BRNO UNIVERSITY OF TECHNOLOGY
VYSOKÉ UČENÍ TECHNICKÉ V BRNĚ

FACULTY OF CHEMISTRY
FAKULTA CHEMICKÁ

INSTITUTE OF MATERIALS SCIENCE
ÚSTAV CHEMIE MATERIÁLŮ

MECHANISMS AND KINETICS OF POLY(3-HYDROXYBUTYRATE) REACTIONS
MECHANISMY A KINETIKA REAKCÍ POLY(3-HYDROXYBUTYRÁTU)

DOCTORAL THESIS
DIZERTAČNÍ PRÁCE

AUTHOR — **Ing. Veronika Melčová**
AUTOR PRÁCE

SUPERVISOR — **Mgr. Radek Přikryl, Ph.D.**
ŠKOLITEL

BRNO 2022

BRNO UNIVERSITY OF TECHNOLOGY
FACULTY OF CHEMISTRY

Assignment Doctoral Thesis

Department:	Institute of Materials Science	Academic year: 2022/23
Student:	**Ing. Veronika Melčová**	
Study programme:	Macromolecular Chemistry	
Study field:	Chemistry of Macromolecular Materials	
Head of thesis:	**Mgr. Radek Přikryl, Ph.D.**	

Title of Doctoral Thesis:

Mechanisms and kinetics of poly(3–hydroxybutyrate) reactions

Doctoral Thesis:

The aim of this dissertation is, firstly, to study poly(3–hydroxybutyrate) degradation during processing with respect to the influence of processing parameters, mainly temperature and mechanical stress and to determine the kinetics of the degradation at processing temperature. Secondly, the goal is to find a compound reactive towards the polymer in a way it will compensate for the negative effects of the degradation reaction on the resulting properties. To accomplish this task, poly(3–hydroxybutyrate) will be processed with selected reagents with different functionality and chemical functional groups. The effect of the additives on the molecular weight, the thermal and thermomechanical properties of the material will be analysed. Moreover, infrared spectroscopy will be utilised to observe changes in the polymer structure. The degradation kinetics of poly(3–hydroxybutyrate) in the presence of these compounds will be measured. And thirdly, the influence of performed reactive modifications of poly(–3–hydroxybutyrate) on its biodegradability will be studied.

Deadline for Doctoral Thesis delivery: 28.10.2022:

Ing. Veronika Melčová student	Mgr. Radek Přikryl, Ph.D. Head of thesis	doc. Ing. František Šoukal, Ph.D. Head of department

In Brno dated 1.9.2021

prof. Ing. Martin Weiter, Ph.D.
Dean

ABSTRACT

This thesis deals with melt reactions of bacterial biopolymer poly(3-hydroxybutyrate) with selected reactive agents. Compounds of different functional groups; isocyanates, carbodiimides, alcohols and epoxides; and functionalities; from two to polyfunctional; were exploited. The aim is to characterize the kinetics of the polymer's thermal degradation during processing with and without the addition of aforementioned reagents in different dosages. For that, rheological measurement consisting of four subsequent frequency sweeps covering a range of 0.1–50 Hz was carried out and obtained data were evaluated to gain a viscosity loss rate. This kinetic parameter enabled the comparison of the effects of individual reagents. Moreover, reactive samples were prepared by kneading, where melt torque was recorded and discussed, and also by solution method, where solution viscosity was measured. The thermal properties, molecular weight and infrared spectra of such prepared samples were studied. Among the tested additives, polymeric carbodiimide Raschig 9000, hexamethylene diisocyanate, poly(glycidyl methacrylate) synthetized for the purpose of this work, and poly(hexamethylene diisocyanate) showed the best overall results in performed experiments. Notably, the sample with a 100-fold molar overdose of Raschig had a 20–30% lower value of the viscosity loss factor than the reference in the frequency region 0.1–5 Hz. In addition, an enzymatic biodegradability test with lipase and in abiotic conditions was carried out. Poly(3-hydroxybutyrate) additivated with poly(glycidyl methacrylate) showed the highest rate of molecular weight decrease.

KEYWORDS

Poly(3-hydroxybutyrate), isocyanates, carbodiimides, hydroxyl compounds, epoxy compounds, melt reaction, degradation kinetics, enzymatic biodegradation

ABSTRAKT

Tato práce se zabývá reakcemi bakteriálního biopolymeru poly(3-hydroxybutyrátu) s vybranými reaktivními činidly v tavenině. Využity byly sloučeniny různých funkčních skupin; isokyanáty, karbodiimidy, alkoholy a epoxidy; a funkcionality; od dvou po polyfunkční. Cílem je charakterizovat kinetiku termické degradace tohoto polymeru během zpracování samotného a s přídavkem výše uvedených činidel v různých množstvích. Za tímto účelem bylo provedeno reologické měření sestávající ze čtyř po sobě jdoucích frekvenčních testů v rozsahu 0,1–50 Hz a ze získaných dat byl vyhodnocen parametr kvantifikující rychlost poklesu viskozity. Tento kinetický parametr umožnil porovnání účinků jednotlivých činidel. Dále byly připraveny reaktivní vzorky hnětením, při němž byl zaznamenán a diskutován kroutící moment, a také v roztocích, u kterých byla měřena viskozita. U takto připravených vzorků byly studovány tepelné vlastnosti, molekulová hmotnost a infračervená spektra. Z testovaných aditiv vykázaly nejlepší celkové výsledky v provedených experimentech polymerní karbodiimid Raschig 9000, hexamethylen diisokyanát, poly(glycidyl methakrylát) syntetizovaný pro účely této práce a poly(hexamethylen diisokyanát). Pozoruhodné je, že vzorek se 100násobným molárním přebytkem Raschigu měl o 20–30 % nižší rychlost poklesu viskozity v oblasti frekvence 0,1–5 Hz. Kromě toho byl proveden test enzymatické biologické rozložitelnosti s lipázou a v abiotických podmínkách. Nejvyšší rychlost poklesu molekulové hmotnosti vykazoval poly(3-hydroxybutyrát) aditivovaný poly(glycidylmethakrylátem).

KLÍČOVÁ SLOVA

Poly(3-hydroxybutyrát), isokyanáty, karbodiimidy, hydroxylové sloučeniny, epoxidy, reakce v tavenině, kinetika degradace, enzymatická biodegradace

MELČOVÁ, V. Mechanisms and kinetics of poly(3-hydroxybutyrate) reactions. Brno: Brno University of Technology, Faculty of Chemistry, 2022. 113 p. Supervisor of thesis Mgr. Radek Přikryl, Ph.D.

DECLARATION

I declare that my doctoral thesis was worked out independently and that the used references are quoted correctly and fully. The content of the above mentioned thesis is considered a property of BUT Faculty of Chemistry and can be used for commercial purpose s only with the supervisor‘s and dean‘s consents.

.....

Student‘s signature

PROHLÁŠENÍ

Prohlašuji, že jsem disertační práci vypracovala samostatně a že všechny použité literární zdroje jsem správně a úplně citovala. Disertační práce je z hlediska obsahu majetkem Fakulty chemické VUT v Brně a může být využita ke komerčním účelům jen se souhlasem vedoucího disertační práce a děkana FCH VUT.

.....

Podpis studenta

ACKNOWLEDGEMENT

The greatest thanks undoubtedly belong to my supervisor Mgr. Radek Přikryl, Ph.D., for having answers when I needed them and always believing that is document will ever come into being. I would also like to express my gratitude to all my colleagues from the end-of-life laboratory, especially to Ing. Štěpán Krobot and Ing. Vojtěch Jašek and also to Ing. Přemysl Menčík, Ph.D. and Ing. Aneta Pospíšilová.

Moreover, I would like to thank the unknown person who infected me with covid for giving me plenty of time I could dedicate to writing. And together with that, also to my dearest, who showed endless patience and support.

TABLE OF CONTENT

INTRODUCTION

Everybody of us has heard about the issue of plastic contamination of the planet Earth. The problem that scientists foretold shortly after the first short-lived plastic products were put on the market to make everyday life easier is finally getting a bit of attention among people and at the government level. The question now stands, how to deal with this problem and, no less importantly, what steps to take to avoid deepening it.

In connection with this, keywords like bioplastics, biodegradability or compostability began to be discussed more frequently. Gradually, the efforts to solve the problem of plastic pollution took a direction aiming to replace all disposable plastic products with a seemingly ecological variant of bioplastics. However, some crucial issues regarding bioplastics are beginning to emerge, for instance:

- Biodegradability – According to the definition of the term bioplastic, not all of them are biodegradable. Moreover, when they are, it is usually under special conditions, which may not be fulfilled in the environment leading to more pollution/microplastic creation.
- End of life – The fate of bioplastic products in the waste system is currently neglected in the legislation. This causes utter confusion among consumers and major protests of recycling and composting institutions against bioplastics generally.
- Resources - In many cases, bioplastics need valuable agricultural resources for their production. This is a problem in terms of greenhouse gas emissions, which are caused by agricultural production by one quarter, and the overall lack of land for food growing.

In order to evaluate the environmental impacts of a material life cycle, while keeping in mind all these effects, life cycle assessment (LCA) analysis is used nowadays. It is noteworthy that the result of LCA for the subject of this work, microbial polyester polyhydroxybutyrate shows lower values of total cumulative energy and net CO_2 emissions than that of mostly used commercial polymers like polyethylene, polypropylene, polystyrene and poly(ethylene terephthalate). Of course, it is a theoretical analysis. Nevertheless, it clearly proves that it is useful to investigate this material further. At the same time, it is extremely important to keep in mind not to treat polyhydroxybutyrate and alike polymers as materials that are produced to be degraded. On the contrary, it is necessary to perceive them as full-blown plastics, which will serve well in a proper application and offer the advantage of ecological degradation.

1. THEORY

1.1. Poly[(R)-3-hydroxybutyrate]

Poly[(R)-3-hydroxybutyrate] (also poly(3-hydroxybutyrate) or polyhydroxybutyrate, abbreviation PHB) is the most discussed polymer and the first to be described from the group of microbial polyesters poly(hydroxyalkanoates) (PHA).[1] Chemically, it is a linear aliphatic polyester comprised of *R* stereoisomers of 3-hydroxybutanoic acid monomeric units, as can be seen in Figure 1. This polymer is known since 1926 when it was discovered by French scientist Maurice Lemoigne while working with *Bacillus megatherium, Bacillus mesentericus,* and *Bacillus vulgatis*.[2] In the cells, PHB exists in an amorphous state in the form of hydrophobic polymer granules (usually 0.2–0.5 μm in size).[3] The role of these inclusions for hosting microorganisms was identified to be mainly a form of energy and carbon reservoir, similarly to glucose or starch in other bacteria[4], and also enhanced robustness upon exposure to various environmentally relevant stress conditions (temperature, oxidation or UV radiation)[5].

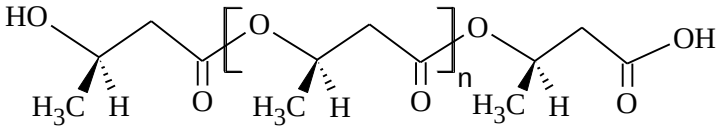

Figure 1 Poly(3-hydroxybutyrate) structure[1]

Since then, biosynthesis has remained the best production possibility for PHB focusing on product quality and cost.[6] Number of bacteria strains are able to produce PHB in special conditions characterised by carbon source excess and deprivation of other nutrients. The most utilized species of PHB bacteria are *Cupriavidus necator* (former *Alcaligenes eutropha* or *Ralstonia eutropha*), *Alcaligenes latus* and recombinant *Escherichia coli* with genes from *C. necator*.[1,3] PHB biosynthesis that occurs in *C. necator* is the most thoroughly described of the eight pathways identified for PHA production. The first step in this biosynthesis is the formation of an acetoacetyl-CoA molecule from two acetyl-CoA molecules, which is catalysed by the enzyme *β*-ketothiolase. Afterwards, acetoacetyl-CoA is transformed into (*R*)-3-hydroxybutyryl-CoA by NADPH-dependent acetoacetyl-CoA reductase. The third and last step is the polymerisation reaction catalysed by PHB synthase leading to PHB formation.[1,3] The regulation of PHB synthesis *in vivo* in polymer granules is made by degradation catalysed by PHB depolymerase, dimer hydrolase, 3-hydroxybutyrate dehydrogenase, and acetoacetyl-CoA synthase.[3]

Various inexpensive carbon sources have been studied in order to be used for PHB production, including agro-industrial wastes (cane molasses, sugar beet juice, rice straw hydrolysate and others), glycerol, glucose or different oils. The motivation to use waste products as a substrate for PHB production is motivated by the fact that the substrate cost constitutes almost 50% of the overall cost.[6,7]

Apart from the cost of the substrate, other crucial factors increasing the overall price of biosynthesised PHB are polymer concentration, yield, and productivity of the production processes. Both the laboratory and large-scale fermentations usually take place in batch reactors in an aqueous

solution at mild conditions. Biosynthesis in batch reactors is a discontinuous process where input substances are added at the beginning of the cultivation and the product is removed at the end. This way, various researchers achieved PHB content of 38–72% dry cell weight.[6] An example of bacteria after fermentation is given in Figure 2.

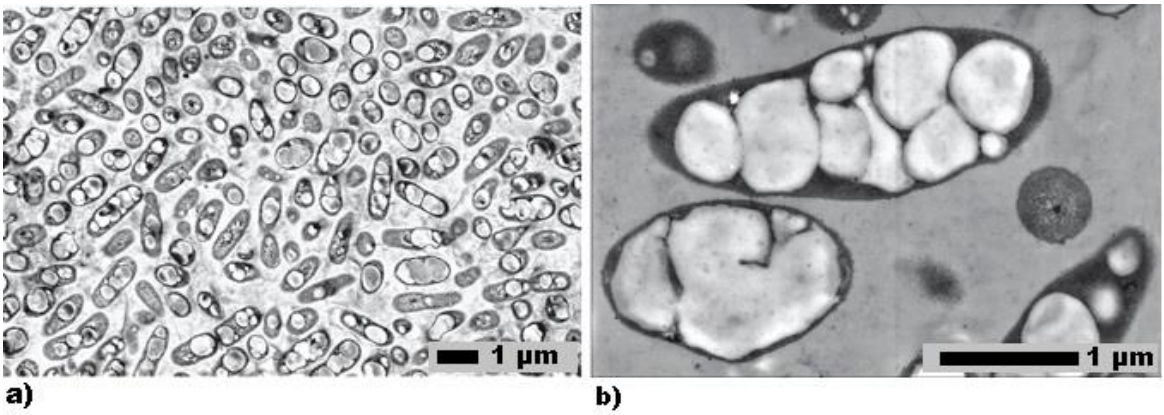

Figure 2 Scanning electron micrographs of PHA-rich C. necator DSM 545 cultivated in a continuous fermentation process on glucose. a) 48% of PHA in a cell mass, magnification ×20,000 b) 65% of PHB in a cell mass, magnification ×72,000[7]

After the fermentation is finished, there are two options for the isolation process.[8] The first method is to destroy the cells mechanically and to dissolve the formed product with a suitable solvent. The best results were achieved with chlorinated hydrocarbons such as chloroform[9,10], methylene chloride[10] or 1,2-dichlorethane[10] with the highest obtained purity of resulting polymer 96, 98 and 98%, respectively. Afterwards, the solid fraction is separated from the PHB solution, and the polymer is precipitated and dried. The second alternative, opposingly to the first one, is to dissolve everything but PHB. These so-called digestion methods exploit the ability of certain chemicals to solubilize cellular mass. There are numerous reported solubilizers for non-PHB biomass, including the combination of surfactant and sodium hypochloride (up to 98% purity)[11], sodium hydroxide (up to 98% purity)[12], surfactant and chelate (purity higher than 96%)[13] or various enzymes (90% purity with pancreatin)[14]. Though more specific details of isolation methods are usually the subject of patents or company secret.

The isolation step is crucial for the following polymer processing as it can highly affect polymer molecular weight and already mentioned purity. Possible contaminants of PHB include residual solvent or building elements of cells, for example, endotoxin, which is a part of cell surfaces.[12]

Biosynthesised PHB shows the molecular weight (MW) from 10,000 to 3,000,000 Da depending on the microorganism, carbon source and its concentration, fermentation time and other factors related to the isolation process.[3] Microbial PHB has strictly periodic isotactic structure and thus is able to crystallize. The molecules are organized into the form of left-handed helix, where each revolution is made by two monomeric units. The unit cell of the PHB crystal structure is orthorhombic and made up by 4 monomeric units.[15]

PHB usually possesses 55-90% crystallinity with melting temperature (T_m) of the crystalline phase between 170–180 °C depending on the crystal size and morphology. Glass transition temperature (T_g)

of the amorphous phase lies between −5 and 5 °C depending on the molecular weight and crystallinity of PHB and the method used.[1,3,16] The heat of fusion was estimated to be 146 J/g.[16] The most appealing attribute of PHB is undoubtedly its biodegradability, while its major drawbacks as a possible material for commercial use are its brittleness and susceptibility to thermal degradation. These three key topics are to be discussed in the following chapters.

1.2. Biodegradability

Biodegradation (biotic or biological degradation) is a special type of degradation where material is completely decomposed through a biological process by enzymes produced by living organisms into small molecules like carbon dioxide or water, biomass and/or mineral salts in a defined environment and in a defined timescale. The process usually happens in mild conditions of temperature and pH.[17,18]

Biodegradation can be divided according to various criteria. According to the oxygen access, aerobic – with oxygen and anaerobic biodegradation – without oxygen, are distinguished. Depending on whether the process takes place inside or outside the cell, intra- and extracellular biodegradation is identified. In addition, in the literature, two types of processes are performed – enzymatic and microbiological biodegradation. The key difference is that enzymatic tests utilize enzymes isolated from the microorganisms and, therefore, allow shorter experiment times.[17]

Overall, the biodegradation of a polymer is affected by the properties of the material itself and environmental characteristics. Environmental aspects include both biotic and abiotic factors. Important abiotic influences are outdoor conditions such as humidity, weather, ageing and burying. Material is exposed to mechanical, light, thermal or chemical actions (pH as well), which may affect its ability to biodegrade further.[18] For instance, the biodegradability of PHB is impaired if it undergoes photodegradation beforehand. This is due to an increase in PHB crystallinity caused by UV irradiation.[19] As for the temperature, it is necessary to keep in mind that T_g of PHB lies around 0 °C, which may be crucial for biodegradation in outdoor conditions. Last but not least, chemicals which may potentially influence the course of biodegradation are mainly oxygen, water, atmospheric and agro pollutants.[18]

Biological aspects are mainly the result of microorganism activity. Important microbiological factors are the type, distribution, abundance, diversity, activity and adaptation of the microbiota and the supplementation of nutrients. Microorganisms act by mechanical, chemical and/or enzymatic means.[18]

The properties of a material which are of interest when it comes to biodegradation are:

1. First-order structure such as chemical composition, comonomers, MW and MW distribution
2. High-order structures such as T_g, T_m, crystallinity and crystal structure
3. The size and geometry (particles, film, bulk) and surface condition of the plastic (pores etc.)

MW directly influences many fundamental physical properties of the polymer, and its increase leads to a decrease in biodegradability. The degree of crystallinity is a key factor affecting biodegradability since enzymes mainly attack the amorphous domains of a polymer.[20]

1.2.1. Biodegradability testing

Biodegradability testing is, of course, a subject of respective standards issued by corresponding bodies like the International Organization for Standardization (ISO), which operates on a supra-national level, and regional standardization bodies, such as the American Society for Testing and Materials (ASTM) or the European Committee for Standardization (CEN).[20,21]

There exist many biodegradability tests in different environments, as depicted in Figure 3. Moreover, all tests may be performed under aerobic and anaerobic conditions. Other special cases, for instance, *in vivo* testing in living tissues, are not part of the scheme.

Currently, standardized methods usually exploit gravimetry and respirometry as tools for biodegradability determination. Gravimetric analysis is a simple method to measure the changes in sample mass or, e.g. CO_2 absorption. However, its key drawback is the impossibility of telling disintegration and real biodegradation of a sample apart. Respirometry, on the other hand, can monitor either oxygen consumed (chemical oxygen demand – COD) or CO_2/methane produced during biodegradation. Both these methods are successfully used for PHB.[22]

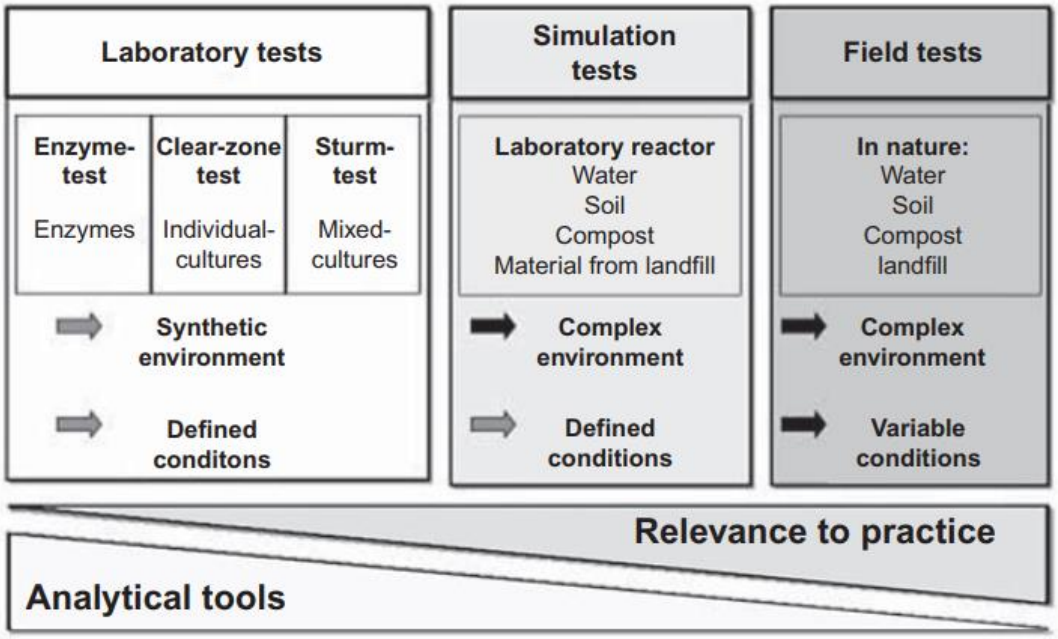

Figure 3 Overview of biodegradability tests[20]

The bacterially produced PHB is fully biodegradable in both anaerobic and aerobic conditions of soil, compost and water environment as well as in marine environments and also without the action of living organisms at a slower rate, as will be described in the following chapters.

1.2.1.1. Abiotic biodegradability of poly[(R)-3-hydroxybutyrate]

In the real natural environments, both non-enzymatic (abiotic) and enzymatic processes can take place. In the case of enzyme absence, PHB can degrade by non-catalysed hydrolysis, in which the water permeates the polymer bulk and causes a random cleavage of polyester bonds independent of the

crystallinity. This leads to a decrease in MW, while the weight remains unchanged up to a great extent of the degradation.[23]

The rate of non-enzymatic hydrolysis is autocatalysed by generated carboxyl end groups (concentration of COOH ends equals the number average molecular weight M_n^t at time t). The kinetics is also proportional to the water and ester bond concentration, which are considered constants hence the relationship:

$$M_n^t = M_n^0 e^{-kt}, \quad \text{Eq. 1}$$

where M_n^0 is the number average molecular weight at time 0 and k is the rate constant, which can be obtained from the semilog plots of $\ln(M_n^t)$ on time. If the chain scission is completely random, the average number of bond cleavage per molecule is linearly dependent on time.[24]

Hydrolysis of PHB is generally a very slow process described many times in the literature, although with inconsistent results due to different sample geometries, sizes and molecular weights.[23] These tests are especially relevant if one is interested in the behaviour of PHB in the human body, as there are no specific PHB depolymerases. The most used medium is phosphate buffer of varied molarity[25–28], others include simple saline solution[26], Hank's solution[26] or blood and blood serum[27].

Bonartsev et al studied the kinetics of non-enzymatic hydrolytic degradation of PHB with different MW *in vitro* in 25 mM phosphate buffer (pH = 7.4, 37 and 70 °C) for 91 days. At 37 °C, PHB with high MW (950 kDa, determined by viscosity measurements) showed 15% weight loss compared to the lower MW sample (150 kDa), which had 38%. The decrease of MW is quite the opposite as it is more profound for higher molecular weight samples.[25] Koyama and Doi observed a decrease of PHB MW in 10 mM potassium phosphate buffer (pH = 7.4) at 37 °C for 150 days at the same time with no change in polymer weight.[28]

1.2.1.2. Enzymatic biodegradation of poly[(R)-3-hydroxybutyrate] in vitro

Degradation through the action of enzymes originates at the surface of a material, where the enzyme adsorbs. Selective degradation and simultaneous removal of low MW degradation products lead to surface erosion and weight loss, while MW and MW distribution do not change as opposed to non-enzymatic hydrolysis. In the initial stages of degradation, preferentially amorphous fraction is consumed.[21,23] PHB is degraded by a number of bacteria and fungi. Extracellular PHB depolymerases consist of 2 separate domains: PHB binding domain and a catalytic domain. The list of PHB depolymerase excreting bacteria was given by Roohi et al. in 2018.[29]

Enzymatic screening tests are convenient because of their speed and are of great use when it comes to the understanding PHB performance in both living tissue and the environment. The tests are usually conducted at 37 °C in a buffer with pH 7.4. PHB depolymerase isolated from *Alcaligenes Faecalis* is extensively used.[28,30] However, it is necessary to note that in real conditions and in living tissue, mainly nonspecific esterases contribute to biodegradation.[23]

For example, Kumagai et al. examined the enzymatic degradation of PHB films at 37 °C and pH 7.4 in aqueous solutions containing extracellular PHB depolymerase from above mentioned *A. faecalis* T1. They concluded that the enzymatic degradation rate decreases with increased crystallinity but is independent on spherulite size.[30]

In order to simulate the conditions of the digestive tract, Freier et al. tested the enzymatic biodegradability of PHB films in Sørensen buffer (37 °C, pH 7.4) with and without pancreatin enzyme. Without enzymatic catalysis, the 70% drop in MW was observed after 32 weeks, whereas with pancreatin, the same was achieved after 12 weeks.[31]

Moreover, lipase, an enzyme that catalyses the hydrolysis of an ester bond between glycerol and fatty acids, is capable of cleavage of PHB ester bonds. Konamni et al. studied the degradation of PHB in a water suspension with the addition of lipase from *B. subtilis* (pH 8, 40 °C). After 72 h of the test, a notable decrease of both molecular weight (21%) and weight (28%) was measured.[32]

1.2.1.3. Biodegradation of poly[(R)-3-hydroxybutyrate] in aqueous conditions

As already mentioned, tests in aqueous conditions may take place under anaerobic and aerobic conditions. For a polymer to be considered biodegradable, it needs to degrade in both cases.

Biodegradability of PHB particles under anaerobic conditions was performed by Abou-Zeid et al. in two anaerobic sludges and monitored with the change in weight and biogas formation. PHB degrading strains were isolated and used for laboratory tests. After 10 weeks of cultivation, 23% weight loss was observed in mixed cultures of methane sludge, while 32% was obtained using a single strain.[33]

Kasuya et al. carried out aerobic biodegradability tests of PHB in water from various sources (river, lake, sea and ocean) at 25 °C for 28 days. Biochemical oxygen demand (BOD) and sample weight loss (WL) was measured. The results are shown in Table 1.[34]

Table 1 The results of PHB biodegradability in various water sources[34]

Biodegradability (%)							
Freshwater				**Seawater**			
River		**Lake**		**Bay**		**Ocean**	
WL	BOD	WL	BOD	WL	BOD	WL	BOD
100 ± 0	75 ± 16	93 ± 7	52 ± 7	41 ± 16	27 ±10	23 ± 13	14 ± 10

At first glance, the difference between results from WL and BOD methods is apparent. Authors explained lower values of BOD with the fact that about 20% of degradation products are water-insoluble. Therefore, these products are not utilized by bacteria for energy generation (lower BOD) and, at the same time, are included in the WL biodegradability.[34] Other important finding is a significantly slower performance of PHB in seawater compared to freshwater.[34]

1.2.1.4. Biodegradation of poly[(R)-3-hydroxybutyrate] in soil and compost

In contrast to enzymatic screening tests, real-world (environmental) biodegradation is a more complex process. Though, we can say that generally, the degradation rates in compost conditions are higher than in natural (soil) conditions because of higher temperatures.

Mergaert et al. studied the biodegradability of PHB in five different soils (pH 3.5, 3.9, 6.3, 6.5, and 7.1) under laboratory conditions. The temperatures used were 15, 28, or 40°C, water content varied from 14 to 22%, and the test ended after 200 days. Degradation was measured through loss of weight (surface erosion), changes in MW and mechanical strength. Weight loss of PHB followed a linear zero-order kinetics defined by this formula:

$$W = k_e \cdot t, \qquad \text{Eq. 2}$$

where W is weight loss, t is time, and k_e is a rate constant. The results clearly showed the biodegradability-temperature relationship as the rate constant rose with increasing test temperature for all soil types. However, the increase was less profound for acidic soils. The highest rate constant, 0.48% per day, was achieved for clay soil with pH 7.1 and a temperature 40 °C; the lowest, 0.03% for sandy soil with pH 6.5 at 15 °C. The authors also gave a list of PHB degrading microorganisms.[35]

Yue et al. performed a compost biodegradability test of PHB using municipal solid waste compost, constant temperature of 55 °C, constant moisture of 54% and pH 6.6–7.4. Biodegradation was measured only through weight loss normalized for thickness. The compost activity was found to be divided into three stages, with the maximum rate of polymer degradation occurring between the tenth and fifteenth day.[36]

1.2.2. Stages of biodegradation

Biodegradation of polymeric material in the natural environment with present degrading bacteria proceeds by following key steps and can stop during each one:

1. Biodeterioration
2. Depolymerisation or biofragmentation
3. Assimilation
4. Mineralisation

Firstly, in a step called biodeterioration, the material is defragmented into small pieces by a combination of microbial activity and abiotic degradation. Acting microorganisms may form a surface layer on a given material, so-called biofilm. Secondly, these microorganisms excrete extracellular enzymes onto the surface of a material or generate free radicals and this way, they cleave long polymeric chains forming soluble oligomers and monomers. In the case of PHB, the mechanism of depolymerisation is hydrolysis catalysed by PHB depolymerases. In the next step, the products of depolymerisation may be transferred into the degrading microorganisms, in other words, assimilated. There, the final step of biodegradation happens. Mineralisation is the process of conversion of organic

products into inorganic ones. This is accomplished by intracellular enzymes, which metabolize polymer fragments as carbon energy, eventually leaving only small by-products, as schemed in Figure 4. In aerobic conditions, these by-products are CO_2, water and microbial biomass, while in anaerobic conditions, CO_2, water, CH_4 and microbial biomass are produced. These simple molecules may afterwards leave intracellular space.[17,18,20]

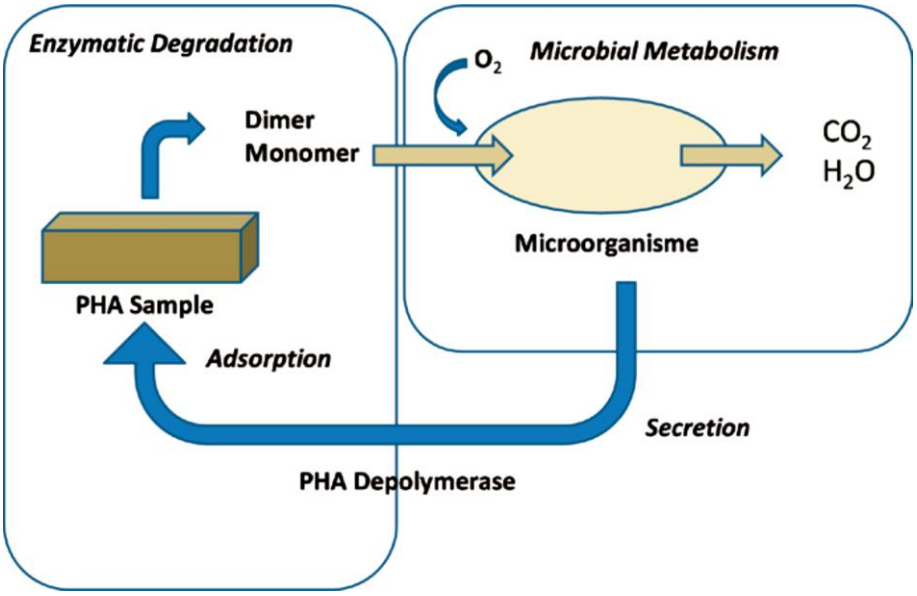

Figure 4 Biodegradation of PHB in the presense of PHB degrading bacteria[17]

1.3. Morphology and ageing of poly[(R)-3-hydroxybutyrate]

As for the often discussed brittleness of PHB, it is caused by the material's phase structure and its change over time, which is usually denoted as ageing.

As studied by Barham et al., PHB develops a banded spherulitic morphology when crystallized from the melt as can be seen in Figure 5.

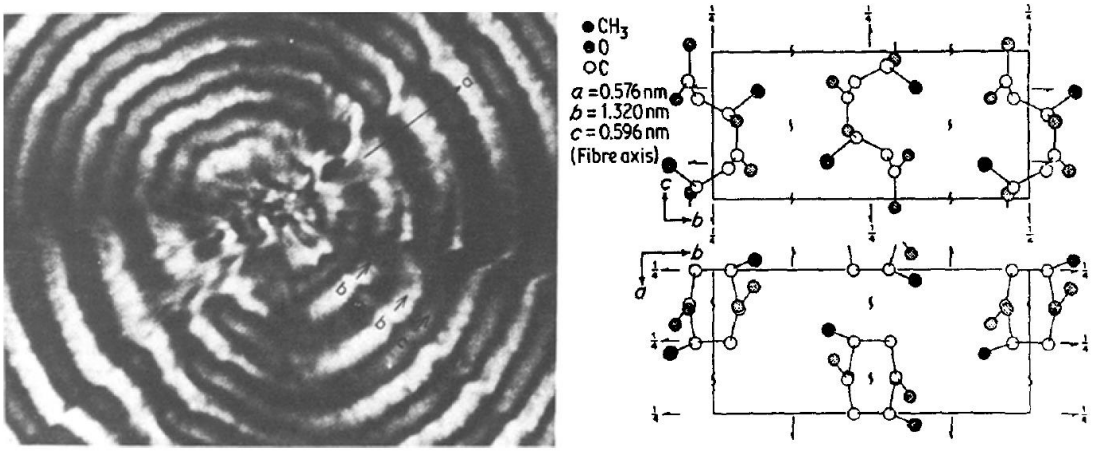

Figure 5 The orientation of crystal axes in PHB spherulite (left) together with a model of PHB unit cell with folded molecules (right)[16]

Spherulite band width and lamellar thickness starts to rapidly increase with crystallization temperature above 85 °C. Due to the low nucleation rate of pure PHB, spherulite diameter is increased

with increasing crystallization temperature as well as studied by polarized optical microscopy (POM).[16] At first, the existence of large crystals with defects was thought to be responsible for the poor mechanical properties of PHB. However, firstly, immediately after processing, PHB exhibits rather ductile behaviour, and secondly, the addition of nucleating agents does not improve the situation.

1.3.1. Secondary crystallization and physical ageing

In the question of PHB brittleness, Scandola et al. were the first to point out the effect of physical ageing of the amorphous phase.[37] De Koning et al. confirmed the ageing phenomenon as an intrinsic property of PHB, which is not related to any foreign compound or molecular weight (MW) deterioration.[38,39] In addition, they examined the influence of storage time on the mechanical properties of PHB and rejected vitrification and physical ageing as the only mechanism of PHB embrittlement. Density measurements shed light on this topic and highlighted the effect increasing of crystallinity upon storage (increase from 56% to 63% in 200 h at 25 °C). X-ray analysis revealed that the increase in crystallinity is due to progressive crystallization rather than crystal rearrangement. From the change of dynamic mechanical characteristics, they concluded that the secondary crystallization of PHB also leads to the constraining of the amorphous phase, which loses its pliability.[39]

The authors also described that annealing the sample at 110 °C for 10 hours restored the original mechanical properties. Furthermore, thus prepared material did not change its properties significantly for 5 months, and it is supposed that after annealing, it underwent only minor changes in the structure due to physical ageing within 20 days.[39]

In the third article in the series, authors studied the effect of annealing of PHB injection moulded samples at temperatures from 90 to 150 °C for the period 10–1225 min on density, crystallinity, dynamic mechanical characteristic and elongation at break. The results clearly showed that annealing led to the increase of crystallinity while unexpectedly, the modulus dropped with a simultaneous increase in elongation at break. In other words, the relaxation strength of the amorphous phase was increased, although its fraction was reduced.[40] Microscopy and X-ray studies showed a much coarser lamellar texture with widened lamellar and amorphous thickness for annealed samples. This coarsening is possible by melting and recrystallization mechanism. As a result, the modified structure of annealed samples with less constrained and more pliable amorphous phase allows the material to deform plastically upon mechanical stress.[40] Remarkable output of this research is the relationship between structural parameters: relaxation strength (represented by a maximum of $\tan\delta_{MAX}$ from dynamical mechanical analysis) and amorphous thickness A with important mechanical parameter: elongation at break, ε_b. The relationship $\varepsilon_b = f(A \cdot \tan\delta_{MAX})$ creates a linear function for annealed and aged samples of PHB, as can be seen in Figure 6.[40]

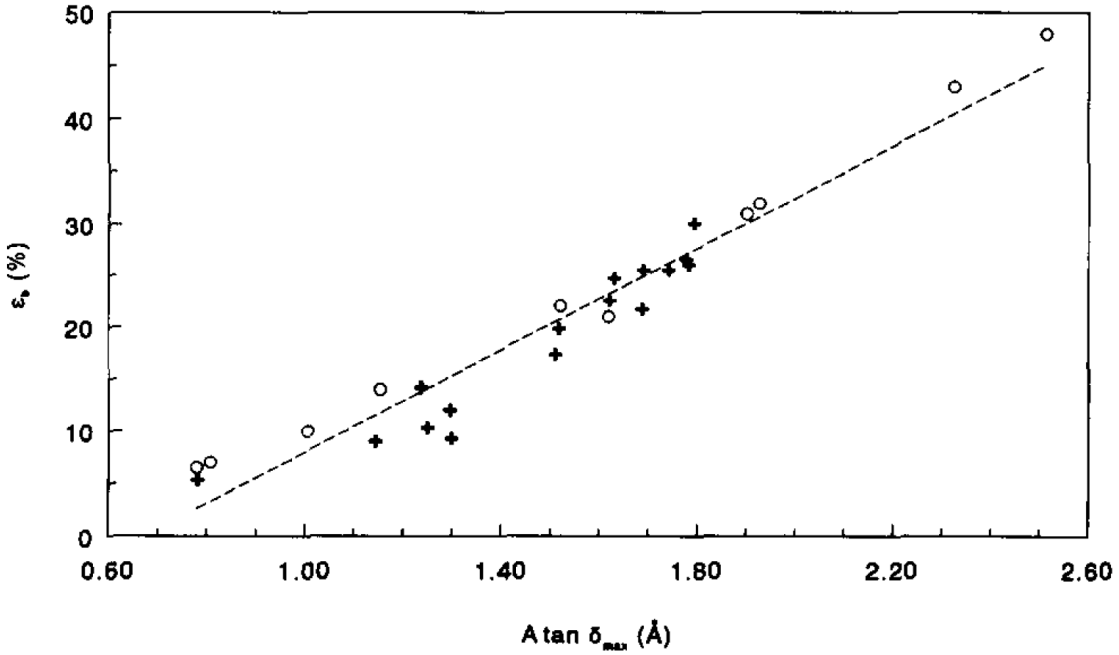

Figure 6 Elongation at break as a function of amorphous thickness and relaxation strength for aged (○) and annealed samples (+)[40]

In short, upon storage, PHB undergoes physical ageing of the amorphous phase and, more profoundly, secondary crystallization. The latter leads to the constraining of the amorphous phase and the loss of its plasticity. These negative ageing effects can be erased through annealing, during which the PHB structure is modified by recrystallization. Equilibrium properties are reached after 20 days.

The effect of plasticizer tri(ethylene glycol) bis(2-ethylhexanoate) on ageing of PHB has also been described. Plasticizer increases PHB crystallinity and, more importantly, lowers the glass transition temperature, which mitigates the effects of physical ageing.[41]

However, while secondary crystallization is easy to describe and measure, the physical ageing of the amorphous phase is harder to comprehend and more complex in its effects on semicrystalline material. Physical ageing can be described as the molecular relaxation that occurs at temperatures below the T_g as polymer chains in a glass state are in a non-equilibrium state. This molecular mobility causes a change in material properties as it becomes stiffer and more brittle with less damping ability.[42] The question now stands how PHB can undergo physical ageing while being stored at ambient temperature meaning above, not under, its T_g.

1.3.2. Three-phase structure

The explanation lies in the phase structure of semicrystalline polymers. In addition to the crystal and the amorphous phase, there is a metastable nano-phase between these two analogically to interphase observed in polymer composites. In the literature, the phases are marked as the crystalline phase (CF), mobile amorphous phase (MAF) and rigid amorphous phase (RAF), respectively.[43] MAF consists of the polymer chains that mobilize at T_g (from now on $T_{g,MAF}$), while RAF is a fraction of immobilized non-organized macromolecules in immediate proximity to CF. Due to the immobilization of RAF

macromolecules, RAF softens at higher temperatures than MAF and, therefore, has its own glass transition temperature or rather temperature range, $T_{g,RAF}$, which usually lies between $T_{g,MAF}$ and the melting temperature of the CF. Hence the physical ageing described for PHB. The identification of $T_{g,RAF}$ is difficult and is usually evaluated from heat capacity measurement by differential scanning calorimetry (DSC).[43]

Di Lorenzo et al. studied nonisothermal cold crystallization of PHB after quenching of the melt and noticed it is a two-stage process. Initial crystal growth up to 70 °C is accompanied by the increase in RAF fraction, both in the expense of MAF. Above 70 °C, reversing melting and reorganization of the metastable PHB structures was observed. Authors concluded, that this recrystallization is possible due to the complete mobilization of the RAF around 70 °C, which is the $T_{g,RAF}$ of PHB.[44] Moreover, they studied the phase structure of PHB after cooling from the melt by three different cooling rates (200, 20 and 5 °C/min) and upon storage at 25 °C at various times.[45] They described the evolution of MAF, RAF and CF fractions for the period of two years. During the storage at 25 °C, crystallization of PHB occurs firstly by crystal growth at the expense of the MAF, and after 240 min, a mechanism changes to local rearrangements of the RAF phase. The ratio between the amount of amorphous and crystalline phase measured soon after crystallization from the melt cooled at 20 °C/min is 1.4 and drops down to 0.06 after 1 year at room temperature.[45]

1.4. Thermodegradation of poly[(R)-3-hydroxybutyrate]

As already mentioned, the other serious problem of PHB is its low thermal stability and narrow processing window. The degradation of PHB and degradation products were extensively studied by Grassie et al.[46–48] Upon heating PHB to temperatures between 170 and 200 °C, which are the typical processing temperatures for PHB, the degradation is first manifested by the change in MW and viscosity of the system. Two competing reactions were identified: random chain scission and condensation reaction. Random scission is carried out by the cis-elimination mechanism, also called McLafferty rearrangement. Ustable α-hydrogen of PHB monomeric unit forms a six-membered ring ester intermediate with adjacent unit resulting in the formation of two shorter molecules. One of the formed sub-molecules has an unsaturated crotonate end group, and the other has a carboxylate end group, as depicted in Figure 7.[47]

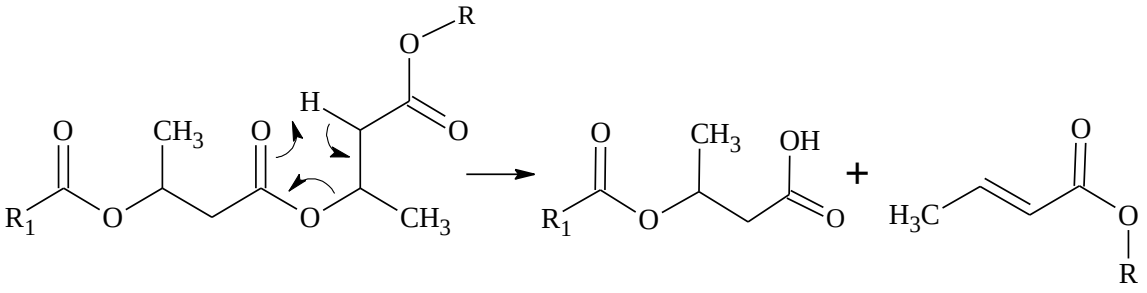

Figure 7 PHB decomposition by cis-elimination[47]

Simultaneously, the condensation reaction proceeds, consuming hydroxyl and carboxyl terminal groups of original PHB together with newly formed carboxyl ends, as can be seen in Figure 8. The new link formed is indistinguishable from the ester groups present. The reaction is slow as it is strictly diffusion controlled. This reaction leads to an increase in MW in the early stages of the reaction, hydroxyl groups are relatively quickly consumed, though. This reaction explains a small amount of water detected as a degradation product.[47]

The esterification reaction ensures that the polymer can resist three heating cycles (1 min at 200 °C) without the drop of MW under the initial value as measured by intrinsic viscosity.[47]

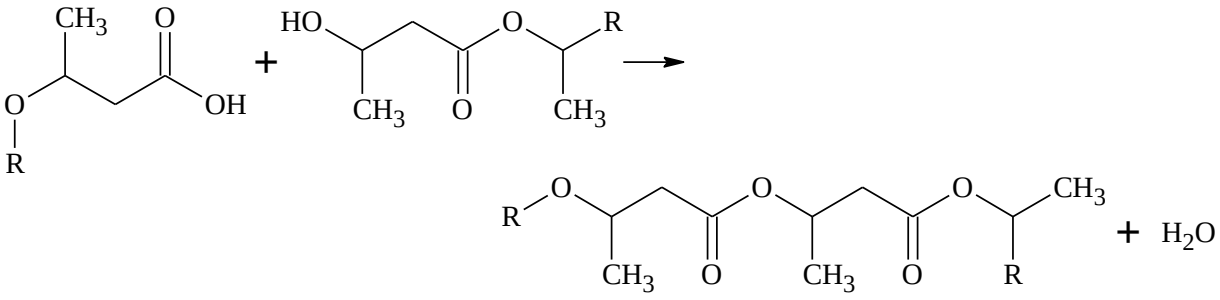

Figure 8 Condensation reaction occurring in PHB[47]

Above 200 °C, the evolution of volatile products becomes significant. Under vacuum, after 120 minutes at this temperature, 20% of PHB mass evaporates. Complete volatilization can be achieved at temperatures up to 338 °C under vacuum. Degradation products, marked as primary degradation products, are the following: 41.2% of dimer, 35.5% of crotonic acid ((E)-but-2-enoic acid, CA), 12.5% of trimer, 2.9% of tetramer and 0.9% of isoctonic acid ((Z)-but-2-enoic acid, Iso-CA). During PHB degradation, MW is reduced by cis-elimination (Figure 7) forming shorter oligomers. Oligomers higher than tetramer are not volatile at these reaction temperatures and are thus broken down further. The relative freedom of movement of the chain ends of larger oligomers may also allow the scission at terminal units.[46]

When PHB is degraded at higher temperatures, around 340–500 °C under vacuum, secondary products are formed. Firstly, *β*-butyrolactone is cleaved from the carboxyl-terminated structure (Figure 9).[46]

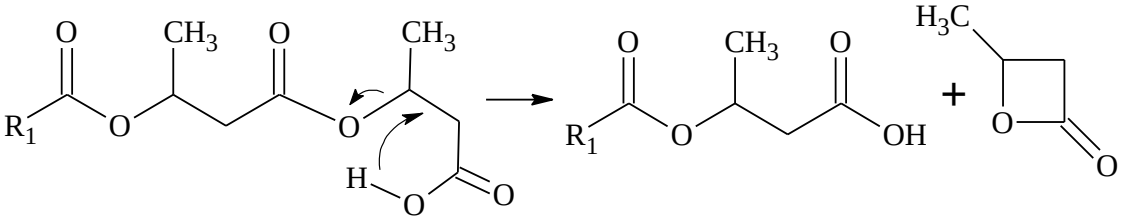

Figure 9 Cleavage of β-butyrolactone from PHB macromolecule[48]

Due to its ring structure, *β*-butyrolactone is highly unstable and undergoes further degradation, as can be seen in Figure 10. Its decomposition leads to the formation of carbon dioxide, propene, ketene and acetaldehyde. All above-mentioned compounds are detected in small amounts as degradation products of PHB when degraded at higher temperatures under vacuum. Under a nitrogen atmosphere, *β*-butyrolactone is not present.[48]

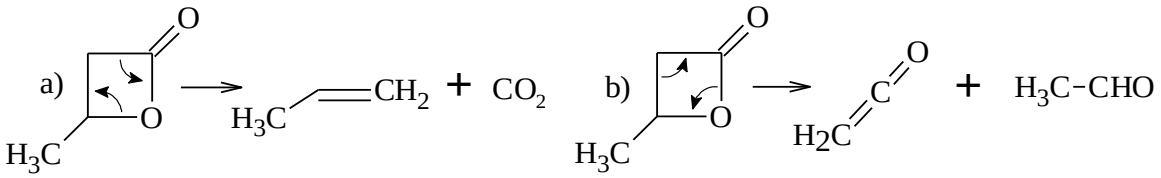

Figure 10 The decomposition of β-butyrolactone by a) O-alkyl scission to form propene and carbon dioxide and b) O-acyl scission to form ketene and acetaldehyde[48]

CA and Iso-CA can undergo decarboxylation forming carbon dioxide and propene as well. Moreover, two CA units may presumably form an anhydride, which is further decomposed into propene, carbon dioxide and carbon monoxide.

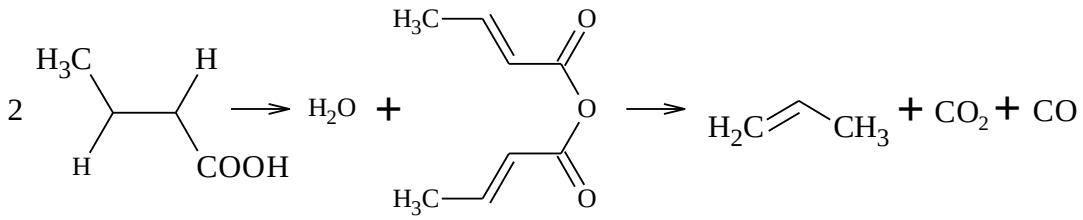

Figure 11 The decomposition of crotonic anhydride[48]

1.4.1. The kinetics of thermal degradation

As Grassie et al. stated that the degradation of PHB follows a kinetic model of random scission during the few hours of the reaction. However, corrections in kinetic relationships derivation have to be made in order to compensate for the increase in MW in the early stages of the reaction due to condensation (see the previous chapter).

When M_{n0} in number average MW of the original non-degraded polymer consisting of carboxyl and hydroxyl ends and S is the average number of bonds broken per original polymer molecule, then the measured value of MW at the time t, M_{nt}, is given by the equation:

$$M_{nt} = \frac{M_{n0}}{S}. \qquad \text{Eq. 3}$$

The theoretical value of MW if no condensation reaction occurred, M_{nt1}, has to be corrected by the factor of one, meaning the one bond regenerated during the condensation reaction:

$$M_{nt1} = \frac{M_{n0}}{S+1}. \qquad \text{Eq. 4}$$

Therefore, measured MW can be expressed as:

$$M_{nt1} = \frac{M_{n0} \cdot M_{nt}}{M_{n0} + M_{nt}}. \qquad \text{Eq. 5}$$

Analogically, the number average chain length during the course of random scission, CL_t, is given by:

$$CL_t = \frac{CL_0}{S+1}, \qquad \text{Eq. 6}$$

where CL_0 is the initial chain length. The degree of degradation, α, is then defined as:

$$\alpha = \frac{S}{CL_0 - 1}, \quad \text{Eq. 7}$$

which can be reduced in the case of large CL_0 to:

$$\alpha = \frac{S}{CL_0}. \quad \text{Eq. 8}$$

If the chain scission is completely random, then at least in the early stages of the reaction, the degree of degradation is a linear function of time:

$$\alpha = \frac{S}{CL_0} = kt, \quad \text{Eq. 9}$$

with k being the rate constant of the reaction. Combining Eq. 6 and Eq. 9 leads to:

$$\frac{1}{CL_t} - \frac{1}{CL_0} = kt. \quad \text{Eq. 10}$$

Indeed, the linear relationship between $1/CL_t - 1/CL_0$ and time was confirmed for temperatures 170–200 °C and activation energy of chain scission was estimated as 247 ± 19 kJ/mol.[47]

Kunioka and Doi monitored the MW change behaviour of PHB and its copolymers poly(3-hydroxybutyrate-co-3-hydroxyvalerate) (PHBV) and poly(3-hydroxybutyrate-co-4-hydroxy-butyrate) (PHB4B) in the temperature region 100–200 °C. They confirmed the random scission kinetics is applied to reaction time up to 20 minutes, with the rate constant being rather dependent on the temperature than the copolymer composition.[50]

However, the auto-acceleration effect was observed for longer reaction times. From a number average MW of around 6000, this effect became significant, and the rate of the reaction rose.[51] The reason for this is that while the carboxylic acid and a saturated ester ends show to induce similar electronic effects on a neighbouring ester cleavage, the crotonate conjugated with an ester group generates an inductive effect. Therefore, the unsaturated end increases the scission rate of the neighbouring ester linkages. Moreover, the addition of palmitic acid or phosphoric acid was shown to affect only slightly the thermal stability of PHB, thus the catalytic effect is not attributed to the higher concentration of acidic carboxylic acid end groups.[52]

Harrison and Melik developed a methodology for characterizing the degradation kinetics using simple rheology measurement, without the need of complicated MW analysis.[53] The authors proceeded from the expression for the change of the chain length given in Eq. 10 and gave a corresponding expression for the change of MW in time, which follows the kinetics of the first-order reaction:

$$\frac{1}{M_{w0}} - \frac{1}{M_w} = -\frac{k}{2M_0}t, \quad \text{Eq. 11}$$

where M_w is weight average molecular weight at time t, M_{w0} is starting weight average molecular weight, k is thermal degradation rate constant and M_0 is monomer MW. In order to eliminate M_w from the equation, the authors used the relationship between M_w and complex viscosity η^*:

$$\eta^* = KM_w^{\alpha(\omega)}, \quad \text{Eq. 12}$$

where K is a material constant and $\alpha(\omega)$ is a power law exponent for given frequency ω. Then, substituting Eq. 12 into Eq. 11, we obtain:

$$\left(\frac{\eta_0^*(\omega,t=0)}{\eta^*(\omega,t)}\right)^{1/\alpha} = 1 + \left(\frac{kM_{w0}}{M_w}\right)t. \quad \text{Eq. 13}$$

Upon the conditions, where we measure complex viscosity as a function of time and frequency – $\eta^*(\omega,t)$ (frequency sweep) and we want to calculate the complex viscosity as a function of frequency at time 0 prior to any degradation – $\eta^*(\omega,t=0)$. This expression can be expanded as:

$$\log \eta^*(\omega,t) = \log \eta_0^*(\omega,t=0) + \sum_{i=1}^{\infty}(-1)^i(R_{vi}t^i), \quad \text{Eq. 14}$$

where R_{vi} is an ith-order viscosity loss rate defined as:

$$R_{vi} = \frac{\alpha}{i}\left(\frac{kM_{w0}}{2M_w}\right)^i. \quad \text{Eq. 15}$$

According to that, complex viscosity as a function of time was plotted for each frequency. For each frequency, there were four points corresponding to four FS measured fitted with first or second order fit. From the regression equation, the values of time zero complex viscosity $\eta^*(\omega,t=0)$, R_{v1} (in the case of first order fit) and both R_{v1} and R_{v2} (in the case of second order fit) were obtained for each frequency.

1.4.2. The effect of impurities on thermal degradation

The kinetics and extent of degradation of PHB are, similarly to other polymers, influenced by impurities present in the polymer matrix. As a biological polymer, PHB does not contain catalyst and monomer residues. However, possible contaminants include bacteria residues like endotoxins, enzymes or coenzymes and residues from the nutrient which sustain the bacteria. The major impurities contain nitrogen, phosphorus and sulphur atoms.[12,16] The specific composition was identified by Hablot et al. by thin-layer chromatography with hexaneediethyl ethereformic acid as the solvent elution system. The separation revealed that the residues are a mixture of lipids like free fatty acids, mono-, di- and triacylglycerols, phospholipids, cholesterol and cholesterol esters. The authors also estimated the total amount of nitrogen in the extracted residues as approximately 0.5% using the titration technique. That corresponds to less than 50 ppm in the raw PHB.[54] However, the amount and composition of impurities in PHB highly vary for different producers of PHB and different batches as well. For instance, Nguyen et al. reported 0.10–0.11% of nitrogen in PHB, which is up to five times less.[51]

The effect of inorganic oxides CaO, MgO, PbO, PbO_2, $A1_20_3$ and ZnO and CaH_2 on the degradation of PHB into volatile products was studied by Csomorová et al. All selected additives led to the decrease in the temperature of maximum degradation rate compared to neat PHB. The smallest drop was observed for Al_2O_3, while the biggest for Ca-containing compounds.[55] The degradation effect of Ca together with Na was confirmed by Kim et al., while the metals Zn, Sn and Al were found to have a negligible influence on PHB thermal stability.[56] Another study was focused on the effect of acetic and carbonic acid salts of alkali metals (Cs, K, Li) and bivalent metal (Ca, Mg, Zn) salts on lowering PHB thermal

stability. The salts of monovalent cations showed increased activity with increasing cation radius (from Li to Cs). Bivalent cations generally caused less degradation effect compared to monovalent ones.[58] High pro-degrading effect was also observed for organic quaternary ammonium salts.[54,59]

Thanks to this sensitivity of PHB to the presence of foreign substances, various purification methods appeared in the literature. Barham et al. started with the raw biomass with 55 wt% of PHB from the fermentation procedure. Dry biomass was washed with hot methanol in order to remove phospholipids. Drying followed, and washed biomass was refluxed with chloroform for 10 min. PHB solution in chloroform was separated from the cell debris by centrifugation and filtration through a 5 μm pore sized cartridge filter. PHB solution was vacuum dried at 60 °C for a minimum of 24 hours.[16] PHB/chloroform solution can as well be precipitated instead of drying. Grassie et al. used petroleum ether as a precipitant. The precipitated polymer was dried and washed with diethyleher, and the procedure was repeated until snow white. Finally, PHB was precipitated in methanol.[46] Hablot et al. used Soxhlet extraction with diethyl ether for extraction of fermentation residues in PHB. The initial amount of impurities in the raw PHB was gravimetrically determined from the liquid phase and estimated to be ca. 2 wt%.[54] Another technique used is simple purification by precipitation in 10-fold volume methanol from 5 vol% chloroform solution.[56] Larsson et al. improved the thermal stability of PHB by simply washing the materials in 1 mM aqueous solution of hydrochloric acid for 30 minutes.[57]

1.5. Prevention and suppression of the effects of thermal degradation

Many different attempts have been made to prevent extensive thermal degradation of PHB or at least to compensate for its negative effects on material properties. The ways to do this can be divided as follows:

1) Non-reactive methods
   a) Additivation
      i) Stabilization
      ii) Plasticization
   b) Blending with other polymer
   c) Composites
2) Reactive methods
   a) Grafting
   b) Copolymer synthesis
   c) Chain extension and crosslinking

The first category includes all options, where a mixture of PHB and other low to high molecular weight components is prepared while the original structure of PHB is preserved. It includes all kinds of additivation and preparation of blends with other polymers (more than 5 wt% addition) and composites. In the second group, there are reactive modifications, which lead to altered PHB structure with changed properties. It is important to note that using any method to overcome PHB drawbacks, emphasis should be placed on maintaining the unique property of PHB – its biodegradability.

1.5.1. Non-reactive options

One of the simplest methods of degradation prevention, and also an inexpensive one, is stabilization, which is often employed in the case of commercial polymers. For instance, antioxidant 1010

(Pentaerythritol tetrakis(3-(3,5-di-tert-butyl-4-hydroxyphenyl) propionate))[60] has been reported to enhance melt properties of PHB/acetyl tributyl citrate blend. The stabilization mechanism on PHB is not satisfactorily explained, though, as other resources claim that commercial stabilizers give no significant improvement in the stability of PHB.[48] Recently, Tochacek et al. performed multiple extrusions of PHB with commercial thermooxidation stabilizers: phenols of different steric hindrance, phosphites, amine oxide, hydroxylamine, lactone, hindered amine, and carbodiimide. Instead of stabilization, the pro-degradation effect was observed, mainly with nitrogen- and phosphorus-containing additives.[49] Biodegradable alternatives of commercial stabilizers, such as tannic acid (1,2,3,4,6-penta-*O*-{3,4-dihydroxy-5-[(3,4,5-trihydroxy-benzoyl)oxy]benzoyl}-D-glucopyranose)[61] or grape pomace extract[62] were found to successfully reduce thermal degradation of PHB. Grape pomace is a mixture rich in natural antioxidants as polyphenols, stilbenes and flavonoids while tannic acid is a polyphenolic substance. Carboxyl-terminated butadiene acrylonitrile rubber (CTBN) and polyvinylpyrrolidone (PVP) were used as polymeric additives and were proven to enhance PHB thermal stability.[63]

Plasticizer addition leads to a drop in the melting temperature of a semicrystalline polymer which subsequently allows to lower processing temperature and minimizes the effects of thermal degradation. Recently, mainly citrate-based plasticizers gained great attention as they are non-toxic derivates of citric acid, for example, acetyl tributyl citrate (ATBC)[60,64], acetyl triethyl citrate[65] or triethyl citrate[66]. ATBC lowers the melting temperature of PHB of approximately 10 °C and does not affect the degradation behaviour distinctively. Non-citrate-based plasticizers include glycerol and triacetin[65], dioctyl (ophthalate), dioctyl sebacate[60], soybean oil, epoxidized soybean oil or dibutyl phthalate[66].

As for polymer blends, the results of numerous studies have been summarized by Ha et al., however, only some of them are focused on the blend's thermal stability.[67] To give some examples, the improvement of overall thermal stability was observed for PHB/soda lignin blends with lignin content up to 40 wt%. The reason for this is ascribed to intermolecular interactions between two polymers via hydrogen bonding leading to a more stable polymer structure.[68] Generally, the existence of hydrogen bonds can promote miscibility, affect the morphology and improve their mechanical properties as well. Hydrogen bonding was also observed for PHB blends with poly(vinylacetate), poly(vinylacetate-co-vinylalcohol)[69] and poly(4,4′-dihydroxydiphenyl ether)[70] although authors did not concentrate on the degradation behaviour of prepared blends. Moreover, hydrogen bonds are reported in the case of PHB with hyperbranched structures – dendrimers[71], bisphenol A[72], where they have a positive effect on enlarging the processing window of PHB; and low molecular weight poly(propylene glycol) (LMWPPG)[73]. In the latter case, a decrease in PHB crystallinity and melting point and an increase in degradation onset temperature was observed for a blend containing 15 wt% LMWPPG. The thermal stabilization observed by TGA could be related to the intermolecular interaction of LMWPPG (as can be seen in Figure 12) with PHB chains hindering the mechanism of β-elimination.[73]

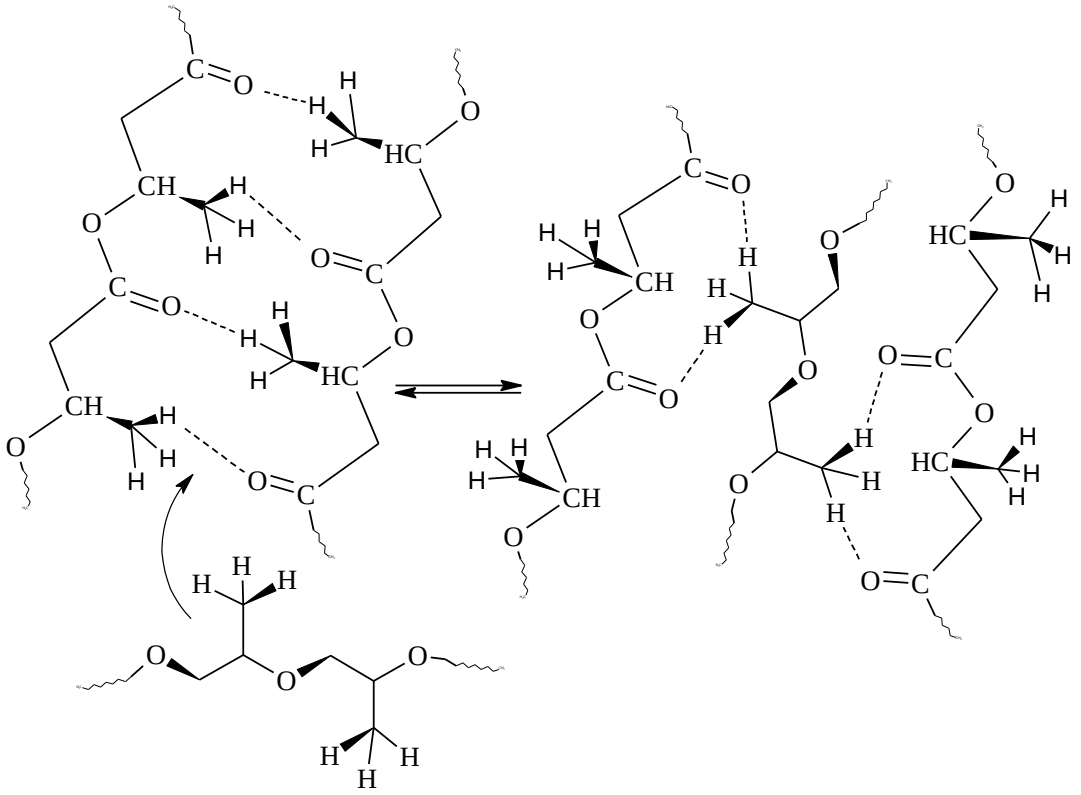

Figure 12 Interactions between PHB and LMPPG[73]

1.5.2. Reactive options

In contrast with the previous chapter, different ways of chemical modifications of PHB structure are given here. Although these methods aim to improve various physical and mechanical properties of PHB and only in a few cases the attention is paid to the thermal stability of newly formed PHB derivate.

In the work of Arkin and Hazer, chlorination of PHB was carried out. From chlorinated PHB-Cl, phenyl, quaternary ammonium, and thiosulfate moieties were synthesised. PHB-Cl showed lower T_m and T_g and radical drop in MW compared to neat PHB.[74]

The majority of chemical modification methods described in the literature deal with the preparation of copolymers. Two types of copolymers to focus on are graft and block copolymers. The former is usually prepared by grafting from technique, in which a monomer is polymerized on a specific site of the existing macromolecule, where there exists a reactive species – most often a radical. Radicals can be generated by the decomposition of thermally unstable compounds (e.g. peroxides) or by the application of radiation. Block copolymers can be prepared by transesterification reaction with other polymers or from PHB macromers with functional end groups.

1.5.2.1. Graft copolymers from PHB

Graft copolymers of PHB were synthesised, for example, using the following monomers: maleic acid or maleic anhydride (MA)[75–77], sodium *p*-styrene sulfonate (SSS), styrene (St) and methyl acrylate (MAA)[78], acrylic acid (AA)[78,79], methyl methacrylate (MMA) and 2-hydroxyethyl methacrylate (HEMA)[80], poly(ethylene glycol) (PEG)[81], isoprene[82] or vinyl acetate[83].

Chen et al. prepared PHB-g-poly(MA) with graft degree from 0.21 to 1.18% and found out that maleation leads to a higher thermal decomposition temperature than that of pure PHB, although the degradation mechanism is the same for PHB and PHB-g-poly(MA).[75] In the subsequent study, they used benzoyl peroxide as an initiator and maleic anhydride as a monomer and prepared PHB-g-poly(MA) with graft degree 0.2–0.85%. Improvement of thermal stability of PHB was confirmed and explained as the replacement of labile tertiary hydrogen of PHB by MA units. The study was also extended by a biodegradability test in phosphate buffer with fungi *Penicillin sp*. at 28 °C for 50 h. According to the results, under these conditions, the biodegradability of PHB was promoted by maleation. Moreover, the weight loss value gradually increased with graft degree, which is attributed to the more hydrophilic nature of PHB-g-poly(MA).[76] Maleic anhydride can be grafted by radiation-induced graft polymerization technique with the same effect on thermal stability.[77]

Hsieh et al. prepared PHB-g-poly(SSS), PHB-g- poly(St), PHB-g-poly(AA), and PHB-g-poly(MAA) copolymers by pre-irradiation with ^{60}Co γ-rays before radiation-induced graft polymerization. Enzymatic degradation of newly formed copolymers was evaluated at 37.8 °C in 0.1 M phosphate buffer (pH 7.4). PHB depolymerase purified from *Ralstonia pickettii* T1 was used. Weight loss after 48 h of the test can be seen in Figure 13.

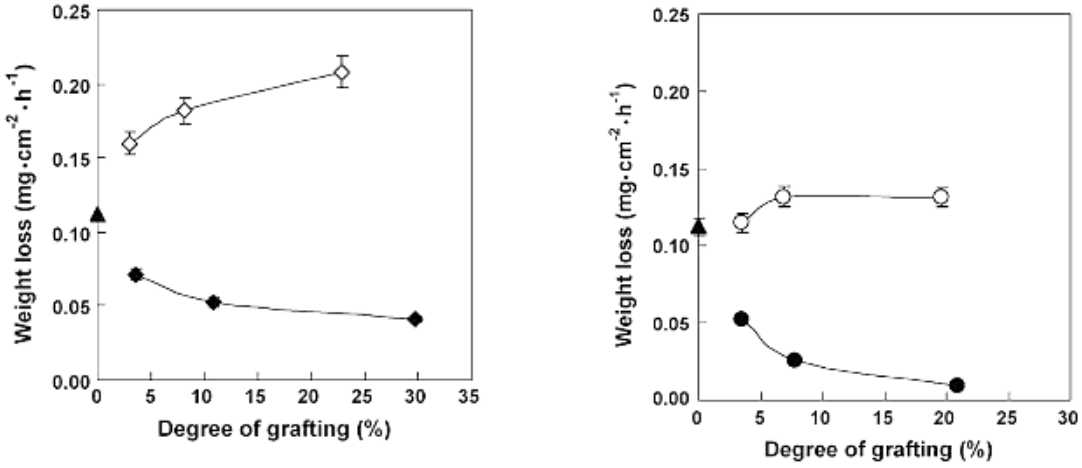

Figure 13 Enzymatic degradation of PHB and grafted PHB films against degree of grafting (%). (▲) PHB film and in the left: (◊) PHB-g-SSS and (♦) PHB-g-St, in the right (○) PHB-g-AAc and (●) PHB-g-MAAc[78]

The results clearly show the influence of hydrophilicity/hydrophobicity of side chains grafted from PHB as the more hydrophilic monomers (SSS and AA) caused higher enzymatic degradability compared to both neat PHB and their hydrophobic equivalent (St and MAA).[78] The study of the effect on thermal stability was not a part of the study.

Mitomo et al. studied the rate of the enzymatic biodegradability of PHB-g-poly(MMA) and PHB-g-poly(HEMA) and reported a decrease for PHB-g-poly(MMA) copolymers of all MMA contents. In the case of PHB-g-poly(HEMA), at first, an increase attributed to the improvement of wettability between the polymer and an enzyme solution was observed. Then a steep decrease in the biodegradability rate with higher content of HEMA was observed.[80]

Zhijiang et al. prepared PHB-g-PEG copolymers via radical grafting in chloroform with azobisisobutyronitrile as an initiator from PHB and functionalized PEG macromer with unsaturated ends. Grafting PEG onto PHB did not change the thermal stability of PHB. Moreover, copolymers had improved biodegradability in both acidic (pH 1) and alkaline (pH 13) solutions and as well in 0.1 M phosphate buffer containing lysozym.[81]

1.5.2.2. Block copolymers from PHB

As for the block copolymers, the focus is generally kept on linear copolymers, which can be prepared by various ways. Transesterification reaction has been employed for the synthesis of block copolymers of PHB with poly(isosorbide succinate) (PIS) and poly((L)-lactide) (PLA)[84], poly(ε-caprolactone) (PCL)[85], poly(1,4-butyleneadipate) (PBA)[86] or poly(hydroxyl ether of bisphenol A) (phenoxy)[87]. Newly formed PHB-block-PIS is reported to have similar thermal stability as neat PHB.[84] PHB-block-PCL copolymers had PHB content ranging from 28 to 81 mol%. PHB-block-PBA was prepared by microwave-assisted transesterifications. Neither thermal stability nor the biodegradability of these copolymers was studied though.[85,86] The same applies for copolymer with phenoxy.

Low-molecular weight PHB prepolymers of PHB can be prepared by various methods, which will not be discussed in detail in this work. These oligomers are subsequently used as components to build block copolymers. For instance, Casarano et al. prepared a copolymer with a sequence PLA-block-PHB-block-IS-block-PHB-block-PLA. They started from a prepolymer of two PHB units bonded to an isosorbide succinate. PLA was polymerized via ring-opening polymerization onto the prepolymer with tin(II) 2-ethylhexanoate as a catalyst.[84]

Saad et al. used dihydroxy-terminated PHB prepolymers with molecular weight of around 3000 Da prepared by transesterification of high molecular weight PHB with1,4-butanediol in $CHCl_3$ at 65 °C in the presence of *p*-toluene sulfonic acid as a catalyst. PHB-diol together with poly(butylene glycol adipate)-diol (PBA-diol) and poly(diethylene glycol adipate)-diol (PDEGA-diol) were used to prepare multiblock polyurethanes with 1,6-hexamethylene diisocyanate (HMDI) as a non-toxic connecting agent. The thermal stability of PHB in prepared copolymers was not changed. Moreover, it is interesting to note that in this case, biodegradability was determined by measuring the biological oxygen demand of insoluble substances in a standard test medium for more than 9 weeks (more about biodegradability in chapter 1.2 Biodegradability). Copolymers with 50 wt% of PHB had a similar degradation behaviour as neat PHB, while lower amounts of PHB made the samples resistible to degradation.[88]

Different type of polyurethane copolymer was synthetized by Zhao et al. from PHB-diol, PEG and HDI. Authors exploited the biodegradation behaviour of prepared copolymers *in vitro*. The test was conducted at 37 °C in phosphate buffered saline and the changes in MW were monitored weekly. Due to the increase in hydrophilicity and drop in crystallinity, the hydrolysis process of copolymers was profoundly accelerated compared to the homopolymer.[89]

1.5.2.3. Chain extension and crosslinking of PHB

Chain extension and crosslinking are other ways how to prevent PHB from extensive degradation or to compensate for the negative effects of degradation, for example, in the case of already processed PHB. These reactive modifications are generally conducted at higher temperatures in the melt state.

For instance, Vogel et al. reported reactive melt spinning of PHB with dicumyl peroxide (DCP) for the purpose of improving the crystallization behaviour of PHB fibres. DCP concentration 0.1 wt% resulted in a distinct increase in melt viscosity, while further addition of DCP had the opposite effect due to chain scissions. Thermal stability and biodegradability of modified PHB was not evaluated.[90]

Similarly, Wei et al. studied the properties of PHB and PLA cross-linked with DCP. The proposed reaction mechanism for PHB is given in Figure 14.[91]

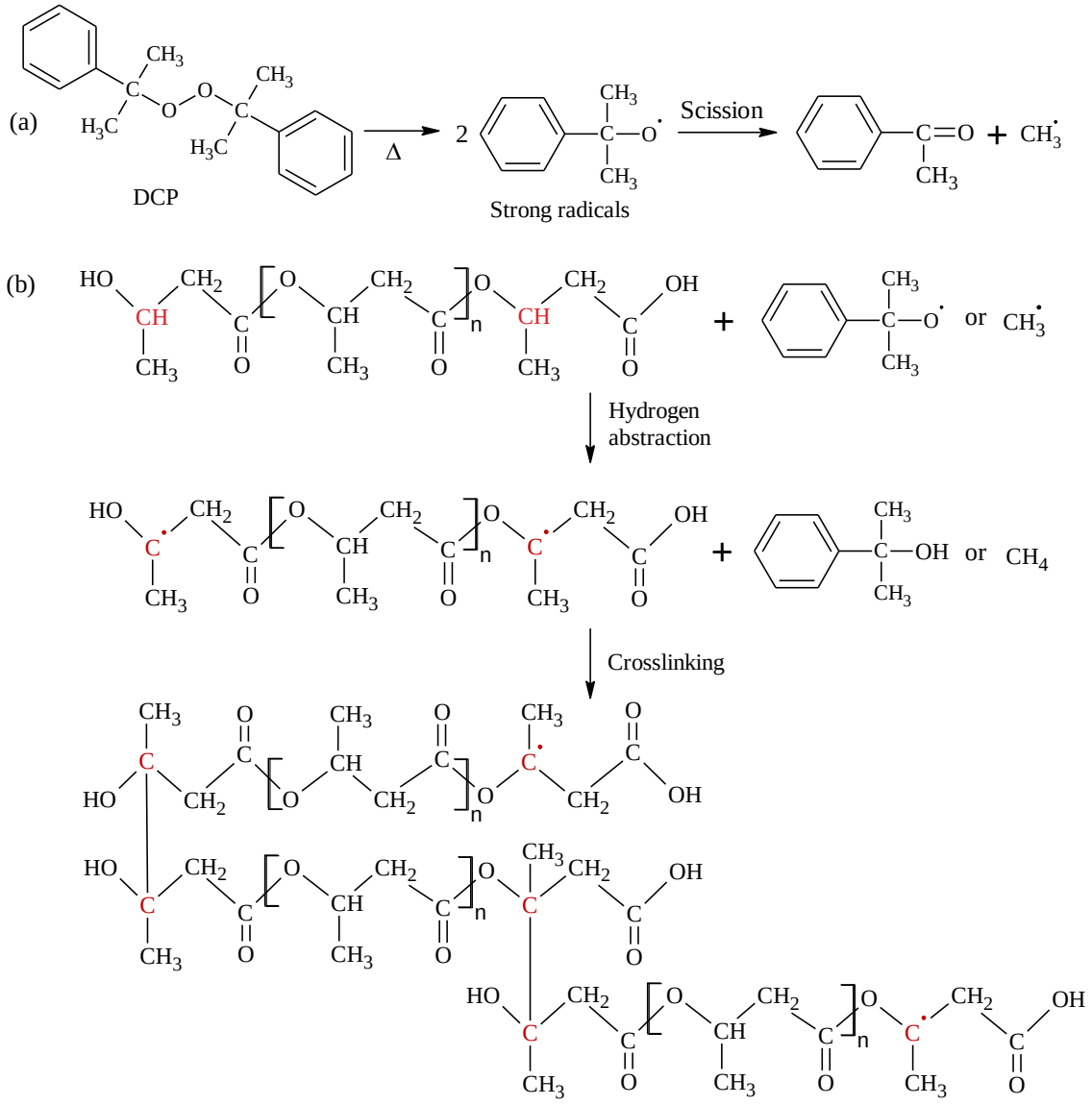

Figure 14 Schematic illustration of DCP induced cross-linking of PHB: (a) thermal decomposition of DCP into primary radicals when exposed to heat and then (b) hydrogen abstraction from PHB chains by primary radicals and bimolecular recombination of polymer radicals[91]

The amount of DCP studied was 0, 0.25, 0.5 and 1 wt% for different reaction times. The gel fraction of reactive samples reached values up to 58% (1 wt% of DCP, 8 minutes' reaction time), and the degree of swelling of isolated gels was measured as well. Cross-linking efficiency and the ratio of the chain scission to cross-linking were determined from the Charlesby-Pinner equation. The authors measured the thermal stability of cross-linked gel fraction by thermogravimetric analysis (TGA). Degradation onset temperature and temperature of 98% degradation were both shifted to higher temperatures, meaning higher thermal stability of cross-linked PHB in comparison with linear PHB. Moreover, cross-linked material exhibited lower T_g, T_m and crystallinity, improved melt strength and showed signs of long chain branching (LCB).[91]

In the work of Kolahchi, PHB was modified through a reactive extrusion with DCP and triallyl trimesate (TAM). During the reaction, DCP forms radicals in the same way as in Figure 14 (a). After tertiary hydrogen abstraction from PHB, the radicals subsequently react with the chain extender to form branched and cross-linked structures, as indicated in the scheme in Figure 15. The changes in the structure of PHB were proven by rheological measurements. Gel content up to the value 65 wt% was reached for the sample containing 0.3 wt% DCP and 1 wt% TAM. The samples with high gel contents showed higher onset degradation temperature than pure PHB as measured by TGA. Furthermore, thermal stability was investigated by rheology using a time sweep test conducted at 190 °C and frequency of 1 Hz. DCP/TAM treated samples showed significantly reduced rate of thermal degradation when compared to PHB, presumably because of delayed kinetics.[92]

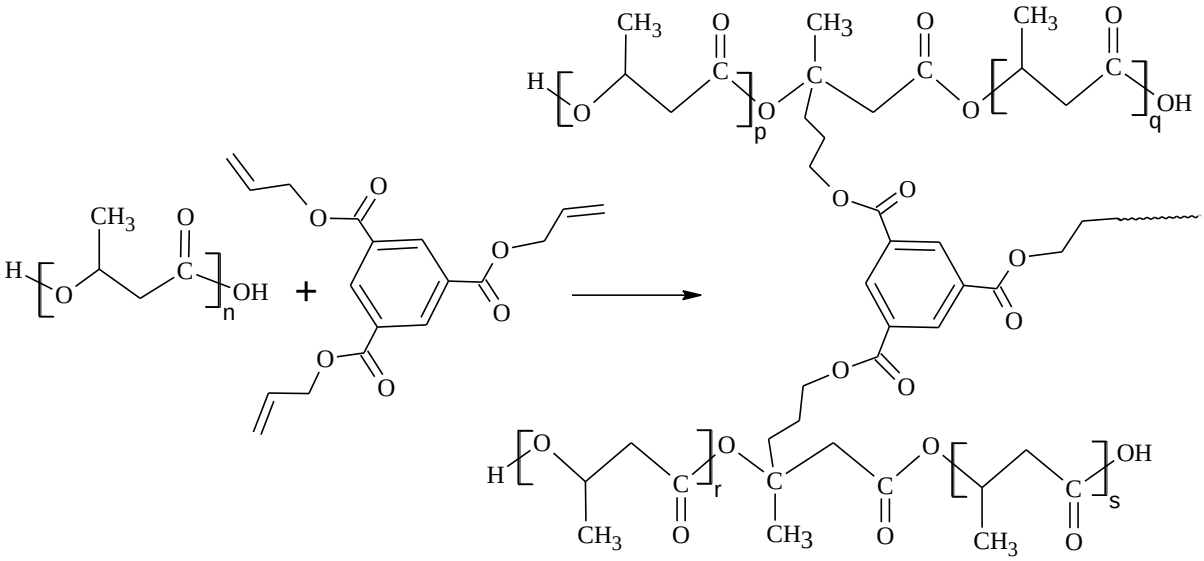

Figure 15 Reaction of PHB with TAM in the presence of free radicals[92]

Apart from radical reactions, the reactive ends present in the original PHB molecule and those generated by the cleavage can be exploited for chain extension or cross-linking of PHB. Neat PHB as a polyester contains hydroxyl and carboxyl chain end. As discussed in chapter 1.4 Thermodegradation of poly[(R)-3-hydroxybutyrate], hydroxyl functional groups enter the condensation reaction with carboxyl groups being consumed in time. On the contrary, carboxyl ends are continuously generated by the *β*-

scission reaction. This opens possibilities for using substances which are reactive towards the carboxyl functional group.

Epoxide group opens one such possibility as a highly reactive specie. Melt reaction between PHB and up to 30% of epoxidized polybutadiene (EPB, degree of epoxidation 43%, Figure 16) has been studied by Choi et al. He described that reaction shown in Figure 16 occurs between these two polymers leading to higher thermal stability of reactive blends against PHB.[93]

Later, H. K. Lee et al. studied the melt reaction of immiscible blends comprising PHB and EPB (degree of epoxidation 50%, Figure 16) of the ratio PHB/EPB from 10/90 to 90/10 via differential scanning calorimetry (DSC). They estimated the heat of the reaction, reaction half-time, $t_{½}$, and other kinetic parameters for all blend compositions and different temperatures. The results indicate that the reactivity of ring-opening reaction in PHB/EPB blends is influenced by the acidity of degraded PHB. Furthermore, it was shown that EPB did not only react with PHB but also increased the degradation rate of PHB as the concentration increased. Therefore, the rate constant for PHB decomposition will always be higher than the rate constant for the carboxylic acid consumption reaction.[94]

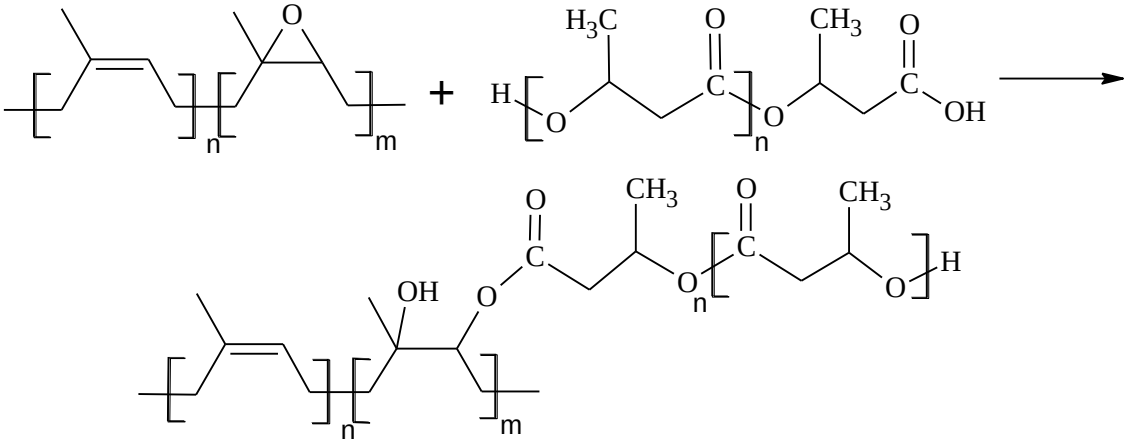

Figure 16 The reaction between PHB and EPB[93]

In addition, another polymer containing epoxy rings capable of reacting with PHB chain ends to form a modified material with higher thermal stability is poly(glycidyl methacrylate) (PGMA). Differential thermal analysis (DTA) confirmed the existence of an exothermic reaction between these two polymers. Cross-linking reaction takes place both before and after severe degradation of PHB due to the enhanced miscibility of PGMA and degraded PHB. Moreover, the temperature of maximum degradation rate was increased by about 24 °C for PGMA/PHB 30/70 compared to pristine PHB.[95]

Another functional group reactive towards PHB is carbodiimide, as investigated by Martelli et al.[96] Commercial polymeric carbodiimide (PCDI) Stabaxol® P200 additive was compounded with PHB in the amount of 1, 3 and 5 wt%. Size exclusion chromatography (SEC) analysis showed an increase in MW, however, a decrease in PHB thermal stability and mechanical properties was observed with the increase of the additive amount. PCDI is supposed to react with the carboxylic end groups of PHB,

forming new *N*-acylurea end groups. The reaction with other PHB molecule on the same mer leads to the formation of acid anhydride and urea as represented in Figure 17.[96]

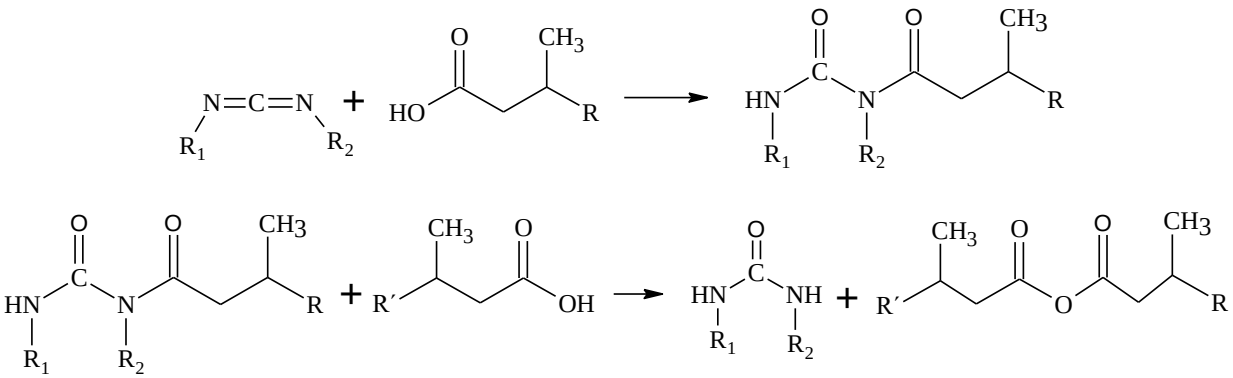

Figure 17 Possible reaction between PHB and PCDI[96]

Arza et al. studied the behaviour of different types of compounds, which should react with carboxyl group, namely bis(3,4-epoxycyclohexylmethyl) adipate (BECMA), 2,2'-bis(2-oxazoline) (BOX), trimethylolpropane tris(2-methyl-1-aziridinepropionate) (PETAP), triphenyl phosphate (TPP), tris(nonylphenyl) phosphate (TNPP), already mentioned PCDI, and poly(methyl metharylate-co-glycidyl methacrylate) (GMA.MMA) towards purified high MW PHB. The structures of individual reagents are depicted in Figure 18.

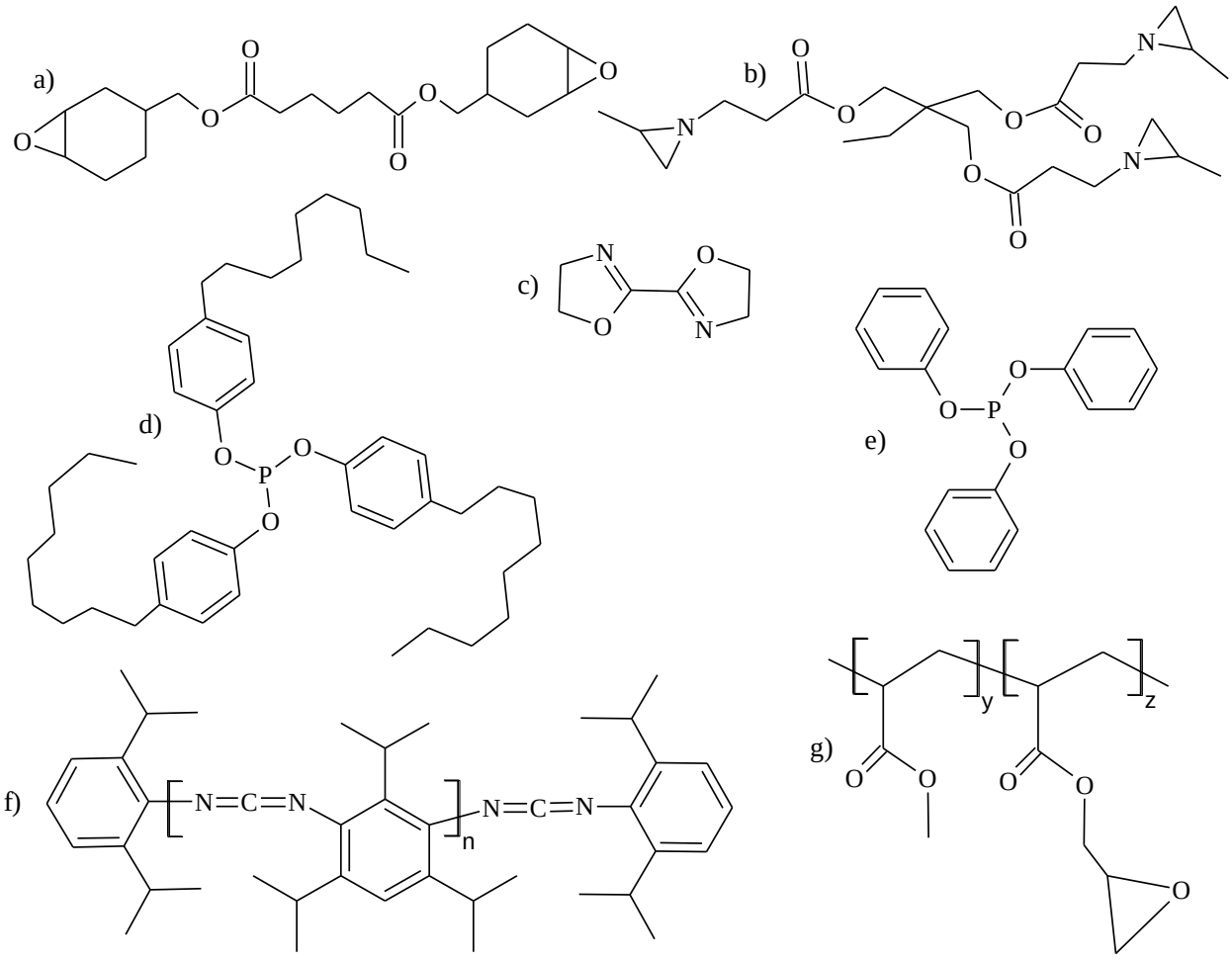

Figure 18 Structures of a) BECMA, b) BOX, c) PETAP, d) TNPP, e) TPP, f) PCDI and g) GMA.MMA[97]

Samples were co-casted from chloroform solution and tested via rheology and SEC. Bi- and tri-functional additives BECMA, BOX and PETAP showed a clear negative effect on the thermal stability of PHB, while triarylphosphites TPP and TNPP showed none. At the same time, minor improvement of PHB melt stability and also the preservation of MW was observed in the case of multifunctional additives PCDI and GMM.MMA as indicated in aforementioned studies.[97]

To conclude, PHB is quite susceptible to modification by radical reactions in the melt with suitable peroxide or a combination of peroxide and co-agent. However, without the use of radicals, PHB seems to be inert to most of the additives. Only EPB and a polymeric variant of carbodiimide and glycidyl methacrylate were successful in the suppression of thermal degradation of PHB. It is important to note that the biodegradability of such modified structures has not been studied although such results would indeed be of great benefit.

1.6. Structure-biodegradability relationship

As already outlined by chapter 1.5.2.1 Graft copolymers from PHB, the biodegradability of PHB can easily be tailored by varying the hydrophilicity of a grafted surface layer of a polymer. Moreover, while studying PHB grafted with AA Wada et al. discovered that grafted samples which lost their biodegradability can regain it after thermal re-moulding. The principle of this is engaging the surface layer of grafted polymer into the bulk and re-access of the degrading microbiota.[98]

However, finding a general relationship between the structure of a material and its biodegradability is difficult and perhaps impossible. In the literature, there are studies aiming to unveil some dependencies. For example, Hongwei et al. extensively studied the quantitative structure biodegradability relationship of low MW aliphatic compounds. They used the analytical hierarchy process, which is a tool for solving multiple-criteria decision problems. This way, they analysed the results from three individual methods of biodegradability evaluation: the biogas production, organic end products present and the activity of microorganisms. Tests themselves were carried out in an inorganic medium incubated with inoculum sludge at pH 7.0 ± 0.2, temperature 35 ± 1 °C for 50 days (ISO 11734). The results showed that the predominant molecular structure descriptors affecting the biodegradability were total energy and molecular diameter of a compound.[99]

In the case of polymers, Commereuc et al. investigated the biodegradability of commercial polyester poly(butylene adipate terephthalate) (PBAT) and synthesised polymers. Synthesised polyesters and copolyesters were based on 1,4-butanediol and three types of dicarboxylic acids: 1,12- dodecanedioic acid (aliphatic), 1,4- cyclohexanedicarboxylic acid (cyclic) and terephtalic acid (aromatic). Similarly to the previous study, an inorganic medium incubated with inoculum from sewage sludge was used. The test was implemented at 30 °C for 19 days, and O_2 consumption and the quantity of CO_2 released were monitored. No biodegradation activity was observed for copolyester containing both aromatic and aliphatic acid, structurally similar PBAT and copolymer prepared from cyclic acid. The sample of purely

aliphatic polyester achieved a mineralization level of 45%, while the copolyester containing both aliphatic and cyclic dicarboxylic acid achieved 63%. However, the authors concluded, that some results may be influenced not only by chemical structure but also by the morphology of individual materials.[100]

The strong influence of supramolecular structure was also described by Kurusu et al. The mechanical properties and biodegradability of 70/30 wt% blend of PHB and poly(ethylene-co-methyl-acrylate-co-glycidyl-methacrylate) (PEMAGMA) were studied before and after thermal annealing. Biodegradation tests were conducted in simulated agricultural soil composed of three equal parts of sand, soil and fertilizer. CO_2 produced was evaluated by respirometry. The results are shown in Figure 19.[101]

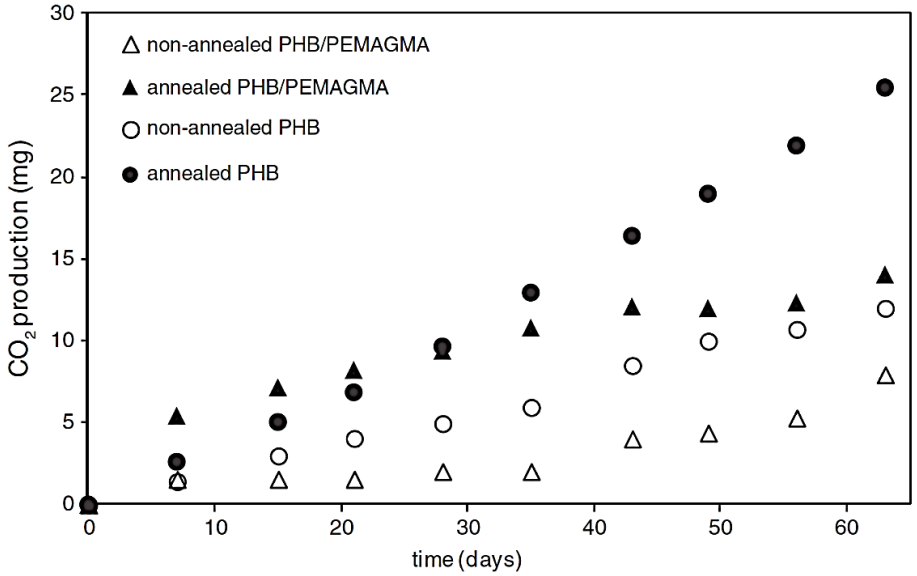

Figure 19 CO_2 evolution during biodegradation of PHB and PHB/ PEMAGMA samples.[101]

Apart from the positive impacts of annealing on the mechanical properties of PHB, which were already described in previous chapters, the change in morphology had a clear effect of enhancing biodegradation. After annealing, the remaining amorphous region has a lower chain density and, therefore, more free volume (voids), which can also contribute to faster biodegradation.[101]

This implies that in order to maintain a biodegradability of material, both chemical structure and morphology changes must be considered.

2. AIMS

The aim of this dissertation is, firstly, to study poly(3-hydroxybutyrate) degradation during processing with respect to the influence of processing parameters, mainly temperature and mechanical stress and to determine the kinetics of the degradation at processing temperature. Secondly, the goal is to find a compound reactive towards the polymer in a way it will compensate for the negative effects of the degradation reaction on the resulting properties. To accomplish this task, poly(3-hydroxybutyrate) will be processed with selected reagents with different functionality and chemical functional groups. The effect of the additives on the molecular weight, the thermal and thermomechanical properties of the material will be analysed. Moreover, infrared spectroscopy will be utilised to observe changes in the polymer structure. The degradation kinetics of poly(3-hydroxybutyrate) in the presence of these compounds will be measured. And thirdly, the influence of performed reactive modifications of poly(-3-hydroxybutyrate) on its biodegradability will be studied.

3. EXPERIMENTAL WORK

3.1. Materials

3.1.1. Poly[(R)-3-hydroxybutyrate]

Poly[(R)-3-hydroxybutyrate] (PHB) with a production name ENMAT batch numbered 2252 was purchased from TianAn Biologic Materials Co., Ltd. in the form of a white powder. Prior to use, the polymer was purified by washing in acetone, filtering and final drying.

The basic material properties of used PHB are listed in Table 2. The information about MW was determined by gel permeation chromatography and thermal properties by differential scanning calorimetry (T_g, T_m, and crystallinity) and thermogravimetry (degradation temperature), the procedures are described in the chapters below.

Table 2 Material properties of used PHB Enmat 2252

Molecular weight		Thermal properties	
Number average MW, M_n (kDa)	150 ± 23	**Glass transition temperature, T_g (°C)**	−0.8 ± 0.2*
Weight average MW, M_w (kDa)	533 ± 56	**Melting temperature, T_m (°C)**	172.8 ± 0.5*
Polydisperzity (-)	3.6 ± 0.5	**Crystallinity (%)**	62.2 ± 0.5*
		Degradation temperature, T_d (°C)	289

* taken from the second heating cycle, average from three measurements.

3.1.2. Isocyanate additives

Isocyanate functional group is highly reactive towards different compounds such as hydroxyls, water, amines, or carboxyls. With carboxyls, in the first step, an anhydride is formed, and in the next step carbon dioxide is released, leaving amide as a final product, as shown schematically in Figure 20.

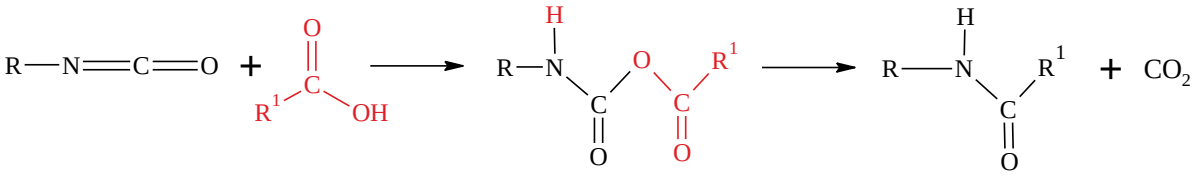

Figure 20 The reaction between isocyanate and carboxyl species

Depending on the functionality of the isocyanate, it can react as a chain extender for PHB connecting two macromolecules or as a branching or crosslinking agent. 1,6-Hexamethylene diisocyanate (abbreviated HMDI) was used as a representative of bi-functional additive. Three-functional isocyanate additive is poly(hexamethylene diisocyanate) (abbreviated PHMDI) with a viscosity at 25 °C 1300–2200 mPa·s, NCO content 22.6-23.7%. Both additives were purchased from ©Merck KGaA (Darmstadt, Germany) and used as received.

PHMDI functionality was calculated from the NCO content given by the producer. The PHMDI contains different oligomers of HMDI, the examples of trimer and pentamer are shown in Figure 21.

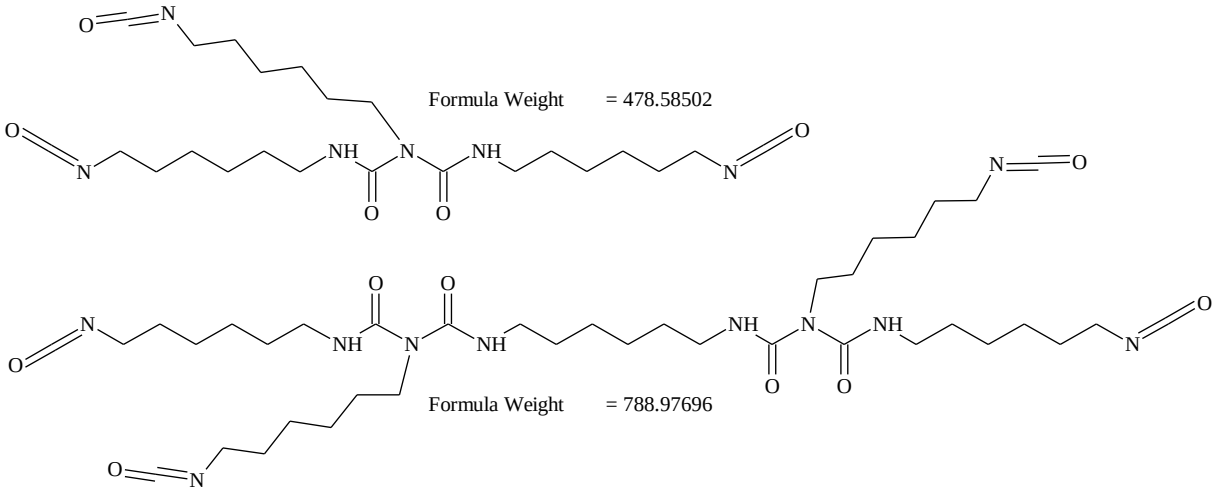

Figure 21 The trimer and pentamer of HMDI

While the trimer has M_{trimer} = 478.59 Da, functionality f_{trimer} = 3 and NCO content = 26.33%, the pentamer has $M_{pentamer}$ = 788.98 Da, functionality $f_{pentamer}$ = 4 and NCO content = 21.29%. Therefore, having an NCO content between 23 and 24%, the average functionality of PHMDI is 3–4. Linear dependency was plotted, where *x* is functionality and *y* is NCO content, with linear regression:

$$\text{NCO } content = -0.050 \cdot f + 0.414. \qquad \text{Eq. 16}$$

The functionality corresponding to the value of NCO content of PHMDI material was calculated using this equation as f_{PHMDI} = 3.61.

3.1.3. Carbodiimide additives

Carbodiimides of different molecular weights and functionalities were kindly provided by Rhein Chemie (Ohio, USA) and RASCHIG GmbH (Germany). Their basic material properties are listed in Table 3.

Table 3 Basic material properties of used carbodiimides

	Stabaxol® 1 LF	**Raschig 9000**
M_n reported (Da)	363	2000–3000
M_n measured by GPC (Da)	-	9500
M_w measured by GPC (Da)	-	21 400
T_m (°C)	40–50	160
Density (g/cm^3)	0.96	-
Min. carbodiimide content (%)	10	16–17
Functionality	2	77

Stabaxol® 1 LF, chemically bis(2,6-diisopropylphenyl)carbodiimide (shown in Figure 22, abbreviated ST-LF), is selected as a bifunctional carbodiimide additive. It is an anti-hydrolysis agent for PU systems, MDI prepolymers, TPU, adhesives, PET and PBT. The recommended dosage is the addition of approx. 1–2 part by weight per 100 parts by weight in PET and PBT during extrusion. It can react with two chain ends of PHB bonding them together, as depicted in Figure 17.

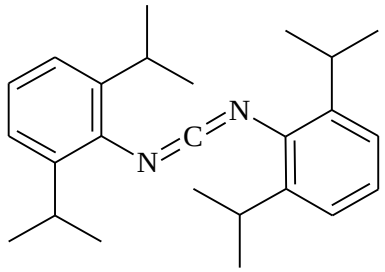

Figure 22 The structure of Stabaxol® 1 LF

Raschig® 9000 (abbreviated R9), is a high-molecular-weight polycarbodiimide used as a water and acid scavenger in polyesters, such as PET. This additive is also reactive towards carboxyl ends, as shown in Figure 17. Because it is a multifunctional additive, PHB carboxyl ends can attach to it along the entire chain lenght, as shown in Figure 23. Both ways, it can act as a chain extender for polyesters, significantly enhancing their melt and other functional properties.

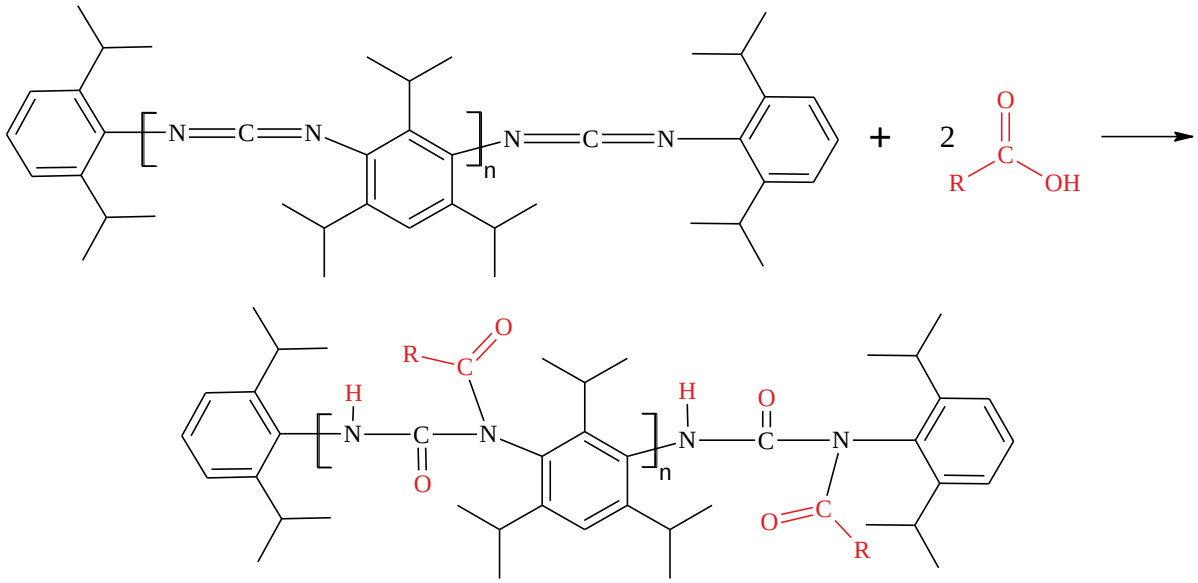

Figure 23 The reaction between polycarbodiimide reagents and carboxyl functional group

The functionality of R9 was calculated from the number average molecular mass obtained from gel permeation chromatography measurement, $M_{n,GPC}$. Each mer of the carbodiimide macromolecule has molecular weight M_{mer} = 242.36 Da, and it consists one N=C=N group with functionality 2. Additionally, each molecule consists of two ends which combined give the structure of the bi-functional additive ST-LF having a molecular weight M_{ends} = 362.55 Da, and functionality 2. Considering this, the functionality of the carbodiimide additives is calculated as follows:

$$f = 2 \cdot \frac{M_{n,GPC} - M_{ends}}{M_{mer}} + 2. \qquad \text{Eq. 17}$$

Which is for R9:

$$f_{R9} = 2 \cdot \frac{M_{n,GPC} - M_{ends}}{M_{mer}} + 2 = 2 \cdot \frac{9534 - 362.55}{242.36} + 2 = 77.7. \qquad \text{Eq. 18}$$

3.1.4. Hydroxy compounds

The hydroxy group reacts with a carboxyl group in a condensation reaction forming an ester bond and releasing water molecule, as depicted in Figure 24. This reaction occurs at the beginning of PHB processing between PHB chain ends until the shortage of OH ends, as described in chapter 1.4 Thermodegradation of poly[(R)-3-hydroxybutyrate]. Therefore, the same reaction could be exploited for chain extending of PHB by external additives.

Diethylene glycol (abbreviated DEG) and glycerol (abbreviated GLYC) were used as low molecular weight additives having the functionality of 2 and 3, respectively. Poly(vinyl alcohol) (abbreviated PVAl) was selected as a multifunctional option.

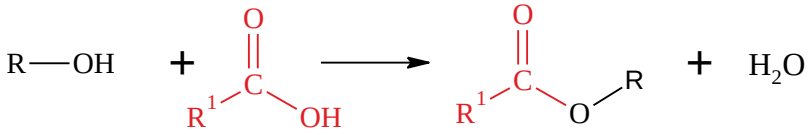

Figure 24 The reaction between hydroxyl and carboxyl species

GLYC was purchased from Fichema (Brno, Czech Republic) and DEG and PVAl Mowiol® 4-88 were purchased from ©Merck KGaA (Darmstadt, Germany), all used as received.

The functionality of PVAl Mowiol® 4-88 (reported M_n = 15500 Da) was calculated from the molecular weight similarly as in the case of polymeric carbodiimide using modified equation Eq. 17. The functionality equals the number average molecular weight minus the MW of chain ends divided by the MW of mer, without the multiplication and addition of 2. For PVAl additive, it is equal to 351.

3.1.5. Epoxy compounds

The epoxy group is generally highly reactive, and in the presence of a carboxyl functional group, it opens and forms *β*-hydroxyester, as shown in Figure 25.

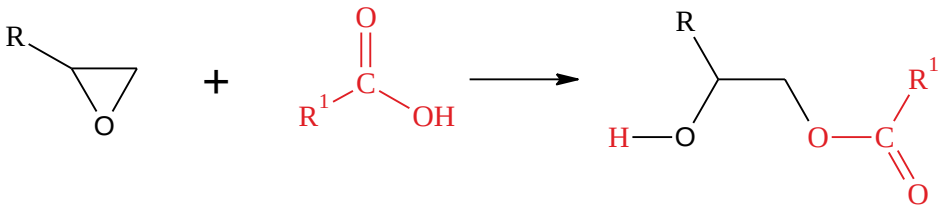

Figure 25 The reaction between epoxy and carboxyl species

As in the previous cases, the functionality of the epoxy compound added to PHB determines the resulting effect on the polymer. Therefore, difunctional, trifunctional and polyfunctional epoxy compounds were used. The first is represented by diglycidyl ether bisphenol A (abbreviated DGE-BPA), which is commonly used for the production of epoxy resin prepolymers. A trifunctional additive is trimethylolpropane triglycidyl ether (abbreviated TMP-TGE), commonly used as crosslinking agent for resins. Both were purchased from ©Merck KGaA (Darmstadt, Germany) and used as received. Multifunctional additive poly(glycidyl methacrylate) (abbreviated PGMA) was synthesised using the procedure described in the chapter below.

3.1.5.1. Poly(glycidyl methacrylate) synthesis

PGMA was synthetized by atom transfer radical polymerization (ATRP) in emulsion according to Haloi et al.[102] The following chemicals were used: glycidyl methacrylate (GMA, CAS 106-91-2), copper bromide 99.999% trace metals basis (CuBr, CAS 7787-70-4), 2,2′-bipyridine (bpy, CAS 366-18-7), methyl 2-bromopropionate (MBrP , CAS 5445-17-0) and Triton™ X-405 70% solution in water (Triton, CAS 9036-19-5); all purchased from ©Merck KGaA (Darmstadt, Germany). All chemicals were used as received.

CuBr was used as catalyst, bpy as ligand and MBrP as initiator. Functionalized polyethylene glycol Triton was used as an emulsifier. Synthesis was carried out in a 3-neck round bottom 250 mL flask under a nitrogen atmosphere and intense mixing (500 RPM). The simple reaction apparatus is shown in Figure 26.

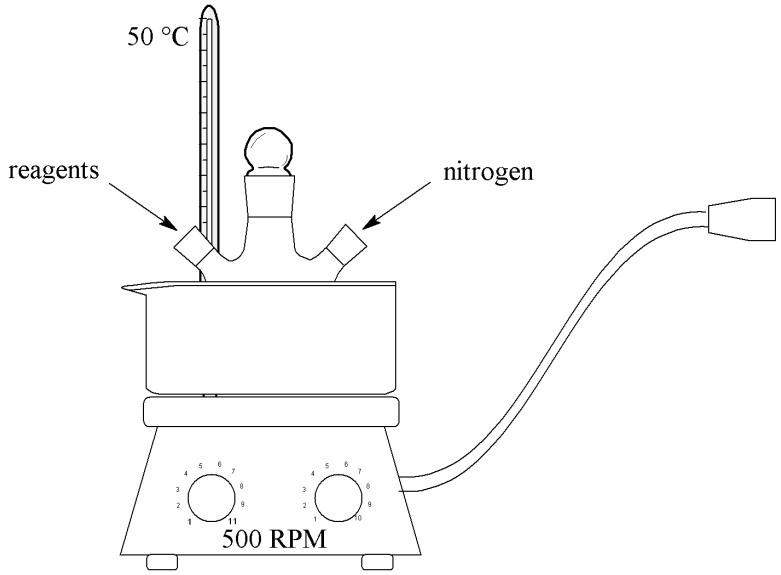

Figure 26 The reaction apparatus for PGMA synthesis

Firstly, CuBr and bpy and secondly, Triton and water were added. Subsequently, GMA was poured into the flask, and the reaction was started by adding the initiator MBrP and putting the system to the water bath tempered at 50 °C. The details of the synthesis conditions of selected PGMA samples are listed in Table 4. The amount of GMA added to the mixture was always 20 g. The weight of the reactants is as follows: 0.13 (0.20) g of CuBr, 0.20 (0.30) g of bpy and 0.13 (0.20) g = 89 (133) μL of MBrP for the ratio GMA/CuBr/Pby/MBrP 150/1/1.5/1 (and for the ratio GMA/CuBr/Pby/MBrP 100/1/1.5/1 in the brackets).

Table 4 Optimisation of PGMA synthesis

	GMA/CuBr/Pby/MBrP	**H_2O (g)**	**Triton (g)**	**Triton (%/GMA)**
PGMA1	150/1/1.5/1	20	3.4	12
PGMA2	150/1/1.5/1	30	5.7	20
PGMA3	150/1/1.5/1	40	4.0	14

The amount of water and emulsifier for the first sample was taken from the article.[102] However, after six minutes, synthetized polymer formed a single bulk, which was stuck to the stirrer and the reaction

was over. Therefore, I prepared two more samples with increased amount of water and surfactant in the system. In both cases, the emulsion was formed and PGMA was successfully synthetized.

3.1.5.2. Poly(glycidyl methacrylate) purification

After the reaction, 60 ml of chloroform was added to the post-reaction mixture and Grahams condenser was connected to the middle neck of the flask. The mixture was heated to the boiling point of chloroform (63 °C) and kept under reflux. After the PGMA dissolved, the mixture was cooled and let to settle. The water and chloroform phases separated, and the upper water part was poured out. The chloroform phase contained obtained PGMA and had a light blue colour given by the oxidised copper. The transition metal compounds of the initialisation system were removed from the product by passing the solution through a 1.5 cm column of neutral alumina. Alumina p. a. (CAS 1344-28-1) was purchased from PENTA s.r.o. (Praha, Czech Republic) and used as received.

The amount of copper after this purification was analysed by inductively coupled plasma atomic emission spectroscopy (ICP-OES). For the measurement, 200 mg of the pure PGMA after purification was decomposed with 5 ml of HNO_3 and 2 ml of H_2O_2 in microwave oven and transferred to 25 ml. The wavelength corresponding to the emission spectrum of copper $\lambda = 324.754$ nm was used for its determination. The amount of copper in the purified polymer was <0.002 mg/g (<2 ppm).

3.1.6. Other chemicals

Chloroform (CAS 67-66-3) stabilized with amylene was purchased from Lach-ner, s.r.o. (Neratovice, Czech Republic) and PENTA s.r.o. (Praha, Czech Republic).

The salts used for the biodegradation tests, NaCl, KCl, $Na_2HPO_4 \cdot 12H_2O$ and KH_2PO_4 were purchased from PENTA s.r.o. (Praha, Czech Republic) and used as received. Lipase type II from porcine pancreas containing 25% of protein was purchased from Merck (Darmstadt, Germany).

3.2. Sample preparation methods

3.2.1. Hot pressing

Controlled degradation of PHB and the preparation of films was performed on QNUBU hydraulic press with maximum pressing force 20 MPa for the area 12×12 cm, thickness range from 0.5 mm to 4 mm, and maximum temperature 200 °C.

For the preparation of samples for controlled degradation, the temperatures above the reported melting point of PHB were used, 180, 185 and 190 °C. Raw PHB in the form of powder was pressed to the form of a 1 mm thin film for 1 and 5 minutes at each of these temperatures.

For the preparation of pre-degraded PHB for solution reaction, 5 g of powder PHB was pressed at 185 °C for 5 min to obtain a 1 mm thin specimen.

3.2.2. Reactions in the melt

A 30 ml internal chamber Brabender laboratory kneader operating at 180–185 °C (oil temperature 200 °C) and 45 RPM was used. The polymer was dried at 60 °C for 2 h before processing. The polymer was fed into the chamber within one minute and was homogenized continuously for 1 min. After that (minute two of the experiment), the reactive agent was added to the mixture, and the kneading continued for additional 3 minutes. Prepared polymer melt was pressed between two metal plates in a laboratory press without additional heating so that after cooling down, the material was in the shape of a 1 mm thin specimen ideal for further handling.

The total sample weight was 25 g of PHB (m_{PHB}) plus the weight of the respective additive. The amount of added reagent was calculated from the number of PHB ends and the functionality of the reagents. PHB molecular weight measured by gel permeation chromatography (chapter 3.4.1 Gel permeation chromatography) is M_{n} = 91 490 Da, and therefore, its substance amount of PHB, n_{PHB}, is:

$$n_{\mathrm{PHB}} = \frac{m_{\mathrm{PHB}}}{\mathrm{M}_{n,\mathrm{PHB}}} = \frac{25}{91490} = 0.273 \text{ mmol.} \qquad \text{Eq. 19}$$

Considering that the polymer is degraded and there is only one reactive group per macromolecule, as one end is carboxyl and the other is crotonyl, the functionality of PHB is f_{PHB} = 1. The functionalities, $f_{reagent}$, of the additives used are organized in Table 5.

Table 5 Additives used for the reactions in the solution and their functionality

	Compound name and functionality			
	Isocyanates	**Carbodiimides**	**Alcohols**	**Epoxy**
Bifunctional	Hexamethylene diisocyanate 2	Stabaxol LF 2	Diethylene glycol 2	Diglycidylether bisphenol A 2
Trifunctional	Poly(hexamethy-lene diisocyanate) 3.6	-	Glycerol 3	Trimethylol-propane triglycidyl ether 3
Polyfunctional	-	Raschig 9000 77.6	poly(vinyl alcohol) 351.2	poly(glycidyl methacrylate) 144.8

The functionality of the additive was taken into consideration when calculating its substance amount. When all PHB ends react with all functional groups of the additive, the molar ratio is:

$$n_{PHB} : n_{reagent} = 1 : \frac{1}{f_{reagent}}, \qquad \text{Eq. 20}$$

where n_{reagent} is the substance amount of the additive.

In the case of an *X*-fold overdose of the reagent, the molar ratio is as follows:

$$n_{PHB} : n_{reagent} = 1 : \frac{X}{f_{reagent}}. \qquad \text{Eq. 21}$$

To give an example, the substance amount of poly(hexamethylene diisocyanate) (MW = 504.57 Da, average functionality 3.6, ρ = 1.12 g·cm^{-3}) for a 10-fold overdose towards PHB is calculated as follows:

$$n_{PHMDI\_10} = n_{PHB} \cdot \frac{X}{f_{reagent}} = 0.273 \cdot \frac{10}{3.63} = 0.753 \text{ mmol;} \quad \text{Eq. 22}$$

and the weight (m_{reagent}) and the volume (V_{reagent}) of the additive for the kneading experiment:

$$m_{reagent} = n_{reagent} \cdot \text{MW}_{reagent} = 0.753 \cdot 504.57 = 380 \text{ mg;} \quad \text{Eq. 23}$$

$$V_{reagent} = \frac{m_{reagent}}{\rho_{reagent}} = \frac{380}{1.12} = 339 \text{ µl.} \quad \text{Eq. 24}$$

In this way, the amounts of reagents for 2-fold, 10-fold, 20-fold, 40-fold and 100-fold overdose were calculated. However, not all the samples could be prepared. In some cases, especially at higher dosages, the release of the reagents after the processing was so intense that these samples were not taken into consideration, and higher amounts were not prepared. The samples, which were successfully kneaded, their abbreviations and the amount of additives (both the weight and weight percentage) are listed in Table 6, Table 7 and Table 8 for bifunctional, trifunctional and polyfunctional additives, respectively.

The used machine allows recording of the time evolution of the torque (M = [N·m]), an indicator of mixture viscosity and a possible reaction, during the whole processing experiment. For presenting the result, parts of these curves from the dosage of the additive to the end of kneading (time 2 to 5 min of the experiment) were used. Relative torque, M_{rel}, towards the torque at 2 minutes of the test, $M_{2\text{ min}}$, was calculated and plotted in order to better compare the effect of different additives and dosages:

$$M_{rel} = \frac{M_t - M_{2\,min}}{M_{2\,min}} \cdot 100\%. \quad \text{Eq. 25}$$

Table 6 Samples with bifunctional additives prepared in the kneader

	Sample name and the amount of the additive			
Overdose	**Hexamethylene diisocyanate**	**Stabaxol® 1 LF**	**Diethylene glycol**	**Diglycidylether bisphenol A**
2-fold	M_HMDI_2	M_ST-LF_2	M_DEG_2	M_DGE-BPA_2
	44 µl	99 mg	26 µl	93 mg
	0.2 wt%	0.4 wt%	0.1 wt%	0.4 wt%
10-fold	M_HMDI_10	M_ST-LF_10	M_DEG_10	M_DGE-BPA_10
	219 µl	495 mg	130 µl	465 mg
	0.9 wt%	1.9 wt%	0.6 wt%	1.8 wt%

Table 7 Samples with trifunctional additives prepared in the kneader

	Sample name and the amount of the additive		
Overdose	**Poly(hexamethylene diisocyanate)**	**Glycerol**	**Trimethylolpropane triglycidyl ether**
2-fold	M_PHMDI_2	M_GLYC_2	M_TMP-TGE_2
	68 µl	13 µl	48 µl
	0.3 wt%	0.1 wt%	0.2 wt%
10-fold	M_PHMDI_10	M_GLYC_10	M_ TMP-TGE_10
	339 µl	67 µl	238 µl
	1.5 wt%	0.3 wt%	1.1 wt%
20-fold	M_PHMDI_20	M_GLYC_20	M_ TMP-TGE_20
	678 µl	133 µl	476 µl
	2.9 wt%	0.7 wt%	2.2 wt%

Table 8 Samples with polyfunctional additives prepared in the kneader

	Sample name and the amount of the additive		
Overdose	**Raschig® 9000**	**Poly(vinyl alcohol)**	**Poly(glycidyl methacrylate)**
2-fold	M_R9_2 67 mg 0.3 wt%	M_PVAl_2 24 mg 0.1 wt%	M_PGMA_2 78 mg 0.3 wt%
10-fold	M_R9_10 335 mg 1.3 wt%	M_PVAl_10 120 mg 0.5 wt%	M_PGMA_10 392 mg 1.5 wt%
20-fold	M_R9_20 671 mg 2.6 wt%	M_PVAl_20 241 mg 1.0 wt%	M_PGMA_20 783 mg 3.0 wt%
40-fold	-	M_PVAl_40 482 mg 1.9 wt%	M_PGMA_40 1 566 mg 5.9 wt%
100-fold	-	M_PVAl_100 1 205 mg 4.6 wt%	M_PGMA_100 3 916 mg 13.5 wt%

3.2.3. Reactions in the solution

The overall aim of the work is to study the reactions of selected additives with PHB in the melt. However, high-temperature processing did not allow preparation of high-dosage samples for most of the additives selected, therefore, the reactions in the solution were performed. In order for the experiments to be as comparable as possible, in other words, to get as close to the conditions of melt reactions as possible, PHB was pre-degraded in the hot press at 185 °C for 5 minutes. These thermal conditions should correspond to the thermal stress the polymer is subjected to during the processing in the kneader.

For the reaction, the polymer (11.76 g) was firstly dissolved in 150 ml of chloroform under reflux (around 63 °C) to form a 5 wt% solution. After complete dissolution, the reactive agent was added, and the mixture was kept under reflux for 6 h. Afterwards, the solution was transferred to a plastic bottle, weighed and stored in the fridge before further analysis. Pre-degraded PHB without any reagent was treated the same way to get a reference sample (marked S_REF).

The amount of the additive was calculated in the same way as for the kneaded samples according to equation Eq. 22. The substance amount for 11.76 g of pre-degraded PHB, n_{PHB}, is equal to 0.129 mmol. All prepared samples, their abbreviations and the amount of additives are listed in *Table 9* for 2-fold molar overdose samples and *Table 10* for 100-fold overdose samples.

In addition, comparison samples were prepared for low molecular weight additives in 100-fold overdose amounts. PHB was dissolved in chloroform and kept under reflux, as already described above. Subsequently, the respective amount of the reagent was added, and the sample viscosity was characterised. Samples were marked with the word “mix” behind the sample name.

Table 9 Samples with 2-fold molar overdose of the additive towards the polymer prepared in the solution

Sample name and the amount of the additive for 2-fold overdose samples				
	Isocyanates	**Carbodiimides**	**Alcohols**	**Epoxy**
Bifunctional	S_HMDI_2 21 µl	S_ST-LF_2 47 mg	S_DEG_2 12 µl	S_DGE-BPA_2 44 mg
Trifunctional	S_PHMDI_2 32 µl	-	S_GLYC_2 6 µl	S_TMP-TGE_2 22 µl
Polyfunctional	-	S_R9_2 32 mg	S_PVAl_2 11 mg	S_PGMA_2 37 mg

Table 10 Samples with 100-fold molar overdose of the additive towards the polymer prepared in the solution

Sample name and the amount of the additive for 100-fold overdose samples				
	Isocyanates	**Carbodiimides**	**Alcohols**	**Epoxy**
Bifunctional	S_HMDI_100 1032 µl	S_ST-LF_100 2330 mg	S_DEG_100 610 µl	S_DGE-BPA_100 2188 mg
Trifunctional	S_PHMDI_100 1595 µl	-	S_GLYC_100 313 µl	S_ TMP-TGE_100 1120 µl
Polyfunctional	-	S_R9_100 1578 mg	S_PVAl_100 567 mg	S_PGMA_100 1842 mg

3.3. *In situ* reactions in the rheometer

Rotational rheometer AR-G2 from TA instrument with the radiation oven was used for the measurements. An Environmental Test Chamber system and parallel plate geometry with a diameter of 25 mm were used for all tests.

3.3.1. Specimen preparation

Specimens for rheology were prepared by pressing PHB Enmat 2252 powder on a laboratory hydraulic press at laboratory temperature. For the reference sample, 1.2 g of polymer powder was weighed and transferred into the mould and pressed with 50 kN of force for 10 s. This way, a rounded specimen of 1 g weight (due to the losses of the mould) with a diameter of 25 mm and constant thickness was obtained. Reactive samples were prepared with the 10-fold molar overdose of the additive for time sweep experiments (Table 11) and with 100-fold molar overdose for frequency sweep tests (Table 12).

Table 11 Samples with 10-fold overdose of the additive for the time sweep test

Sample name and the reagent amount	**Isocyanates**	**Carbodiimides**	**Alcohols**	**Epoxy**
Bifunctional	R_HMDI_10 8.8 µl 0.9 wt%	R_ST-LF_10 19.8 mg 1.9 wt%	R_DEG_10 5.2 µl 0.6 wt%	R_DGE-BPA_10 18.6 mg 1.8 wt%
Trifunctional	R_PHMDI_10 15.2 mg 1.5 wt%		R_GLYC_10 2.7 µl 0.3 wt%	R_ TMP-TGE_10 9.5 µl 1.1 wt%
Polyfunctional		R_R9_10 13.4 mg 1.3 wt%	R_PVAl_10 4.8 mg 0.5 wt%	R_PGMA_10 15.7 mg 1.5 wt%

For 10-fold overdose samples, firstly, 0.6 g of PHB was put into the mould, then the reagent was added, and another 0.6 g of PHB was placed on the top. The layers were pressed with the same force and time as the non-reactive reference. This ensured the encapsulation of the additive in the polymer.

Table 12 Samples with 100-fold overdose of the additive for the frequency sweep test

Sample name and the reagent amount	Isocyanates	Carbodiimides	Alcohols	Epoxy
Bifunctional	R_HMDI_100 88 µl 8.4 wt%	R_ST-LF_100 198.1 mg 16.5 wt%	R_DEG_100 52 µl 5.5 wt%	R_DGE-BPA_100 186.0 mg 15.7 wt%
Trifunctional	R_PHMDI_100 151.9 mg 13.2 wt%		R_GLYC_100 27 µl 3.2 wt%	R_ TMP-TGE_100 95.2 µl 9.9 wt%
Polyfunctional		R_R9_100 134.1 mg 11.8 wt%	R_PVAl_100 48.2 mg 4.6 wt%	R_PGMA_100 156.6 mg 13.5 wt%

For the 100-fold overdose samples, the amount of PHB was weighed so that the total amount of PHB plus the additive was 1.2 g. The additive was added to the powder, and the mixture was homogenized and pressed with 50 kN of force for 10 s, such as for the previous samples.

3.3.2. Time sweep test

Time sweep (TS) of the material was used to monitor the polymer properties over time at a constant frequency, amplitude and temperature, which mimics the traditional processing techniques.

The TS procedure, which was used for the measurements, had three steps:

1. preheating to 185 °C for 1 min with a set of normal force for 1 N,
2. deactivation of normal force control,
3. time sweep at 185 °C for 10 min at 1% amplitude of deformation and 1 Hz frequency.

Preheating was optimized to ensure that the sample was melted and, at the same time, no degradation occurred. Moreover, active control of the normal force in the first step was chosen so that all the samples had the same starting point for the measurement.

A total drop of complex viscosity (from time 0 to 5 min) and the slope of the relative change of the viscosity were evaluated from obtained data.

3.3.3. Multiple frequency sweeps

For 100-fold overdose samples, the scan consisting of four subsequent frequency sweeps (FS) was measured. The test was performed in the linear viscoelastic region (LVR) with a 1% amplitude of deformation. The FS procedure used was as follows:

1. preheating to 185 °C for 1 min with a setting of normal force for 1 N,
2. deactivation of normal force control,
3. FS at 185 °C, 1% amplitude of deformation and frequencies from 0.1 to 50 Hz,

4. conditioning for 5 s,
5. repeating from step 3 for 3 times.

The FS method was selected so that as broad a frequency range as possible within the machine range is covered, and at the same time, the duration of the test was kept as short as possible due to the severe degradation of PHB observed during processing and time sweep. The overall length of this test was 18 minutes.

Obtained data were evaluated according to Harrison and Melik.[53] Complex viscosity as a function of time was plotted for each frequency. Therefore, for each frequency, there were four points corresponding to four FS measured fitted, and these were fitted with a first or second-order fit. From the regression equation, the values of time zero complex viscosity $\eta^*(\omega,t = 0)$, R_{v1} (in the case of first-order fit) and both R_{v1} and R_{v2} (in the case of second-order fit) were obtained for each frequency.

3.4. Samples characterisation methods

3.4.1. Gel permeation chromatography

Molecular weight was determined by gel permeation chromatography (GPC) on Agilent Technologies 1100 Series instrument with PLgel 5 μm mixed C column thermostated to 30 °C with chloroform as the eluent at a flow rate of 1 ml/min. Linear polystyrene standards with narrow distribution were used for calibration (10 points). A refractive index detector was used for the eluent analysis. For each analysis, 5 mg of the sample was weighed and dissolved in 1 ml of solvent. The solution was always filtred using a 0.2 μm PTFE syringe prior to the analysis. All samples to be compared were measured in one run.

3.4.2. Infrared spectroscopy

Fourier transform infrared spectrophotometry (FTIR) measurements were conducted on Bruker Tensor 27 machine in attenuated total reflection mode in spectral area 4000–600 cm^{-1}, with resolution 4 cm^{-1} and number of scans 32. For the samples with hydroxyl and epoxy functional reagents, a diamond crystal was used due to its low refractive index and high hardness. Because diamond has absorbance in the region 2200–1800 cm^{-1}, for the samples with nitrogenous reagents, germanium crystal was used.

3.4.3. Thermal characterisation

3.4.3.1. Differential scanning calorimetry

Measurements were performed on DSC 2500 model from TA Instruments. All samples (10-15 mg) were hermetically sealed in aluminium pans. All measurements were carried under a nitrogen atmosphere. Two heating scans from −30 to 200 °C with a temperature ramp 10 °C/min were measured.

Crystallization temperature was evaluated from the first cooling cycle, as the second one was influenced by the thermal degradation during the measurement. The glass transition and melting temperatures and melting enthalpy were evaluated using TRIOS software from the second heating cycle,

which reflects the sample thermal properties unaffected by its thermal history (cooling, the length of storage etc.).

Crystallinity X_c was calculated from measured data using the following equation:

$$X_c = \frac{\frac{\Delta H_m}{w_{PHB}}}{\Delta H_m^0} \cdot 100\%, \qquad \text{Eq. 26}$$

where ΔH_m and ΔH_m^0 (J/g) are melting enthalpy of the second cycle and theoretical enthalpy of melting of 100% crystalline polymer (146 J/g for PHB[16]) and w_{PHB} is mass fraction of PHB in the sample composed of the polymer and the reagent.

3.4.3.2. Thermogravimetric analysis

Thermogravimetric analysis (TGA) was performed on TGA Q500 machine from TA Instruments. For the basic degradation assessment, the following heating programme was utilized:

1) equilibration at 40 °C,
2) heating to 600 °C at 10 °C/min under a nitrogen atmosphere,
3) 10 minutes at 600 °C in air atmosphere.

In order to characterize the weight loss of the additives at the processing temperature, the method was as follows:

1) equilibration at 40 °C,
2) heating to 185 °C at 50 °C/min under a nitrogen atmosphere,
3) isothermal stay for 5 minutes,
4) heating to 600 °C at 10 °C/min under a nitrogen atmosphere,
5) 10 minutes at 600 °C in air atmosphere.

3.4.4. Viscosimetry

The viscosity of solutions was measured using a Brookfield RVDV-II + PX rotational viscometer with spindle number 3 (the measured viscosities lay at around 10% of its measuring range). The solutions were firstly tempered overnight at laboratory temperature and refilled with chloroform to the weight, which was measured directly after the sample preparation. This prevents the errors in measurement caused by the evaporation of chloroform from the solutions, which changes their concentration. Approximately 150 ml of solution was used for the measurement. The solution temperature was 22 °C.

3.5. Biological properties

Laboratory biodegradability test *in vitro* was performed in order to test whether biodegradability, the key property of PHB, will be remained after processing (and possible chemical modification caused by the additives). In order to have a comparison among all tested additives, the kneaded 10-fold overdose samples, together with the reference PHB sample, were selected for both tests. Tests were conducted on

rounded testing specimens with 6 mm diameter, which were shape cut from the thin pressed discs prepared during kneading experiments.

The biodegradability *in vitro* was performed in two enviroments:

1) in phosphate buffer saline (PBS) with pH 7.4 prepared according to Table 13 in order to study purely abiotic contribution,
2) in PBS with the addition of lipase, a representative of non-specific enzyme capable of degrading PHB. This way, we will study if the addition of selected reagents will block the enzymatic degradation of PHB.

Table 13 PBS composition

Compound	Amount (g)	Molarity (mol/dm^3)
NaCl (MW 58.44 g/mol)	8.0	0.1370
KCl (MW 74.55 g/mol)	0.2	0.0027
$Na_2HPO_4 \cdot 12H_2O$ (MW 358.14 g/mol)	3.6	0.0100
KH_2PO_4 (MW 136.09 g/mol)	0.2	0.0018

The lipase concentration was 10 μg/ml. Considering that the lipase contains 25 wt% of protein an the biodegradation is performed in 20 ml of PBS, 0.8 mg of lipase was added the respective samples.

All measurements were performed in triplicates. The samples were firstly dried at 60 °C for 2 hours and their dry weight at time 0, m_{D0}, was measured. Afterwards, the samples were put in the medium and kept at 37 °C in the incubator with their medium being regularly changed. Three sets of samples were prepared, which were incubated for 30, 60 and 90 days. After this, the samples were dried and analysed. The extent of biodegradation was monitored by measuring their weight, and MW.

4. RESULTS AND DISCUSSION

4.1. Synthetized poly(glycidyl methacrylate)

The structure of purified PGMA samples was checked using FTIR spectroscopy. The representative of the obtained spectrum is in Figure 27. The characteristic peaks of epoxy group are visible at 905 cm^{-1} (stretching of C-O of oxirane ring) and at 843 cm^{-1} (stretching of C-O-C of oxirane group). At 1146 cm^{-1} stretching C-O-C of ethers has a high intensity peak. The peak at 1723 cm^{-1} corresponds to the ester bond present in each PGMA mer, and the peaks around 3000 cm^{-1} to aliphatic C-H and -CH_2 groups.[103] These results show that there is a portion of epoxy groups of glycidyl methacrylate monomer, which was not affected during the polymerization reaction.

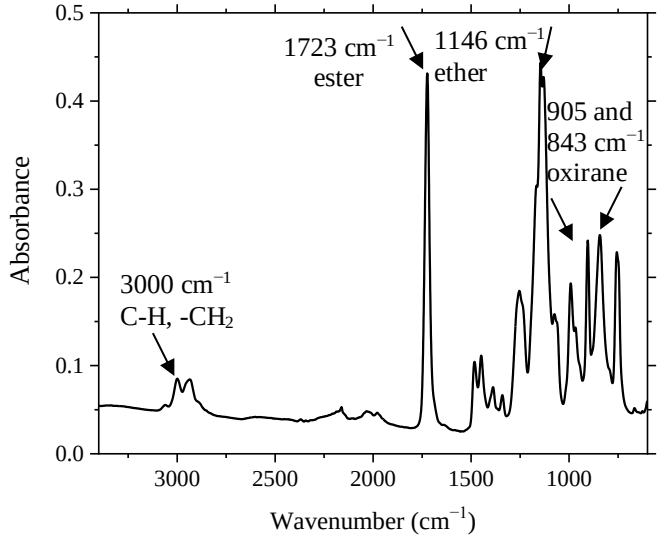

Figure 27 FTIR spectrum of prepared purified PGMA

For the purpose of the work, the most important was to measure the molecular weight of the resulting polymer. The aim was not to achieve as high MW as possible, but rather to produce a short chain length polymer. MWs obtained from GPC are in Table 14. During the preparation of PGMA1 with reactant amounts taken directly from the values reported by Haloi et al., it was clear, that the emulsification system did not function properly.[102] The conditions for a living polymerization were not met, as seen from a really high polydispersity index of this sample. Two samples prepared with a modified amount of water and emulsifier, PGMA2 and PGMA3, showed a stable emulsion. PGMA3 has a lower MW and satisfying polydispersity index and was therefore, chosen for further work.

Table 14 Synthesis conditions and molecular weight of prepared PGMA

	GMA/CuBr/Pby/MBrP	H_2O (g)	Triton (%/GMA)	M_n (kDa)	M_w (kDa)	PDI
PGMA1	150/1/1.5/1	20	12	19.5	107.3	5.52
PGMA2	150/1/1.5/1	30	20	46.9	149.4	3.19
PGMA3	150/1/1.5/1	40	14	20.9	23.1	1.11

The degradation behaviour of selected PGMA3 was studied using TGA with the resulting curve in Figure 28. The polymer starts to decompose at relatively low temperatures compared to PHB. At 185 °C,

which is the temperature of processing used in this work, there is a 4% weight loss. The maximum degradation rate is at 335 °C. Glass transition temperature of PGMA3 is 37.7 °C as measured by DSC.

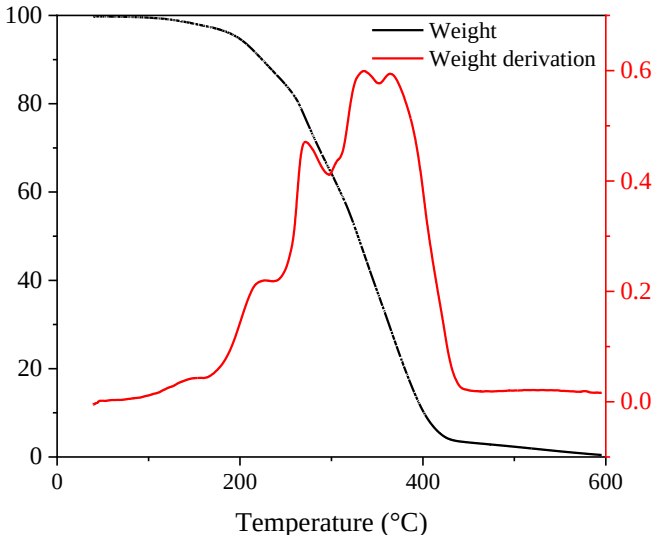

Figure 28 TGA curve of PGMA3

4.2. Thermal degradation of neat poly[(R)-3-hydroxybutyrate]

Wanting to prevent or alter the degradation reaction of PHB in the melt during processing, one must also understand the process of degradation itself. PHB degrades rapidly during the processing, which manifests in the change of colour as can be seen in Figure 29, showing PHB pressed at three temperatures, 180, 185, and 190 °C, for 1 and 5 minutes. Original white powder turns to beige after 1 min at 180 °C and up to orange/brown after 5 min at 190 °C.

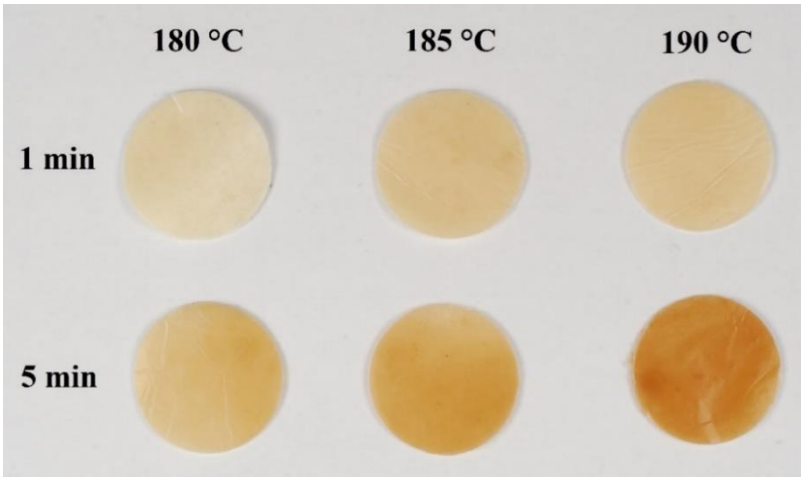

Figure 29 The colour change of PHB after thermal treatment (disc is 25 mm in diameter)

The change in MW of PHB after pressing is in the graphs in Figure 30. As you can see from the figure, M_w drops rapidly after the polymer is melted, from 530 kDa for raw powder PHB to less than 400 kDa for all pressed samples, regardless of the residence time and temperature. After one minute of pressing, the M_w is decreased to approximately 68% of the original value for all temperatures used. After 5 minutes, the M_w drops to 53% of the original value when 180 or 185 °C is used and to 43% when the

temperature 190 °C is used. This agrees well with the data in the literature, where around a 50% drop in MW is reported for the temperature of 190 °C.[47,104]

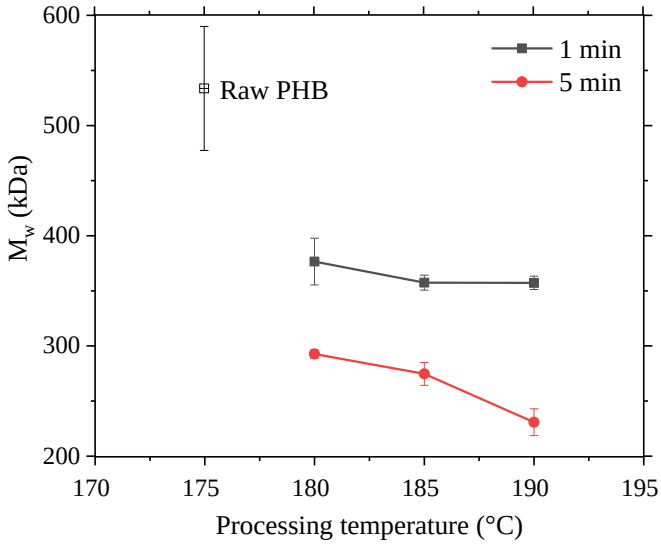

Figure 30 Weight average MW of PHB after being subjected to a thermal stress (n = 3)

While a drop in MW during the processing is profound, the effect on thermal properties is not significant. Generally, all pressed samples had no visible glass transition during the first heating cycle due to the extent to which they crystallized during storage, as described in chapter 1.3 Morphology and ageing of poly[(R)-3-hydroxybutyrate]. Also, the first melting point has a higher peak temperature than the second one, and it is also accompanied by a small shallow endothermic peak starting at 50 °C corresponding to the secondary crystalline fraction. During the second heating cycle, the glass transition is apparent, although still very broad and occasionally still hard to detect. In the temperature range of 50–120 °C, there is a mild cold crystallization directly followed by melting. The melting point of the second heating cycle (not affected by thermal history) for raw PHB is not significantly different from pressed PHB samples despite the drop in MW, as evident from Figure 31.

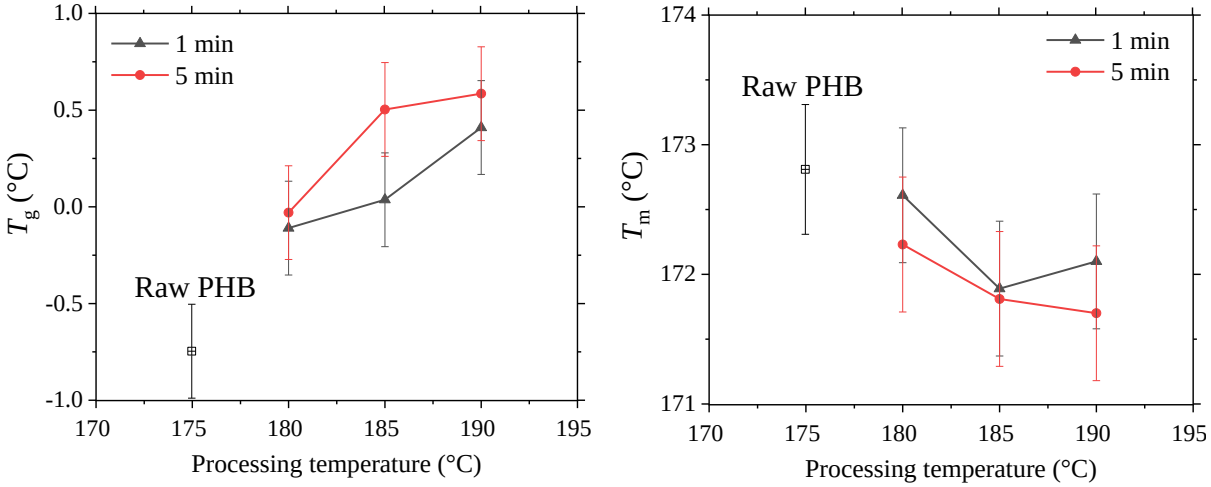

Figure 31 Thermal properties of degraded PHB, second melting point on the left and glass transition temperature on the right (n = 3)

Glass transition temperature of PHB increases by approximately 1 °C with processing, compared to −0.8 °C for raw PHB.

The high shear stress during kneading ensures conditions comparable to large-scale polymer processing techniques, such as extrusion. The effect of shear on PHB is clearly visible in Figure 32, showing the MW of polymer processed in the kneader and in a hydraulic press at 185 °C for 5 minutes, also in comparison to the raw polymer.

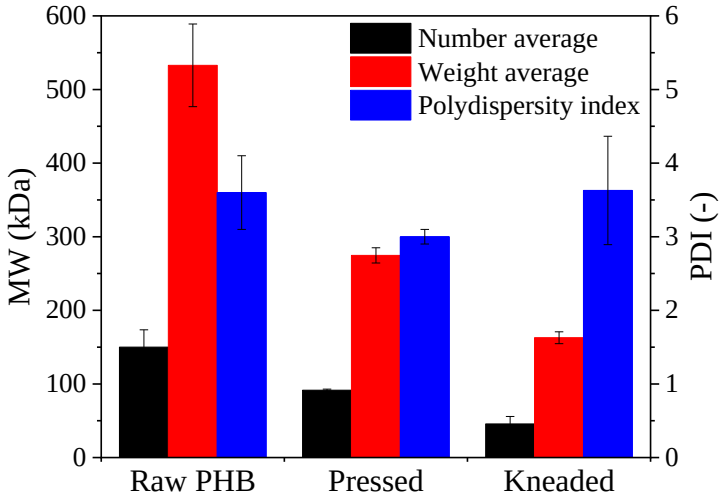

Figure 32 Molecular weight of raw PHB and processed at 185 °C for 5 minutes in the kneader and hydraulic press (n = 3)

Kneaded sample reaches M_n 46 kDa, which corresponds to only 50% of the value of the pressed sample. The M_w of kneaded sample is 163 kDa (59% of the pressed sample). The values corresponding to kneaded PHB were not achieved by pressing even at higher temperature. Similarly to pressing experiments, the changes in thermal properties of kneaded PHB do not match the changes in MW. The glass transition temperature increased further to 2.2 ± 0.7 °C; however it is not a profound change taking into consideration its evaluation difficulties. The average melting point of kneaded sample was around 1 °C higher than neat PHB.

4.3. Melt reactions in the kneader

Laboratory kneaders offer a convenient way of polymer processing due to low requirements for sample amount (likewise the amount of reagents), variable retention time, and the possibility of direct torque monitoring. The general shape of the processing torque record is very similar for all prepared samples PHB + additive. Firstly, the curve consists of the PHB feeding part, which is characterised by an overall steep rise of torque with many spikes. When the polymer is fed into the chamber, the torque starts to decrease slowly as the material melts and starts to degrade. In two minutes' time, the reagent is added, which is in some cases manifested by a small and short drop in the torque, which disappears upon homogenizing of the reagent. Afterwards, the torque decreases steadily due to thermal degradation.

Studied additives had different functional groups reactive towards carboxyls present in the chain end of PHB. They also varied in their functionality. Bifunctional reagents can act as a chain extender in case of the reaction with two carboxyl chain ends so they can compensate the degradation of PHB. The addition of the trifunctional additives can lead to chain extension as well but also to the formation of star-like molecules. Polymeric additives with reactive groups on each monomer can act as a backbone onto which PHB molecules are bonded so that branched structures form. If any of these happens, it should be manifested in the change of viscosity and, therefore, also a processing torque we measure during kneading experiments. The absolute values of processing torque and the slope and extent of its decrease (also possible increase) give us indirect information about the change of melt viscosity over time. It is, therefore, suitable for comparing the differences between the processing of pure PHB versus PHB with studied reagents. In order to easily evaluate the effect of the additives and to neglect torque differences caused by the addition of low viscosity component, the parts of measured curves after reagent feeding were normalized towards the torque at minute 2 to observe a relative change of the torque in %. At the same time, the absolute value of the torque at the end of processing as an indicator of the degradation extent was discussed.

4.3.1. Thermal stability of studied reagents

As indicated in the experimental part, during the kneading of higher dosages of low MW bifunctional additives (especially HMDI and ST-LF), the reagents strongly released from the mixture and therefore, only 2-fold and 10-fold molar overdose samples were prepared for all bifunctional reagents. Figure 33 shows a weight loss of these reagents during heating and subsequent 5 min isothermal stay at 185 °C measured by TGA.

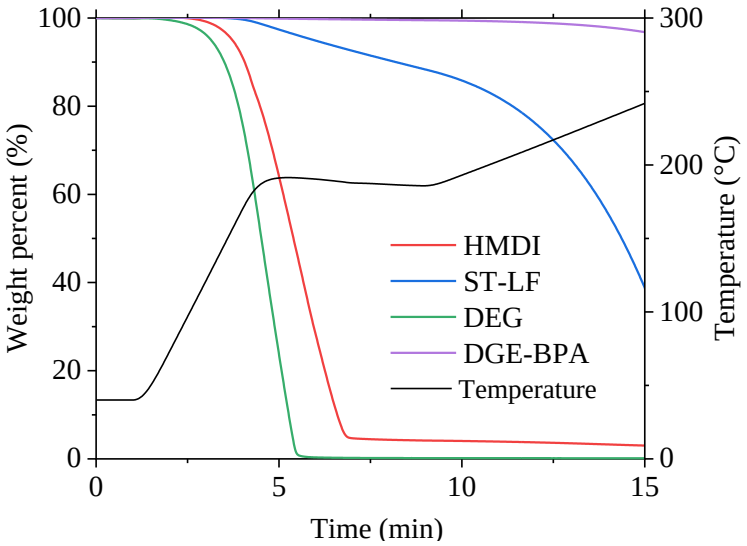

Figure 33 Thermal stability od bifunctional reagents during isothermal stay at 185 °C

Although their boiling point lies above this temperature, both DEG (MW = 106 g·mol^{-1}, boiling point B_p = 245 °C, vapour pressure at 25 °C P_{25} = 0.8 Pa) and HMDI (MW = 168 g·mol^{-1}, B_p = 255 °C, P_{25} = 6.7 Pa) reached a complete weight loss during the first seven minutes of the measurement. During

kneading, the amount of the reagent is higher than during TGA measurement, and rapid mixing into the polymer melt takes place, however a fraction of the reagent may still be lost. As for ST-LF (MW = 363 g·mol^{-1}, B_p = 478 °C, P_{20} = 0.006 Pa), in the end of the isothermal stay 87% of weight is remained. DGE-BPA (MW = 340 g·mol^{-1}, estimated P_{25} = 0.015 mPa) is stable for 5 minutes at 185 °C and also up to 200 °C according to TGA measurement.

The rest of the additives were subjected to TGA measurement as well, with results in Figure 34. Studied trifunctional compounds were more stable than bifunctional ones with the same functional group. The most volatile among them is glycerol (MW = 92 g·mol^{-1}, B_p = 290 °C, P_{25} = 0.4 Pa), with 61% of remained weight in the end of 5 minutes of isothermal stay at 185 °C. Glycerol also has the lowest molecular weight out of all tested regents.

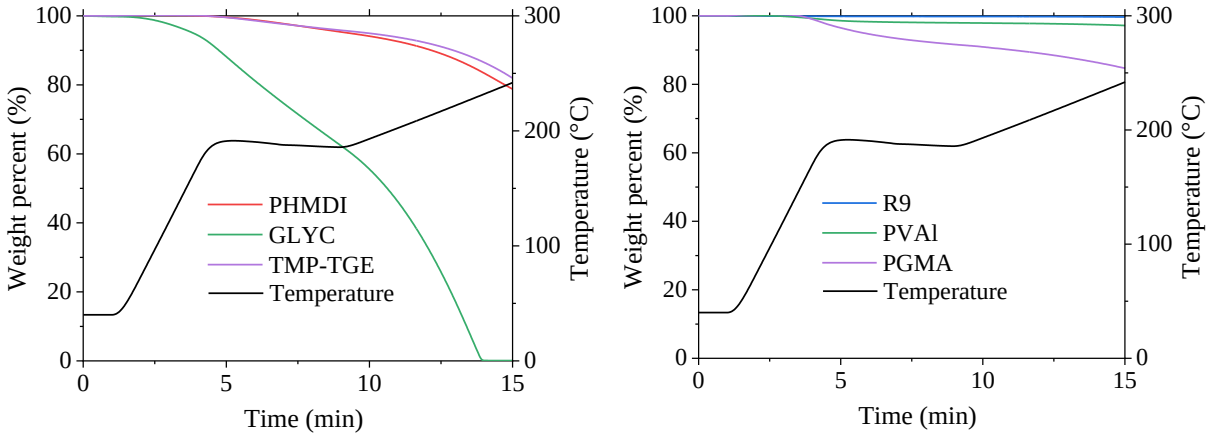

Figure 34 Thermal stability of tri- (on the left) and polyfunctional (on the right) reagents during isothermal stay at 185 °C

PHMDI (MW = 505 g·mol^{-1}, P_{20} = 0.1 Pa) and TMP-TGE (MW = 302 g·mol^{-1}, B_p = 411 °C, P_{25} = 0.01 mPa) both reach around 4–5% of weight loss during the temperature profile matching the processing. Therefore, also 20-fold overdose samples were prepared with trifunctional additives.

For high molecular weight additives, 2-; 10-; 20-; 40- and 100-fold overdose samples were prepared. The polymeric additives were the most stable during the TGA measurements and as well as during the processing therefore, the samples with higher dosages could be prepared. As you can see on the right in Figure 34, R9 and PVAl have negligible weight loss (< 2%) while PGMA has about 8% weight loss during the 5 minutes isothermal stay.

4.3.2. Isocyanates addition

Two isocyanate additives were studied – bifunctional hexamethylene diisocyanate (HMDI) and its trimeric form poly(hexamethylene diisocyanate) (PHMDI). The relative torque during kneading for reference PHB sample, and both isocyanate samples is shown in Figure 35 and further evaluation of the experiment and the results of sample characterization by GPC and DSC are in Table 15.

As for HMDI, the sample with 2-fold molar overdose shows a more profound decrease of relative torque than the reference, and also its final torque after 5 min processing at 185 °C (M_{5m}) is 19% lower,

however within a measurement error. These results are in agreement with the MW results, especially the weight average molecular weight of this sample, which is significantly lower than the reference (10% decrease). Moreover, the melting temperature of M_HMDI_2 is −1.3 °C lower than for the reference.

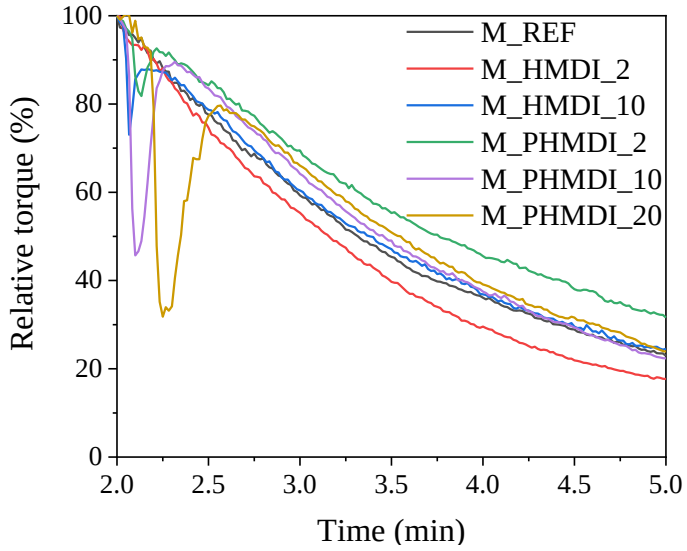

Figure 35 Relative torque during kneading of PHB after the addition of isocyanate additives

On the other hand, the sample with a higher dosage of HMDI (10-fold overdose, 0.9 wt.%) exhibits a similar course of the curve as the reference PHB sample, but its absolute torque at the end is 29% higher than neat PHB. At the same time, the number average MW increased by 59% and the weight average by 13% compared to the kneaded PHB. Also, the melting temperature of this sample is slightly higher compared to the reference.

The addition of HMDI led to a significant increase in T_g for both samples. Changes can also be observed in these samples' crystallization and melting behaviour, as shown in the DSC curves in Figure 36.

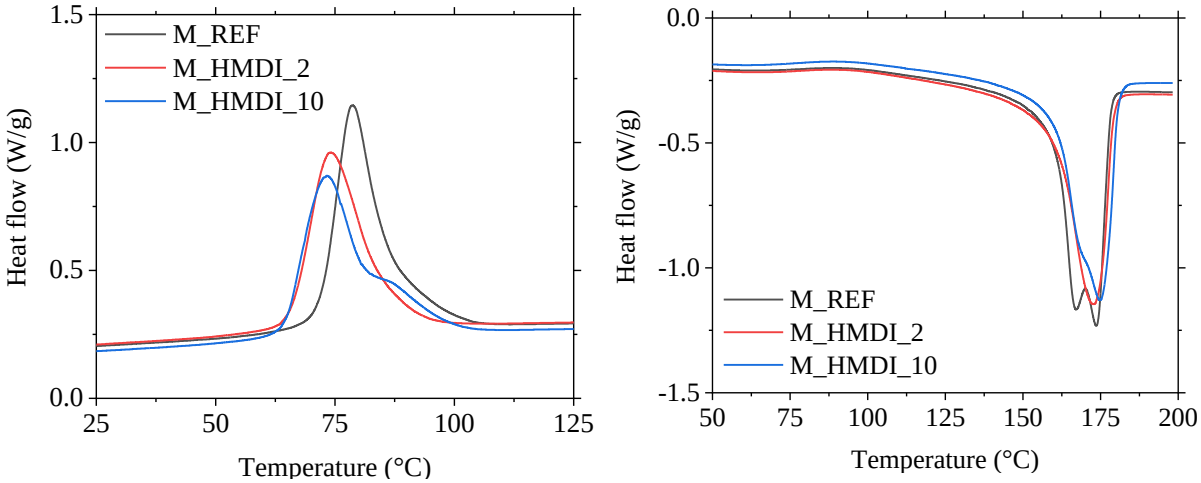

Figure 36 Crystallization (on the left) and corresponding melting (on the right) of HMDI samples and the reference (exo up)

Both HMDI samples have lower crystallization temperatures that reference PHB. There is a shoulder on the M_HMDI_10 crystallization peak, which is reflected in the shape of the melting peak as well.

This indicates the existence of a two-phase crystalline structure. The melting behaviour of both reacted samples is different from that of neat PHB. Due to the recrystallization, PHB exhibits a melting double peak, with the first peak temperature around 167 °C and the second one at 174 °C during the second heating cycle. HMDI addition in both amounts has a single melting peak with peak temperatures closer to the higher temperature of the neat PHB double peak. Therefore, the crystallinity decreases by a few percent as well.

Table 15 The results of kneading experiment, GPC and DSC analysis for neat PHB expressed as mean value ± standard deviation from 5 measurements and for kneaded samples with isocyanate additives expressed as the change of mean values (values differing for more than 2σ are underlined)

	Kneading	**GPC results**		**DSC 2nd cycle**			
Sample name and reagent amount	M_{5m} **(mN·m)**	M_n **(kDa)**	M_w **(kDa)**	T_g **(°C)**	T_m **(°C)**	X_c **(%)**	T_c **(°C)**
REF	1720 ± 160	46 ± 10	163 ± 8	2.2 ± 0.7	173.9 ± 0.3	59.8 ± 0.3	78.0 ± 1.6
	ΔM_{5m} **(mN·m)**	ΔM_n **(kDa)**	ΔM_w **(kDa)**	ΔT_g **(°C)**	ΔT_m **(°C)**	ΔX_c **(%)**	ΔT_c **(°C)**
M_HMDI_2 0.2 wt%	−240	−5	−17	+3.2	−1.3	−5.0	−3.8
M_HMDI_ 10 0.9 wt%	+624	+27	+21	+2.5	+0.7	−3.3	−4.4
M_PHMDI_2 0.3 wt%	+1208	+3	+31	−1.0	+0.9	+0.3	−12.4
M_PHMDI_10 1.5 wt%	+315	+21	+17	+0.3	+1.1	−6.4	−9.6
M_PHMDI_20 2.9 wt%	+644	+21	+16	+1.2	+1.4	−2.1	−9.1

Three samples were prepared with the second isocyanate compound, poly(hexamethylene diisocyanate), PHMDI, from the addition of 0.3 wt% (2-fold overdose) up to 2.9 wt% (20-fold overdose). The kneading curves of these samples and the results of performed analyses are in Figure 35 and Table 15, respectively.

The sample with a 2-fold overdose of PHMDI has 61% higher torque at 5 min than PHB, and the slope of torque change is less steep than the reference during the whole kneading. In addition, M_PHMDI_2 has a 19% increase in weight average MW and a small increase in T_m as well, which makes it the most effective out of isocyanate samples. Higher amounts of the additive than 0.3 wt% did not show any further increase in studied characteristics compared to the sample with a 2-fold overdose of PHMDI.

The sample M_PHMDI_10 had final torque comparable to the reference within the method error. Nevertheless, it reached a significant increase in MW, 45% in M_n and 10% in M_w. Its melting temperature is higher than the reference as well. The sample with a 20-fold overdose of PHMDI reached a 38% increase in the torque after 5 min of processing, its weight average MW is unchanged within the measurement error. Both M_PHMDI_10 and M_PHMDI_20 also showed an increase in the melting

temperature, and their relative torque during kneading exceeded that of the reference up to minute 4 of the processing.

Glass transition temperature shifts slightly to higher temperatures with reagent addition but within the estimated error of the measurement. DSC curves showing the crystallization and melting of the reference and three PHMDI samples are in Figure 37.

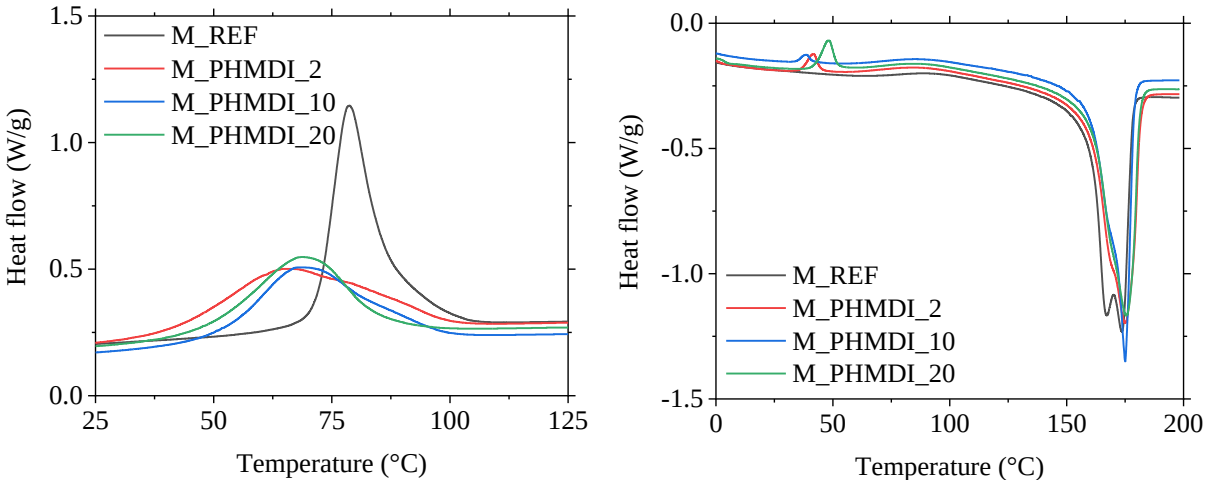

Figure 37 Crystallization (on the left) and corresponding melting (on the right) of PHMDI samples and the reference (exo up)

It is visible that the crystallization ability of PHB is profoundly hindered by PHMDI addition. The crystallization peak is broader, and its maximum is shifted to lower temperatures by 9–12 °C. Moreover, all samples with PHMDI have a small peak of cold crystallization around 50 °C. This may be caused by the low nucleation activity of PHB ends onto which the reagent is attached. The crystallinity is decreased for the samples with 10- and 20- fold overdose. Melting behaviour shows a similar trend to HMDI, neat PHB double peak is changed to a single peak with low temperature shoulder.

4.3.3. Carbodiimides addition

Additives with carbodiimide functional group with two functionalities were studied – bifunctional bis(2,6-diisopropylphenyl)carbodiimide, Stabaxol® 1 LF (ST-LF), and its polymeric form Raschig® 9000 (R9) with around 40 monomers which each can react with two carboxyl PHB ends. The change of relative torque during kneading for PHB reference, and the samples kneaded with ST-LF and R9 addition is shown in Figure 38 and further evaluation of the experiment and the results of sample characterization by GPC and DSC are in Table 16.

The sample with a 2-fold overdose of ST-LF showed a significantly steeper decrease of torque during kneading and reached 31% lower final torque than kneaded PHB, which is the lowest value measured among all tested reagents and amounts. In other measured characteristics, the sample did not differ from the reference significantly. On the contrary, M_ST-LF_10 has 36% higher torque at the end of the test than the reference sample despite the 1.9 wt% addition of low MW reagent. The curve of relative torque for this sample lies above the reference during the whole experiment. The observed positive effect on

the melt viscosity is in agreement with GPC results. Compared to the reference, the increase is 76% and 16% in M_n and M_w, respectively. Measured M_n is the highest measured value from kneaded samples. The glass transition temperature is increased by around 2 °C for this sample, while the melting temperature remains unchanged.

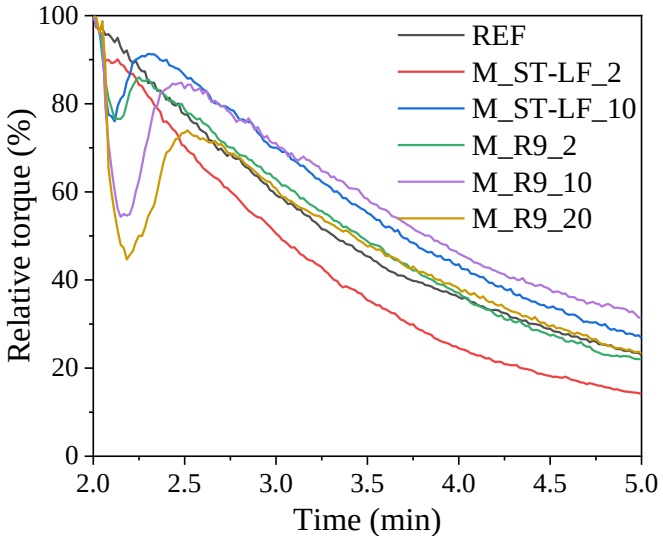

Figure 38 Relative torque during kneading of PHB after the addition of carbodiimide additives

As can be seen in Figure 39, the shape of the crystallization peak for the sample M_ST-LF_2 is identical to that of neat PHB and shifts to lower temperatures for the M_ST-LF-10 sample. With the reagent addition, PHB melting double peak continuously diminishes to a single peak with a small shoulder, as observed for isocyanate-additivated samples.

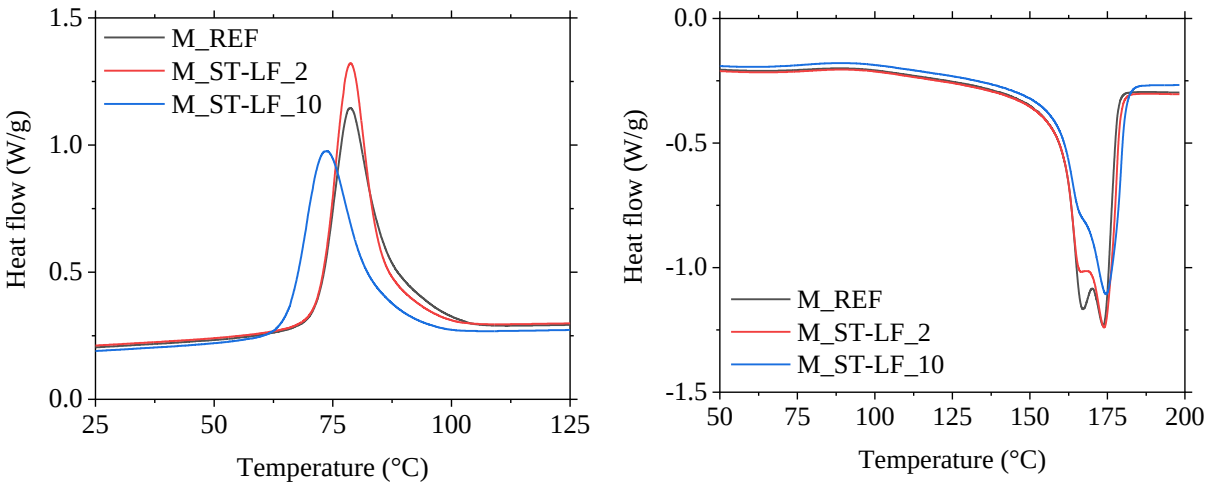

Figure 39 Crystallization (on the left) and corresponding melting (on the right) of ST-LF samples and the reference (exo up)

The addition of polymeric carbodiimide in the 2-fold overdose amount had a negligible effect on studied characteristics, such as in the case of its bifunctional version. Raschig showed the highest impact in the 10-fold overdose (1.3 wt%), reaching 72% higher final torque. The effect on molecular weight is apparent only for M_n though, the change of M_w is positive but within an error. Further increase in the additive amount in the blend, to 2.6 wt%, had an ambiguous effect. The relative decrease of torque of M_R9_20 copied that of the reference PHB sample and ended with a 23% higher value at the end of

processing. The number average MW decreased substantially by 48% while the weight average increased by 14%, which is the highest value out of carbodiimide-additivated samples. At the same time, the glass transition and the melting temperatures decreased.

Table 16 The results of kneading experiment, GPC and DSC analysis for neat PHB expressed as mean value ± standard deviation from 5 measurements and for kneaded samples with carbodiimide additives expressed as the change of mean values (values differing for more than 2σ are underlined)

	Kneading	**GPC results**		**DSC 2nd cycle**			
Sample name and reagent amount	M_{5m} **(mN·m)**	M_n **(kDa)**	M_w **(kDa)**	T_g **(°C)**	T_m **(°C)**	X_c **(%)**	T_c **(°C)**
REF	1720 ± 160	46 ± 10	163 ± 8	2.2 ± 0.7	173.9 ± 0.3	59.8 ± 0.3	78.0 ± 1.6
	ΔM_{5m} **(mN·m)**	ΔM_n **(kDa)**	ΔM_w **(kDa)**	ΔT_g **(°C)**	ΔT_m **(°C)**	ΔX_c **(%)**	ΔT_c **(°C)**
M_ST−LF_2 0.4 wt%	−539	−6	−5	+0.8	+0.0	−0.3	+0.9
M_ST−LF_10 1.9 wt%	+766	+36	+25	+1.9	+0.5	−3.0	−3.7
M_R9_2 0.3 wt%	+217	+18	−14	−1.1	+0.3	−2.6	−2.8
M_R9_10 1.3 wt%	+1232	+28	+13	+1.0	−0.2	−4.7	−5.7
M_R9_20 2.6 wt%	+389	−22	+22	−1.9	−0.6	−3.4	−7.9

More detailed information about the change in thermal properties is gained from the curves in Figure 40. Raschig 9000, with increasing addition, gradually slowers the PHB crystallization process, shifting crystallization temperature to lower temperatures and broadening the peak. There is a mild cold crystallization for all PHB samples just before the melting. It is interesting to note that the sample with the highest amount of R9 exhibits a small cold crystallization peak with a maximum of around 54 °C and enthalpy of 1 J/g in addition to that. The change in the melting behaviour is consistent with what we have observed with the previous reagents. PHB double melting peak disappears with the increment of the additive to one single peak.

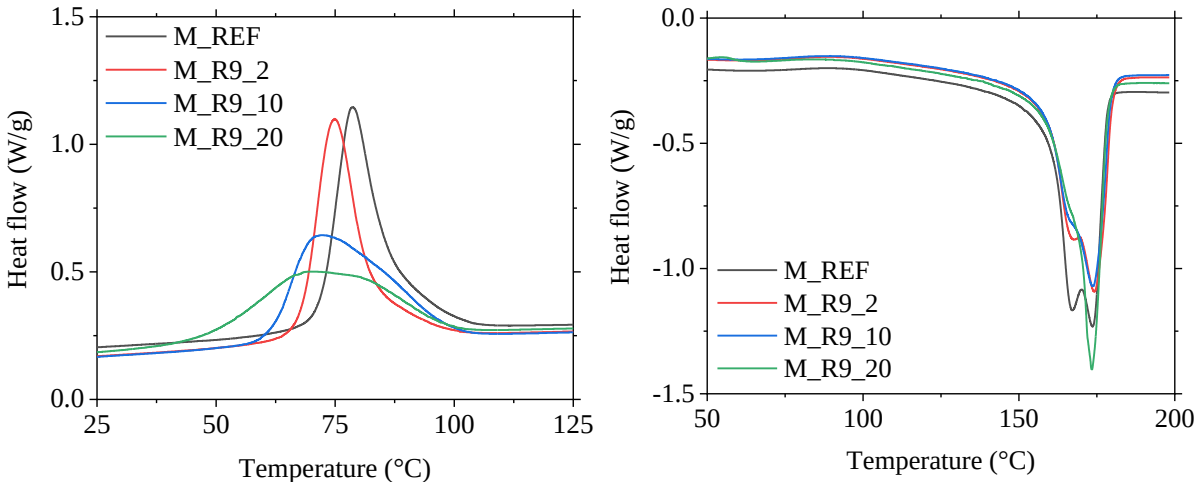

Figure 40 Crystallization (on the left) and corresponding melting (on the right) of R9 samples and the reference

4.3.4. Hydroxy compounds addition

Tested compounds with hydroxyl functional groups were:

- bifunctional diethylene glycol (DEG),
- trifunctional glycerol (GLYC),
- poly(vinyl alcohol) Mowiol® 4-88 with approximately 350 functional monomers (PVAl).

The graphs of relative torque change during the kneading of neat PHB and PHB with hydroxyl reagents are in Figure 41, and all results are in Table 17, such as in previous chapters.

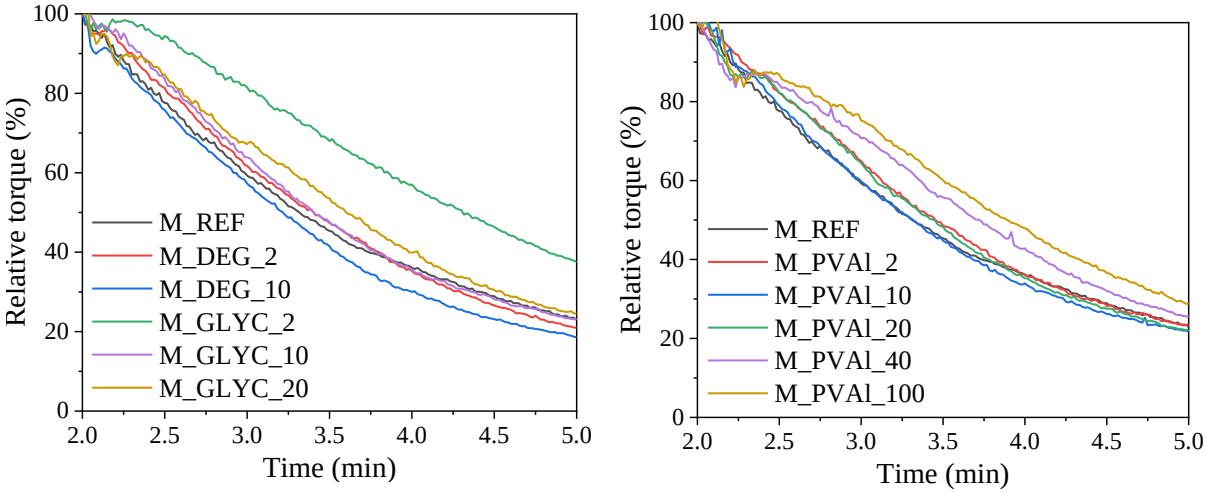

Figure 41 Relative torque during kneading of PHB after the addition of bifunctional alcohol DEG and trifunctional GLYC (on the left) and poly(vinyl alcohol) (on the right)

As far as DEG is concerned, the relative torque during processing lies close to the reference for both tested amounts. The final torque value is comparable to neat PHB within the measurement error. Likewise, the shift in molecular weight is inconclusive. The change in crystallinity and temperature of crystallization is also less meaningful than for the rest of the additivated samples.

On the contrary, the sample with a 2-fold overdose of glycerol (only 0.1 wt%) had the highest torque at the end of the test of all samples, reaching more than two times higher value than the reference (139%). Correspondingly, it had the highest weight average MW obtained, 234 kDa, 44% higher than the reference processed at the same conditions. The melting temperature is among the highest measured for studied PHB samples. Other thermal characteristics remained untouched. However, a further increase in glycerol addition was counterproductive. Both M_GLYC_10 and M_GLYC_20 have higher final torque than the reference, but their curves of the relative decrease of the torque resemble that of the reference. Also, their measured molecular weight is comparable to neat PHB except for a 61% increase in M_n for M_GLYC_20.

Thermograms of kneaded PHB and samples with added glycerol are in Figure 42. The samples with 2- and 20-fold overdose have similar crystallization and melting peaks, the former being shifted to lower temperatures and the latter having already familiar single peak with a low-temperature shoulder. The sample M_GLYC_10 stands out, as its crystallization temperature is higher than the reference T_c. Its

melting peak has similar a shape as the reference, however the first of the double peak is more prominent and therefore, the evaluated melting temperature in Table 17 is the lowest measured.

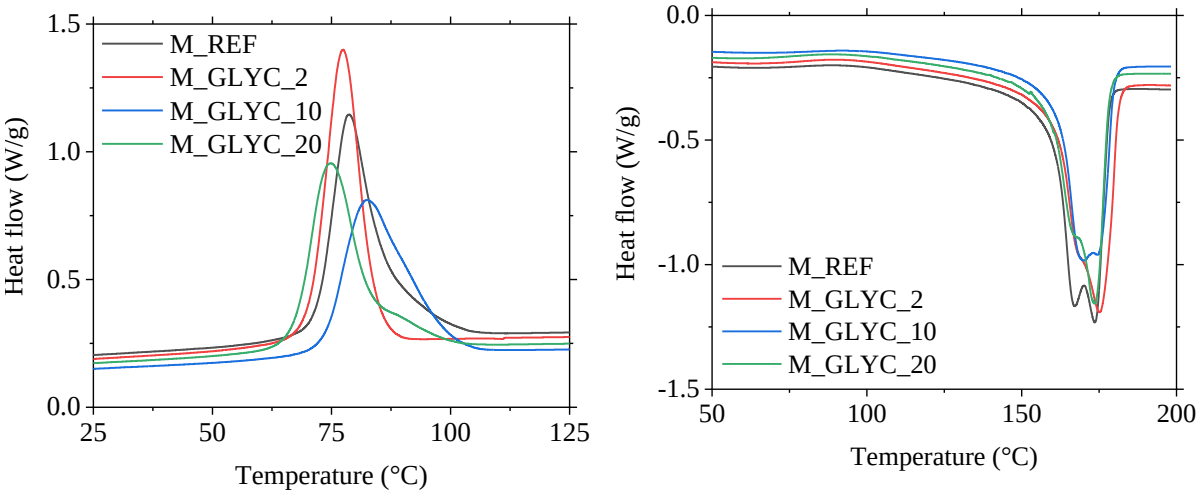

Figure 42 Crystallization (on the left) and corresponding melting (on the right) of glycerol additivated samples and the reference (exo up)

Table 17 The results of kneading experiment, GPC and DSC analysis for neat PHB expressed as mean value ± standard deviation from 5 measurements and for kneaded samples with hydroxy additives expressed as the change of mean values (values differing for more than 2σ are underlined)

	Kneading	**GPC results**		**DSC 2nd cycle**			
Sample name and reagent amount	M_{5m} **(mN·m)**	M_n **(kDa)**	M_w **(kDa)**	T_g **(°C)**	T_m **(°C)**	X_c **(%)**	T_c **(°C)**
REF	1720 ± 160	46 ± 10	163 ± 8	2.2 ± 0.7	173.9 ± 0.3	59.8 ± 0.3	78.0 ± 1.6
	ΔM_{5m} **(mN·m)**	ΔM_n **(kDa)**	ΔM_w **(kDa)**	ΔT_g **(°C)**	ΔT_m **(°C)**	ΔX_c **(%)**	ΔT_c **(°C)**
M_DEG_2 0.4 wt%	+295	+6	+10	+1.2	+1.0	−2.6	−0.2
M_DEG_ 10 1.9 wt%	−166	+19	−3	−0.7	+0.4	−2.3	−0.2
M_GLYC_2 0.3 wt%	+2385	+7	+71	+0.3	+1.2	−1.0	−0.4
M_GLYC_10 1.3 wt%	+389	+19	+7	+0.1	−3.8	−6.9	4.6
M_GLYC_20 2.6 wt%	+545	+30	+10	−0.6	−0.5	−5.2	−2.8
M_PVAl_2 0.1 wt%	+555	+19	−9	−1.7	+0.5	−3.4	−0.9
M_PVAl_10 0.5 wt%	+305	+23	+26	−2.4	+0.2	−2.6	0.8
M_PVAl_20 1.0 wt%	+374	+9	+31	−1.5	+0.0	−4.3	5.1
M_PVAl_40 1.9 wt%	+761	+26	+35	−2.5	−0.1	−3.8	−5.1
M_PVAl_100 4.6 wt%	+1120	+26	+24	−1.3	−0.9	−3.2	−15.4

As can be seen from the relative torque evolution in Figure 41 on the right and also on the evaluation in the table above, there is a positive influence of the increment of poly(vinyl alcohol) in PHB on studied characteristics. PVAl addition led to the increase of 5 min torque for all tested dosages. Moreover, the values have a linear trend of -the higher the dosage, the higher the final torque- with the exception of the 2-fold overdose sample. The most increased final torque, 65% higher than neat PHB, was achieved for the sample with 100-fold overdose, which contained 4.6 wt% of PVAl. The relative torque evolution is also the most promising for this sample. However, the molecular weight increase was more profound for the M_PVAl_10, M_PVAl_20 and M_PVAl_40 samples, reaching 16, 19 and 21% higher M_w than the reference, respectively. For all PVAl samples, the glass transition temperature decreased slightly, and the crystallinity dropped by 3–4%.

Figure 43 shows the thermal properties of the samples with PVAl addition compared to the reference in more detail. Firstly, the crystallization temperature increases with the addition of PVAl and reaches the maximum for the sample M_PVAl_20. With further addition, the crystallization of PHB is impaired, and the T_c drops reaching a minimal temperature observed among all samples, 62.5 °C for M_PVAl_100. The melting point of this sample is decreased consequently as well. The melting follows the already observed trend, narrowing the peak with the addition of the reagent. Due to PVAl crystallization, the effect on crystallinity cannot be evaluated.

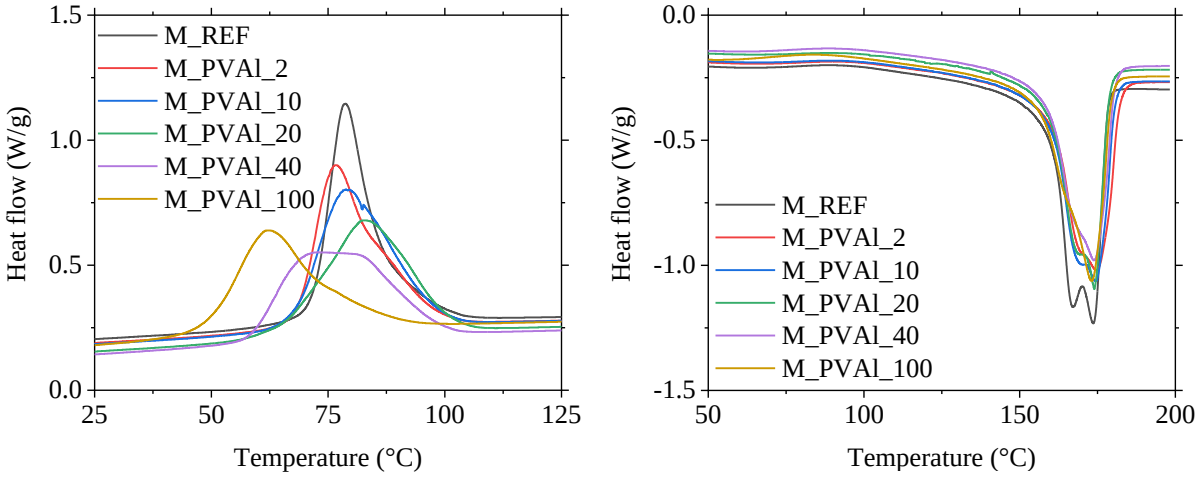

Figure 43 Crystallization (on the left) and corresponding melting (on the right) of PVAl samples and the reference (exo up)

4.3.5. Epoxy compounds addition

Last but not least are the additives with the highly reactive epoxy groups:

- bifunctional diglycidyl ether of bisphenol A (DGE-BPA),
- trifunctional trimethylolpropane triglycidyl ether (TMP-TGE),
- synthesised poly(glycidyl methacrylate) with average functionality of 157 (PGMA).

The change of relative torque during kneading for PHB reference and the samples with the addition of these compounds is in Figure 44 in two separate graphs. The rest of the results of sample characterization by GPC and DSC is in Table 18.

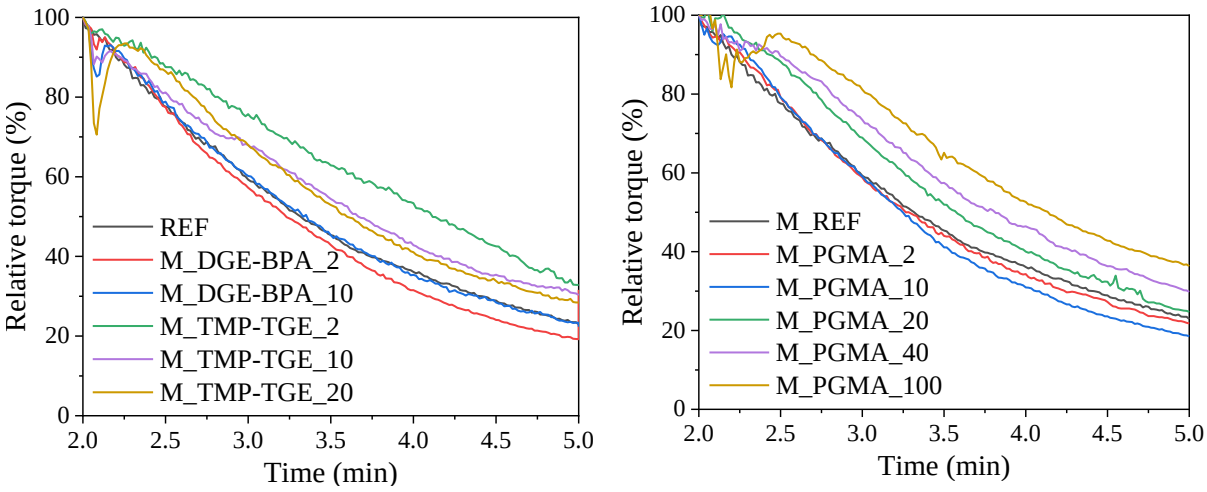

Figure 44 Relative torque during kneading of PHB after the addition of DGE−BPA and TMP-TGE (on the left) and poly(glycidyl methacrylate) (on the right)

Similarly to other bifunctional reagents, the addition of DGE-BPA in the 2-fold overdose amount (0.4 wt%) did not cause any convincing changes in PHB's relative torque, the absolute value of processing torque after 5 min at 185 °C, MW or thermal properties, except for a minor drop in crystallinity. The sample M_DGE-BPA_10 has an identical slope of relative torque decline as the reference, notwithstanding it reached 22% higher torque at the end of the test. Together with that, the molecular weight of PHB increased by 65% for M_n and 16% for M_w.

In Figure 45, there are the crystallization and melting curves of the reference and the samples with DGE-BPA. The crystallization onset of cM_DGE-BPA_2 is higher than for the reference, although the maximum temperature is unchanged. The melting shows a recrystallization double peak similar to neat PHB. The sample M_DGE-BPA_10 exhibits lower T_c and a typical melting peak with a shoulder.

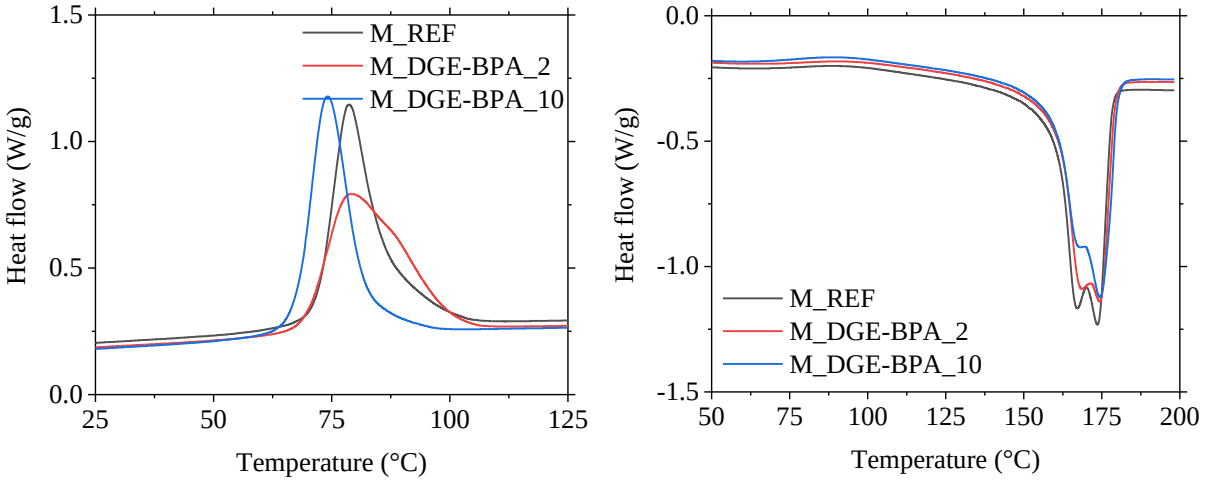

Figure 45 Crystallization (on the left) and corresponding melting (on the right) of DGE-BPA additivated samples and the reference (exo up)

TMP-TGE, on the contrary, showed the best performance in the lowest dosage (0.1 wt%). The sample M_TMP-TGE_2 reached 89% higher torque at the end of the kneading than PHB. The effect on weight average MW was also the most prominent, a 30% increase compared to the reference PHB. With increasing the dosage of the reagent, the observed end torque linearly decreased, and so did the value of

M_w, melting and glass transition temperatures and even the crystallinity and crystallization temperature. The sample with the highest dosage, M_TMP-TGE_20 (2.2 wt% in the mixture), still had 55% higher 5 min torque than the reference PHB, the effect on molecular weight was negligible.

Table 18 The results of kneading experiment, GPC and DSC analysis for neat PHB expressed as mean value ± standard deviation from 5 measurements and for kneaded samples with epoxy additives expressed as the change of mean values (values differing for more than 2σ are coloured)

	Kneading	**GPC results**		**DSC 2nd cycle**			
Sample name and reagent amount	M_{5m} **(mN·m)**	M_n **(kDa)**	M_w **(kDa)**	T_g **(°C)**	T_m **(°C)**	X_c **(%)**	T_c **(°C)**
REF	1720 ± 160	46 ± 10	163 ± 8	2.2 ± 0.7	173.9 ± 0.3	59.8 ± 0.3	78.0 ± 1.6
	ΔM_{5m} **(mN·m)**	ΔM_n **(kDa)**	ΔM_w **(kDa)**	ΔT_g **(°C)**	ΔT_m **(°C)**	ΔX_c **(%)**	ΔT_c **(°C)**
M_DGE-BPA_2 0.4 wt%	+25	+10	−6	+1.3	+0.2	−1.9	1.0
M_DGE-BPA_10 1.8 wt%	+374	+30	+26	+1.2	+0.5	−2.5	−3.5
M_TMP-TGE_2 0.1 wt%	+1534	+15	+49	+0.3	+1.0	−1.8	−1.3
M_TMP-TGE_10 1.1 wt%	+1193	+21	+22	−0.3	+0.3	−1.9	−2.2
M_TMP-TGE_20 2.2 wt%	+948	+18	−6	−2.0	−0.5	−3.2	−4.0
M_PGMA_2 0.3 wt%	+217	+14	−24	−2.0	−0.3	−2.7	−1.1
M_PGMA_10 1.5 wt%	−4	+28	+13	−1.1	−0.3	−3.6	3.9
M_PGMA_20 3.0 wt%	+698	+19	+7	−2.1	+0.1	−1.0	5.8
M_PGMA_40 5.9 wt%	+1198	+30	+24	−1.7	−1.0	−2.8	5.0
M_PGMA_100 13.5 wt%	+1487	+30	+41	−2.1	−1.7	−1.8	−12.5

The glass transition temperature of TMP-TGE additivated samples was very shallow, and hard to detect. Its T_c continuously moved to lower temperatures, and the peak got smaller, as seen on the left graph of Figure 46. The melting peak has a similar shape as other PHB samples with reagents.

Poly(glycidyl methacrylate) addition caused significant improvement compared to the reference from the amount of 3.0 wt% (20-fold overdose). The sample M_PGMA_20 had 41% higher final torque, and its curve of relative torque exceeded that of the reference PHB. It also led to a substantial increase in M_n, although the effect on M_w was within the measurement error. The sample M_PGMA_40 showed even better processing performance, 70% higher 5 min torque. For this sample, also the weight average MW increased by 15%. Maximum final torque among PGMA samples and one of the highest achieved was measured with the 100-fold overdose - 87% more than the neat PHB. Together with that, M_w rose by 25 %.

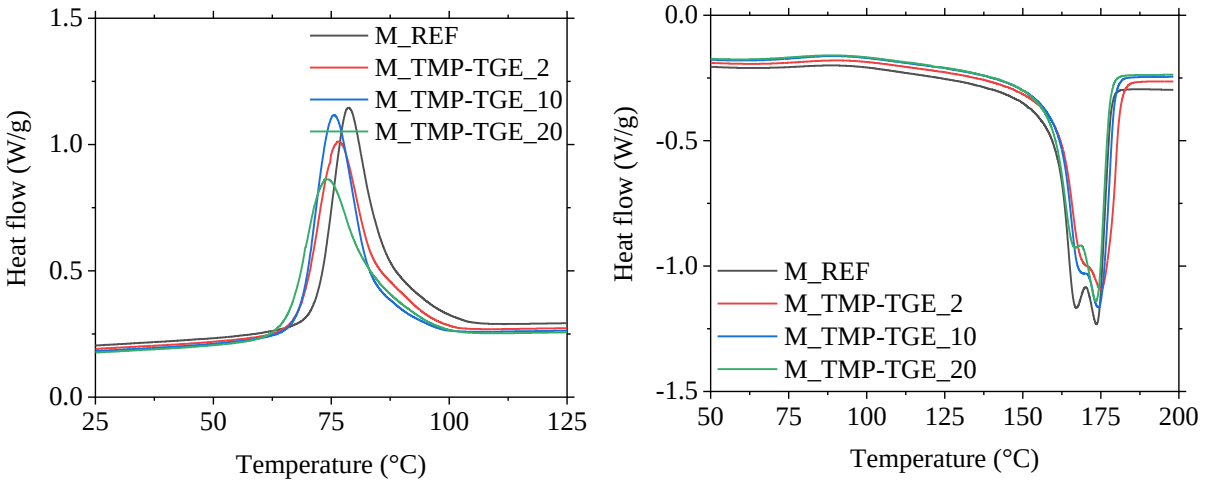

Figure 46 Crystallization (on the left) and corresponding melting (on the right) of TMP-TGE additivated samples and the reference (exo up)

The addition of PGMA, especially in the highest dosages tested, also altered the thermal properties of PHB, as depicted in Figure 47. Up to the 20-fold overdose amount, the crystallization temperature rose, and from the 40-fold it decreased again. However, the onset of crystallization indicating the nucleation ability of the sample was similar for all PGMA samples but M_PGMA_100. For the sample with the highest amount of PGMA, the crystallization temperature was 12.5 °C lower than for the reference, and even the melting temperature decreased considerably.

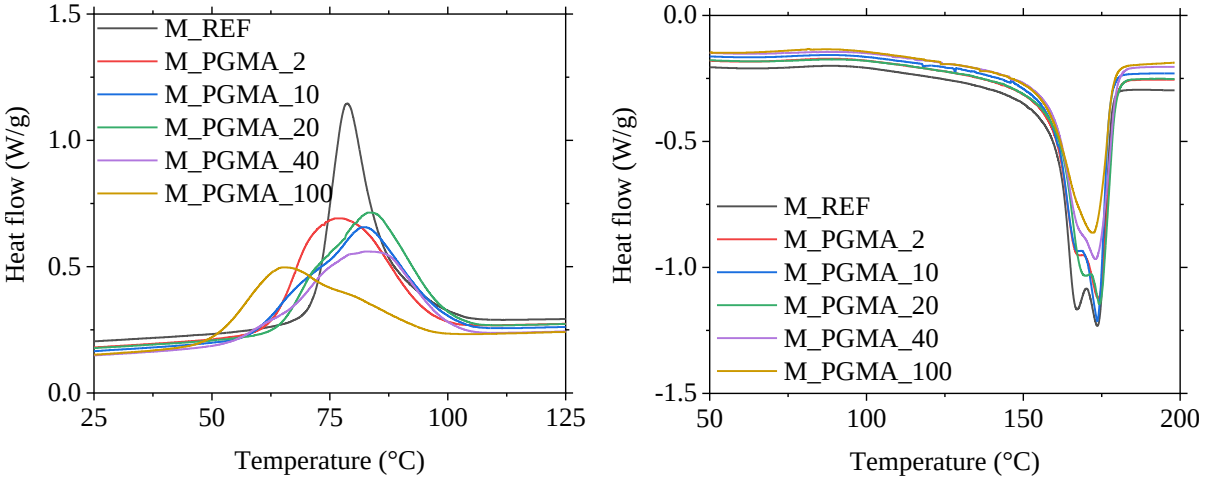

Figure 47 Crystallization (on the left) and corresponding melting (on the right) of PGMA additivated samples and the reference (exo up)

4.3.6. Discussion

A laboratory kneader was used to study the processing changes in poly(3-hydroxybutyrate) with and without the addition of selected reagents with different chemistry and functionality. Prepared samples were characterised by means of processing performance, molecular weight and thermal properties determination, and some profound changes were observed.

Generally, all bifunctional additives showed better performance for the higher tested dosage, as expected due to the higher probability of the additive finding two polymer ends. The only exception is diethylene glycol, which showed no effect on PHB as far as the processing torque values, molecular

weight, and thermal properties are concerned. Hexamethylene diisocyanate, bis(2,6-diisopropyl-phenyl)carbodiimide and diglycidyl ether of bisphenol A in 10-fold molar overdose towards PHB chain ends led to a rise in torque values at the end of the processing. The highest value was measured for carbodiimide reagent Stabaxol® 1 LF, 45% higher than neat PHB. In addition, the sample M_ST-LF_10 was the only one among the bifunctional additives with relative torque during kneading, surpassing that of the reference. It is important to note that all three led to 13–16% higher weight average molecular weight compared to the reference, which indicates the stabilization effect of these three reagents or chain extension reaction between them and PHB chain ends.

As opposed to bifunctional ones, all trifunctional additives were effective in increasing the absolute values of processing torque and compensating for the loss of molecular weight in all tested dosages. Quite surprisingly, they were the most effective in the smallest amounts tested, as manifested by a profound change in the slope of the relative processing torque. On the contrary, the curves of 10- and 20-fold overdose samples lie close to each other and for glycerol and poly(hexamethylene diisocyanate) even over the reference curve. However, we have to take into consideration the possible plasticizing effect of the reagents, which might play a role, especially for 20-fold samples. Nevertheless, glycerol in 2-fold dosage exhibited the greatest suppression of the relative torque decrease among all tested reagents and amounts and reached more than two times higher torque after 5 minutes of kneading at 185 °C than the reference. M_GLYC_2 is the sample with the highest MW measured as well – 44% more than the neat PHB. Trimethylolpropane triglycidyl ether and poly(hexamethylene diisocyanate) additivated samples in the 2-fold overdose amount follow, both with better results than all bifunctional reagents.

As far as polyfunctional additives are concerned, their effect on final processing torque and molecular weight increases with higher dosages with few discrepancies. The highest numbers were achieved for the sample M_PGMA_100, which has an 87% higher value of torque after 5 min of processing and 25% higher weight average molecular weight.

When discussing the molecular weight change with the addition of reagents with the functionality of more than 2, we also have to take into consideration the limits of gel permeation chromatography, which gives the most reliable numbers for linear polymers. As the analysis takes pleace in a diluted solution where the polymer is in the form of a random coil, its retention time is given by its intrinsic viscosity, which is lower for a branched polymer compared to a linear one with the same molecular weight. Therefore, for tri- and polyfunctional additives, we have to look also at other characteristics.

The thermal properties of prepared samples were characterised by differential scanning calorimetry. However, the changes in thermal properties are not easy to interpret. If the additive reacts with one chain end, it can alter the nucleation activity of the given macromolecule and lower the crystallization temperature. If it reacts with two chain ends, increasing the molecular weight, it can increase the glass transition and melting temperatures. At the same time, the crystallization ability of the polymer can be affected, which leads to lower T_m. The situation is even more complicated for the formation of branched

structures. In addition to that, an unreacted additive can have a nucleating or plasticizing effect, which can combine with what was already described.

All samples except two, which showed no change, exhibited a decrease in PHB crystallinity, which is very positive given the poor mechanical properties of PHB caused, among other things, by its high crystallinity. The highest decrease was observed for the samples with glycerol. For PHMDI, Raschig, PGMA and high dosage PVAl samples, the crystallization peaks were broadened profoundly and most of them also shifted to lower temperatures, showing worsened ability of PHB to crystallize. All of them had also an increase in molecular weight, suggesting that the reagent incorporated into the polymer structure, changing its thermal behaviour.

To conclude, we can see that the addition of some of the studied compounds really showed profound changes in PHB processing performance and resulting properties. For isocyanate and carbodiimide additives, bifunctional representatives in the 10-fold molar overdose were the most promising, while for hydroxy and epoxy compounds, trifunctional additives in the 2-fold overdose reached the most remarkable values of measured characteristics.

4.4. The reactions in the solution

The results of high-temperature processing of PHB with studied compounds indicated some of them are reactive towards the polymer and can stabilize or compensate molecular weight loss and a corresponding decrease of processing torque. However, due to the high temperature of processing, there is a risk of reagent loss, hence, for some, only a small dosage samples could be prepared. Therefore, the reactions in the solution were carried out having the following advantages over the melt reactions:

- lower processing temperature – less degradation and additive volatilization, but also a possible decrease in the reaction rate,
- higher mobility of polymer chains,
- increasing the time of the reaction,
- no loss of the reagent,
- possibility of preparing higher dosage samples.

Longer reaction and higher mobility of macromolecules in the solution compared to the melt mean increased probability for two chain ends to meet the reagent. Furthermore, the samples with higher dosages can be studied by infrared spectroscopy, which was not possible in the case of most of the melt-prepared samples due to the low amounts of the additive, often below 1 wt%.

For the reactions in the solution, powder PHB was pre-degraded for 5 min at 185 °C in the press in order to get closer to the melt processing conditions. This way, the polymer was sufficiently melted, and its MW dropped to around 270 kDa, as visible in Figure 30. Moreover, after the pre-degradation in the press, the PHB macromolecules are expected to have only one reactive end. As described in chapter 1.4

Thermodegradation of poly[(R)-3-hydroxybutyrate], initial hydroxyl ends of PHB are consumed, and the new ends formed by chain scission are carboxyl and crotonyl ends, the former being reactive towards used additives. In the same way as in the melt, studied reagents can act as chain extenders, single or multi-way branching points for PHB. This change of structure should reflect in infrared spectra, molecular weight and the solution viscosity, which was measured on the prepared 5 wt% solutions using an oscillation viscometer.

4.4.1. Isocyanates reagents

Prepared solutions of PHB treated with studied isocyanate compounds, hexamethylene diisocyanate (HMDI) and poly(hexamethylene diisocyanate) (PHMDI), and the reference PHB were firstly subjected to the viscosity measurement, with results in Figure 48.

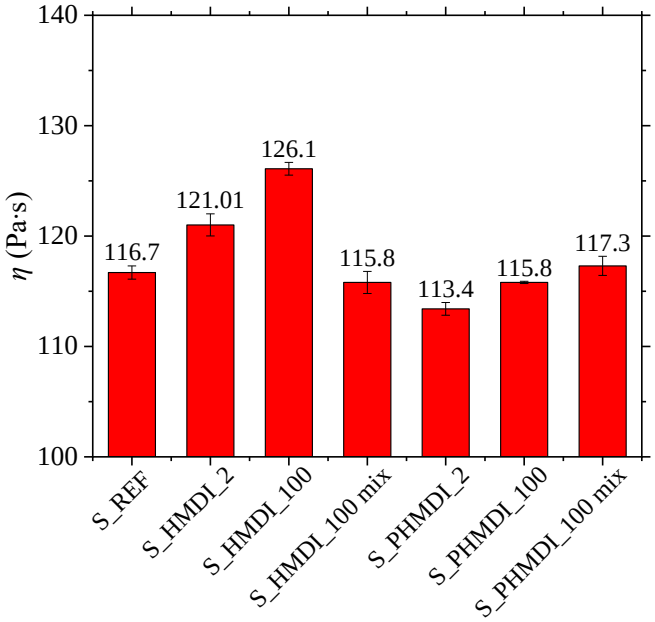

Figure 48 The comparison of viscosity of 5 wt% solutions of PHB (REF) and PHB with isocyanate reagents

The solution of neat PHB pre-degraded in a press and kept in chloroform under reflux for 6 hours has a viscosity of 116.7 Pa·s. The simple addition of 8.4 wt% HMDI (100-fold overdose, named S_HMDI_100 mix) prior to the measurement has a negligible effect on the viscosity value. On the contrary, the solutions to which HMDI was added before the reflux time show an increase in viscosity by 4% and 8% for 2-fold and 100-fold overdose samples, respectively. If HMDI functions as a chain extender, we should observe an increase in the molecular weight as well. However, looking at Table 19 with the results of the sample characterization after drying, this applies only for the sample S_HMDI_100. This sample has a 19% higher weight average but, at the same time 33% lower number average molecular weight than the reference. Number average MW is very sensitive to low molecular weight fractions in the polymer. For processing characteristics, M_w is of greater importance. Looking closely at MW distribution of the reference and S_HMDI_100 in Figure 49, it is clear that the whole peak shifted to higher numbers. The drop in M_n is due to the peak tailing of the reactive sample.

The effect on thermal properties can be observed in the slight increase of the glass transition temperature for both samples with HMDI. The melting temperature of PHB is unchanged, and crystallinity increases substantially for the sample HMDI_100.

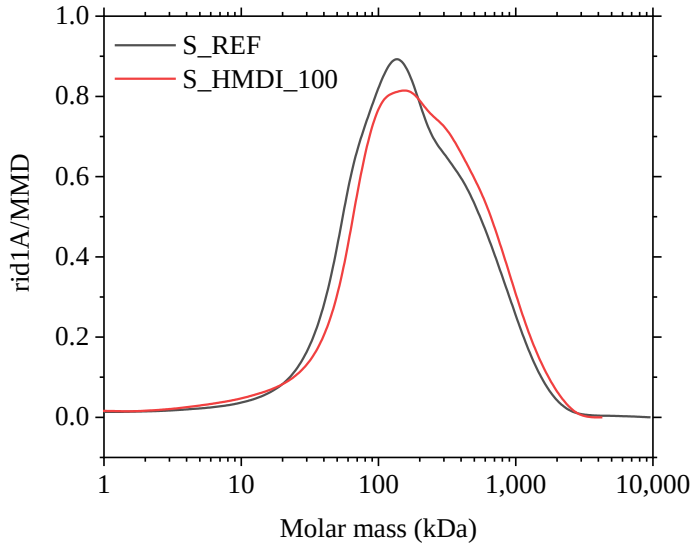

Figure 49 MW distribution of reference PHB sample and S_HMDI_100 from GPC

The FTIR spectra of the samples with bifunctional additive HMDI (S_HMDI_100 and only mixture of PHB and the reagent, S_HMDI_100 mix) and the reagent itself were measured and are shown in Figure 50. Pure HMDI has a very simple IR spectrum with the most intensive absorption peak corresponding to its functional isocyanate group NCO at 2251 cm^{-1} (the other characteristic peak is 1354 cm^{-1}). Peaks such as 2937, 2861 or 1462 cm^{-1} are attributed to the -CH_2- group.[105] The NCO peak at 2251 cm^{-1} is also visible in the spectrum of the sample S_HMDI_100 mix, although it is very weak. On the other hand, in the spectrum of the reactive sample S_HMDI_100, the NCO peak is absent while a mild peak of –NH bonds between 3200–3500 cm^{-1} and amide peaks around 1600 cm^{-1} appears. This proves the reaction between isocyanate and carboxyl groups forming amides as described in Figure 20.

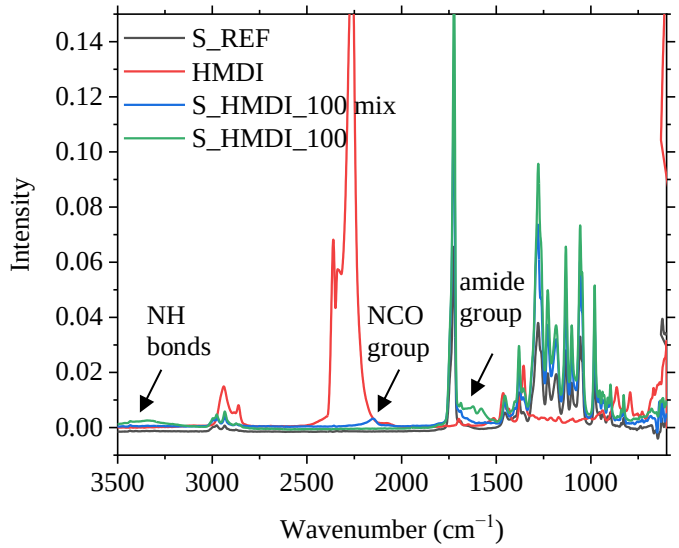

Figure 50 FTIR spectra of PHB reference, pure HMDI, the sample S_HMDI_100 mix (as prepared), and S_HMDI_100 (after the reaction)

In the case of PHMDI, the viscosities in Figure 48 do not look very promising at first sight. A simple addition of this reagent in 13.2 hm% did not affect the viscosity, and the reactive sample S_PHMDI_100 did neither. Moreover, the sample with a 2-fold overdose amount of the reagent showed 3% lower viscosity than the reference without any additive treated in the same way. The weight average MW was not changed, only for the higher dosage sample the M_n is 81% higher than for PHB (Table 19). It is important to note that this does not disprove the reaction between PHMDI and PHB. PHMDI has a functionality slightly higher than 3 and therefore, star-like branched macromolecules may possibly form. These structures have a lower viscosity than their linear analogues, as their viscosity is more dependent on the arm MW than on the overall MW.[106] As discussed in the previous chapter, also GPC measurement has its limits when it comes to the more complex polymer structures.

Table 19 The results of GPC and DSC analysis for neat PHB expressed as mean value ± standard deviation from 5 measurement and for samples prepared by solution method with isocyanate additives expressed as the change of mean values (values differing for more than 2σ are underlined)

	GPC results		**DSC 2nd cycle**			
Sample name and reagent amount	M_n **(kDa)**	M_w **(kDa)**	T_g **(°C)**	T_m **(°C)**	X_c **(%)**	Tc **(°C)**
REF	47 ± 6	268 ± 16	−4.4 ± 0.7	172.2 ± 0.3	60.0 ± 0.6	73.8 ± 1.2
	ΔM_n **(kDa)**	ΔM_w **(kDa)**	ΔT_g **(°C)**	ΔT_m **(°C)**	ΔX_c **(%)**	ΔT_c **(°C)**
S_HMDI_2 0.2 wt%	<u>−17</u>	+7	<u>2.2</u>	−0.4	<u>−2.4</u>	0.7
S_HMDI_ 100 8.4 wt%	<u>−16</u>	<u>+51</u>	<u>3.7</u>	0.0	<u>6.4</u>	2.3
S_PHMDI_2 0.3 wt%	−8	−10	<u>3.6</u>	<u>3.1</u>	<u>−9.7</u>	<u>−4.1</u>
S_PHMDI_100 13.2 wt%	<u>+39</u>	−8	<u>2.1</u>	−0.1	<u>8.0</u>	<u>−2.9</u>

The sample S_PHMDI_2 has a higher glass transition and melting temperatures, while its crystallization temperature is significantly lower and its crystallinity is the lowest measured – 50%. At the same time, the sample with 100-fold overdose has the highest crystallinity measured – 68%.

The infrared spectra of the reference and PHB with 13.2% PHMDI added pre, and after 6 hours under reflux in chloroform are in Figure 51. PHMDI spectrum is more complicated than in the case of HMDI, as there are also amide bonds. PHMDI has clear peaks at 2361 and 2271 (NCO group), 1762 cm^{-1} (C=O group), 1683 cm^{-1} and 1520 cm^{-1} (amide NH). The sample, where PHMDI was only mixed with PHB without any reaction time (as prepared) contains peaks corresponding to the reagent's functional group. These are absent in the sample S_PHMDI_100, which indicates that the reaction consuming isocyanate functional groups took place.

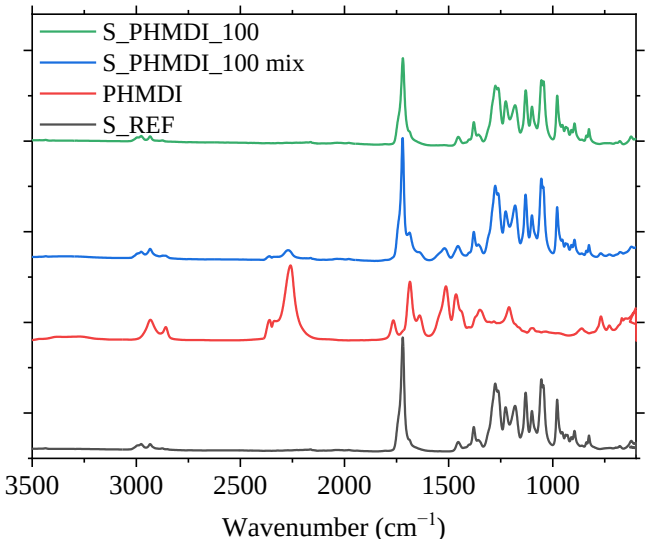

Figure 51 FTIR spectra of PHB reference, PHMDI, the sample S_PHMDI_100 mix (as prepared), and S_PHMDI_100 (after the reaction)

4.4.2. Carbodiimide reagents

The viscosity of prepared samples with carbodiimide additives Stabaxol and Raschig are in Figure 52. In Table 20, there are the results of MW and thermal characterization.

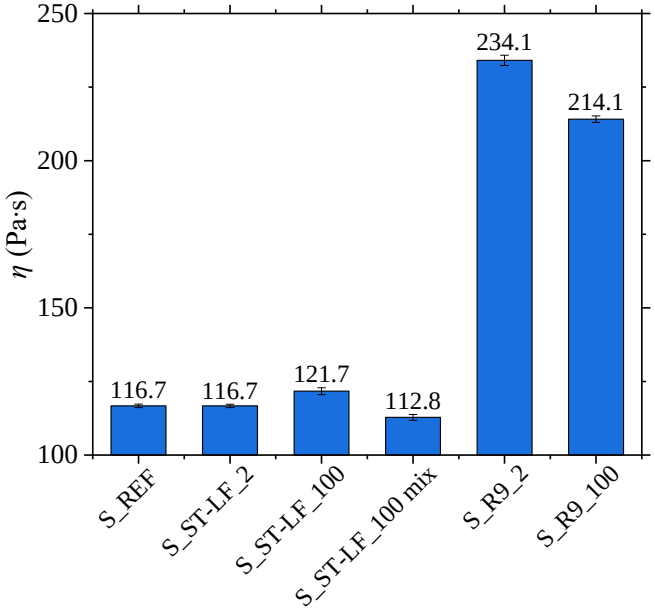

Figure 52 The comparison of viscosity of 5 wt% solutions of PHB (REF), and PHB with carbodiimide reagents

Firstly focusing on Stabaxol, the addition of a 2-fold molar overdose did not have any positive effect on observed properties, such as in the case of melt reactions. The number average MW is 47% lower compared to the reference PHB, while the viscosity and thermal properties remained unchanged. On the other hand, when a 100-fold overdose of ST-LF was used, the solution viscosity is 4% higher than the reference, even though the simple addition of ST-LF without any reaction time decreased the viscosity by 3%. The increase in molecular weight for the sample S_ST-LF_100 is profound – 82% increase in M_n and 19% in M_w. From the distribution curves in Figure 53, we can see that the peak position for the

reference and S_ST-LF_100 are the same, and the changes occurred at the peak tail and the shoulder at around 400 kDa, which is present at both samples.

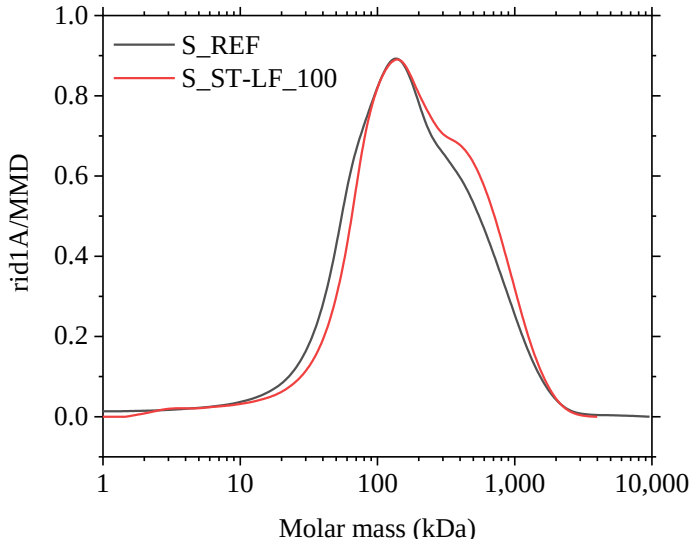

Figure 53 MW distribution of reference PHB, and S_ST-LF_100 from GPC

The effect on thermal properties is significant as well. The glass transition temperature of S_ST-LF_100 increased by 4 °C, and its melting and crystallization temperatures dropped majorly.

The FTIR spectra of bifunctional carbodiimide Stabaxol LF, reference PHB and the samples with a 100-fold overdose of ST-LF can be found in Figure 54. The most intensive peak of Stabaxol is 2156 cm^{-1}, corresponding to its functional group N=C=N. There are also peaks attributed to the benzene ring: =C–H stretch at 3059 cm^{-1}, C–C vibrations of carbons within the ring at 1584 and 1459 cm^{-1}, and intensive peak at 751 cm^{-1} for the substituted benzene ring. Peaks around 2900 cm^{-1} correspond to the =C–H of isopropyl substituent.[107]

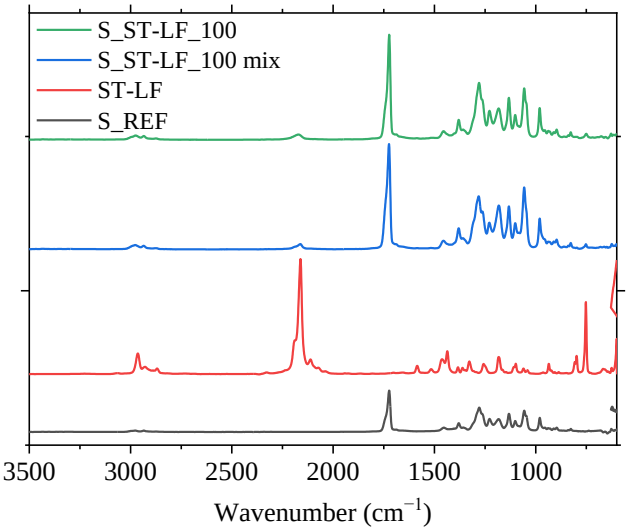

Figure 54 FTIR spectra of PHB reference, pure ST-LF, the sample S_ST-LF_100 mix (as prepared), and S_ST-LF_100 (after the reaction)

Peaks of the benzene ring of Stabaxol at 1584 and 750 cm^{-1} are also visible in the spectrum of both S_ST-LF_100 samples with similar intensity. The NCN group of Stabaxol LF should be consumed

during the reaction with carboxyl ends forming urea derivate with NH-C=O-NH bonds with new characteristic FTIR peaks (Figure 23). However, there is no visible N-H peak between 3500–3300 or amide characteristics peaks, as described for HMDI. Although there is an indisputable effect on PHB's MW and solution viscosity, the reaction was not proven by FTIR. This is probably caused by the high overdose, as there are so many bonds that are supposed to be consumed that you can't see the decrease.

Table 20 The results of GPC and DSC analysis for neat PHB expressed as mean value ± standard deviation from 5 measurement, and for samples prepared by solution method with carbodiimide additives expressed as the change of mean values (values differing for more than 2σ are underlined)

	GPC results		**DSC 2nd cycle**			
Sample name and reagent amount	M_n **(kDa)**	M_w **(kDa)**	T_g **(°C)**	T_m **(°C)**	X_c **(%)**	Tc **(°C)**
REF	47 ± 6	268 ± 16	−4.4 ± 0.7	172.2 ± 0.3	60.0 ± 0.6	73.8 ± 1.2
	ΔM_n **(kDa)**	ΔM_w **(kDa)**	ΔT_g **(°C)**	ΔT_m **(°C)**	ΔX_c **(%)**	ΔT_c **(°C)**
S_ST-LF_2 0.4 wt%	<u>−22</u>	−7	−0.1	−0.1	+0.8	<u>+3.1</u>
S_ST-LF_ 100 16.5 wt%	<u>+39</u>	<u>+50</u>	<u>+4.3</u>	<u>−5.5</u>	<u>+3.0</u>	<u>−8.7</u>
S_R9_2 0.3 wt%	<u>+86</u>	<u>+130</u>	<u>+3.1</u>	<u>+0.8</u>	<u>−4.8</u>	<u>−4.0</u>
S_R9_100 11.8 wt%	<u>−28</u>	−28	−1.3	<u>−1.2</u>	<u>−4.7</u>	<u>−5.3</u>

The polymeric analogue of Stabaxol, Raschig 9000, reached tremendous 101% higher viscosity compared to the reference on 2-fold molar overdose (only 0.3 wt%), as can be seen in Figure 52. From the results in Table 20 above, it is clear that the increase in solution viscosity can be attributed to the changes in molecular weight. The sample S_R9_2 has 181% higher M_n and 49% higher M_w than the reference PHB sample, which are the highest values achieved for all samples prepared by the solution method. Its thermal properties were affected as well, T_g and T_m rose while crystallinity and crystallization temperature dropped. The sample with a 100-fold overdose of R9 additive showed an increase in viscosity as well, 83% more than neat PHB. However, there was no positive influence of MW observed. In fact, both values of MW were the lowest measured in this sample set. The reason can be found by looking at the molecular weight distribution of Raschig samples in comparison with the reference and pure additive in Figure 55. It is clear that there is a great amount of unreacted Raschig in the S_R9_100 sample. This is the reason for the MW difference between pure PHB and this sample, and it proves this overdose is not effective.

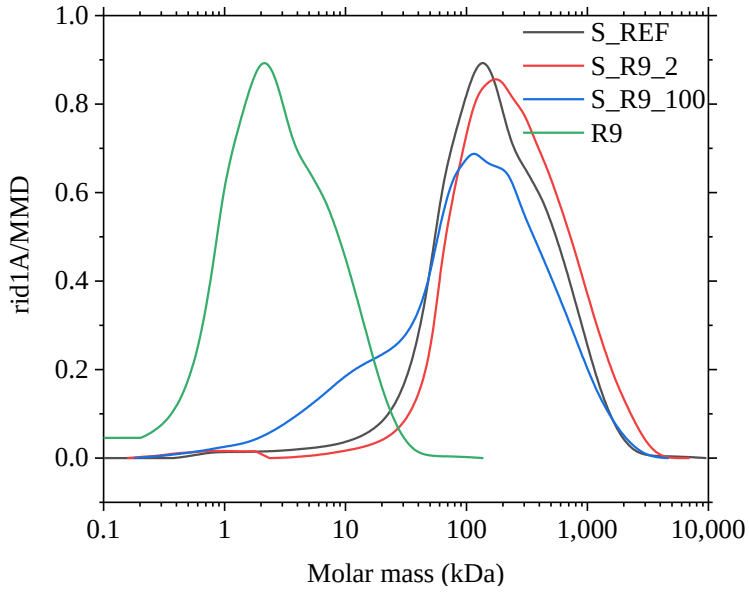

Figure 55 MW distribution of the reference PHB, raschig 9000, and the samples with Raschig from GPC

The existence of unreacted R9 is also confirmed by the FTIR spectrum of the S_R9_100 sample in Figure 56. The peak corresponding to the original functional group N=C=N (also present in Stabaxol) at 2156 cm^{-1} is visible in the spectrum, as it is for the sample made by simple mixing the reagent into the polymer matrix. Similarly to the case of its dimer analogue, the reaction between Raschig and PHB was not proven for solution-prepared samples.

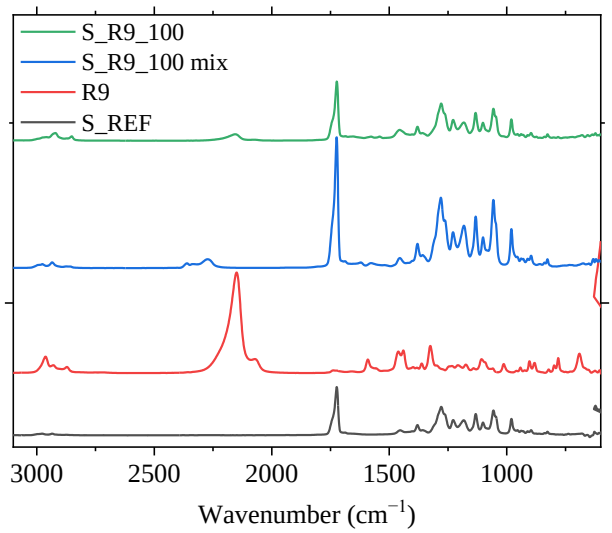

Figure 56 FTIR spectra of PHB reference, pure Raschig 9000, the sample S_R9_100 mix (as prepared), and S_R9_100 (after the reaction)

4.4.3. Alcohol reagents

Due to polyvinyl alcohol's insolubility in chloroform, it could not be used in this test. Therefore, only samples with diethylene glycol and glycerol were prepared. The results of viscosity measurement for all samples are in Figure 57, and further characterization is in Table 21.

Comparing the reference sample and the sample S_DEG_100 mix, in which the PHB was treated the same way and 5.5 wt% od DEG was added into it, we can see no difference in the solution viscosity. On

the other hand, the samples after the reaction time show a 10 and 13% increase in viscosity for 2-fold and 100-fold samples with DEG, respectively. Moreover, the sample S_DEG_2 shows a distinctly increased number average MW (by 36%) and a hint of an increase in weight average MW. The glass transition temperature is slightly lower, and the crystallization temperature higher than the reference. The sample with a 100-fold overdose of DEG has lower M_n than neat PHB, and its M_w is unchanged. The melting point of this sample is decreased slightly.

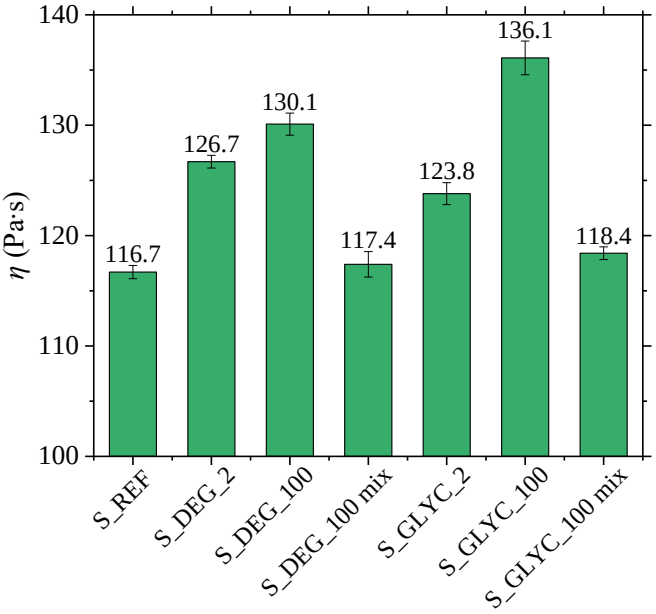

Figure 57 The comparison of viscosity of 5 wt% solutions of PHB (REF), and PHB with hydroxyl reagents

The FTIR spectra of diethylene glycol, reference PHB and the sample S_DEG_100 are in Figure 58.

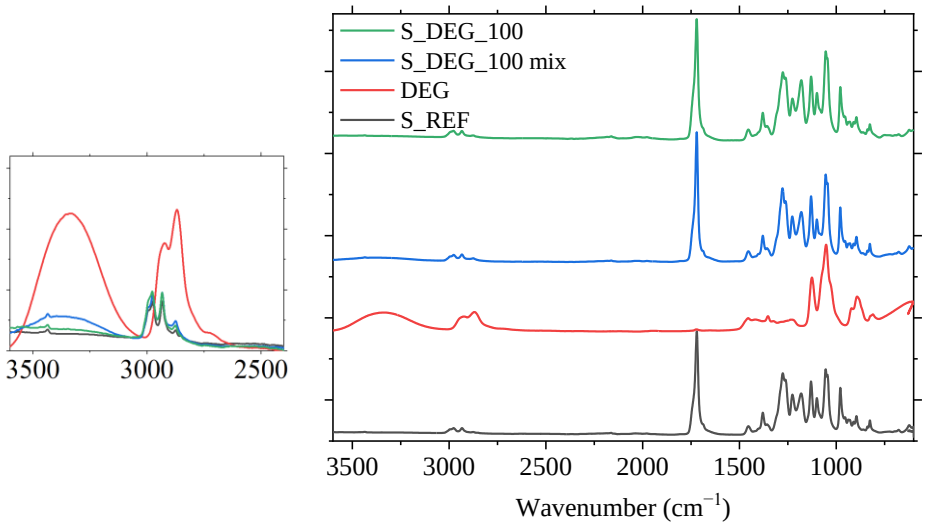

Figure 58 FTIR spectra of the reference PHB, pure diethylen eglycol, the sample S_DEG_100 mix (as prepared), and S_DEG_100 (after the reaction) with close-up of the OH group characteristic peak

DEG has prominent peaks at 3336 and 1125 cm^{-1} corresponding to its end hydroxyl groups. In addition, there is an intensive peak at 1052 cm^{-1} attributed to the C-O-C bond of a saturated ether and peaks of C-H stretching slightly under 2900 cm^{-1}. While the hydroxyl peak at 1125 cm^{-1} is not traceable in the PHB blends, the wide peak of hydroxyl groups above 3000 cm^{-1} is visible in the spectrum of the non-reactive sample S_DEG_100 mix. This peak is not observed in the S_DEG_100 sample, which

suggests the functional groups have been consumed. However, the ester group, forming in the reaction of PHB and DEG (Figure 24), cannot be tracked quantitatively in the PHB spectrum, as it is polyester.

Table 21 The results of GPC and DSC analysis for neat PHB expressed as mean value ± standard deviation from 5 measurements, and for samples prepared by solution method with hydroxy additives expressed as the change of mean values (values differing for more than 2σ are underlined)

	GPC results		**DSC 2nd cycle**			
Sample name and reagent amount	**M_n (kDa)**	**M_w (kDa)**	**T_g (°C)**	**T_m (°C)**	**X_c (%)**	**T_c (°C)**
REF	47 ± 6	268 ± 16	−4.4 ± 0.7	172.2 ± 0.3	60.0 ± 0.6	73.8 ± 1.2
	ΔM_n (kDa)	**ΔM_w (kDa)**	**ΔT_g (°C)**	**ΔT_m (°C)**	**ΔX_c (%)**	**ΔT_c (°C)**
S_DEG_2 0.1 wt%	<u>+36</u>	+27	<u>−1.5</u>	+0.0	+0.4	<u>+3.4</u>
S_DEG_ 100 5.5 wt%	<u>−22</u>	+7	−0.4	<u>−2.3</u>	<u>+3.3</u>	+0.1
S_GLYC_2 0.1 wt%	<u>+41</u>	+13	+0.1	+0.2	<u>−1.5</u>	<u>−2.4</u>
S_GLYC_100 3.2 wt%	<u>+33</u>	+3	+0.3	<u>−3.5</u>	+0.8	+2.3

In the case of glycerol, the pure addition of 3.2 wt% into the PHB solution caused a slight 1% increase in the solution viscosity. The samples prepared by refluxing the additive with PHB reached substantially higher values. S_GLYC_2 has 6% higher and S_GLYC_100 17% higher viscosity than the reference PHB. Both samples showed a profound increase in the number average MW measured. The 2-fold overdose sample showed an 87% increase, and the 100-fold sample showed a 70% increase compared to the neat PHB. Such as for DEG, the 100-fold sample had a lower melting point than non-additivated PHB, other thermal characteristics did not change. The infrared spectra of both prepared samples in the amount of 100-fold overdose (3.2 wt%), reactive sample S_GLYC_100 and non-reactive sample S_GLYC_100 mix were measured, and are shown in Figure 59, together with glycerol spectrum.

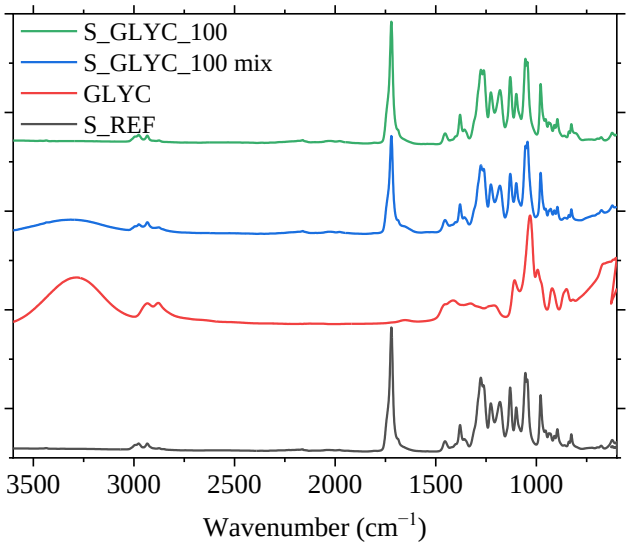

Figure 59 FTIR spectra of the reference PHB, pure glycerol, the sample S_GLYC_100 mix (as prepared), and S_GLYC_100 (after the reaction))

In the sample S_GLYC_100 mix as well as in glycerol, we can see a dominant peak of the hydroxyl functional group at 3284 cm^{-1} (analogous to the case of DEG). This peak is not present in the S_GLYC_100 sample after the reaction. This means that the functional groups of the additive have been consumed during the reaction time in the solution.

4.4.4. Epoxy reagents

The last subchapter will present the results for tested additives with the epoxy group: diglycidyl ether of bisphenol A, trimethylolpropane triglycidyl ether and poly(glycidyl methacrylate). Obtained values of solution viscosity are presented in Figure 60, and the thermal and molecular weight characterization is given in Table 22.

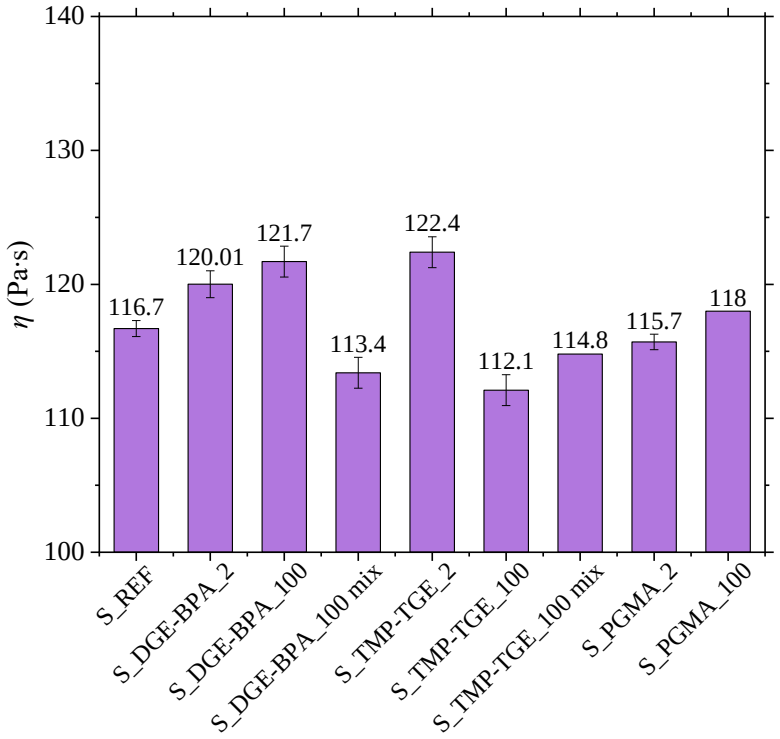

Figure 60 The comparison of viscosity of 5 wt% solutions of PHB (REF), and PHB with epoxy reagents

Starting with the bifunctional DGE-BPA, a viscosity increase was observed for both tested dosages, 3% for a 2-fold overdose and 4% for a 100-fold overdose sample. This increase is especially noticeable when we take into consideration the fact that the addition of 15.7% DGE-BPA causes a 3% decrease in viscosity (see the sample S_DGE-BPA_100 mix). Both samples also showed an increase in the number average molecular weight, for the sample S_DGE-BPA_2, the M_n is 72% higher than the reference PHB, and for the sample S_DGE-BPA_100, 109% higher. Weight average MW was untouched for a 2-fold overdose sample, and for the higher dosage sample, it seems to be higher, but the value is right below the measurement error.

The sample S_DGE-BPA_100 also shows interesting thermal behaviour. As can be seen in Figure 61, while S_DGE-BPA_2 showed an almost identical DSC curve as neat PHB, the higher dosage sample showed worsened crystallization ability with 20 °C lower crystallization temperature than PHB (the

lowest value among all prepared samples both in the melt and in the solution). Moreover, this sample exhibited a small peak of cold crystallization during the following heating cycle, just under 50 °C. Its melting was affected as well, dropping by almost 7 °C.

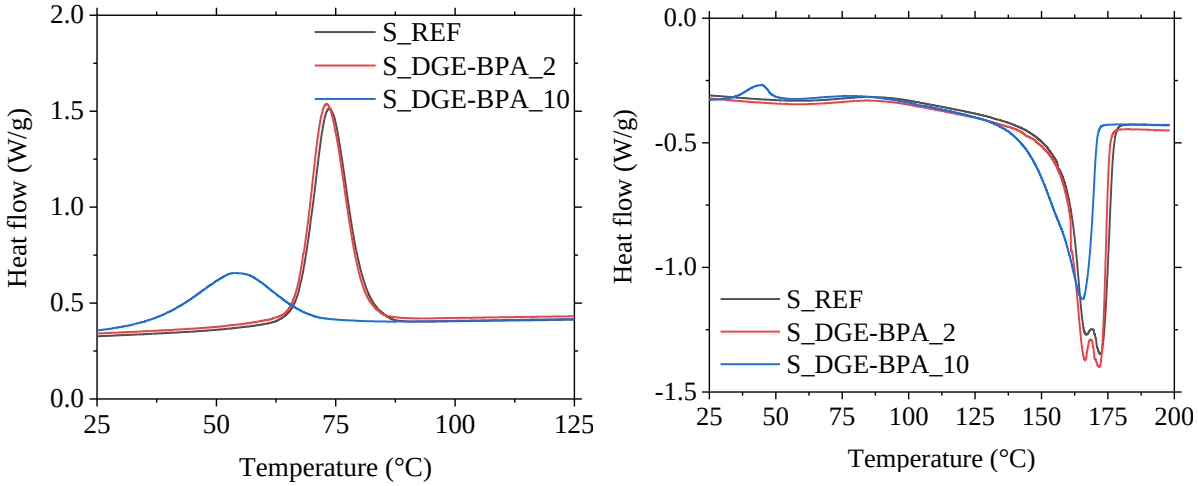

Figure 61 DSC thermographs of crystallization (on the left), and corresponding melting (on the right) of the reference and DGE-BPA additivated samples made in solution (exo up)

In Figure 62, there are the FTIR spectra of diglycidyl ether bisphenol A reagent, reference PHB and the sample S_DGE-BPA_100 and S_DGE-BPA_100 mix. DGE-BPA itself has already described peaks of the benzene ring at 3059 cm^{-1}, 1606 cm^{-1}, and 1507 cm^{-1}. There are also peaks of aliphatic >C–H around 2900 and 1230 cm^{-1}. The characteristic peaks of the oxirane ring are visible at 1230 cm^{-1} asymmetric stretching of the C–O; at 1032 cm^{-1} stretching of the C–O–C of ethers; at 914 cm^{-1} stretching of the C–O; and at 827 cm^{-1} stretching of the C–O–C of oxirane ring.[103,108] Comparing the two 100-fold samples, we can see similar intensities of the characteristic peaks of DGE-BPA, not only those which should be untacked in possible reaction (aromates) but also the peak of interest at 827 cm^{-1}.

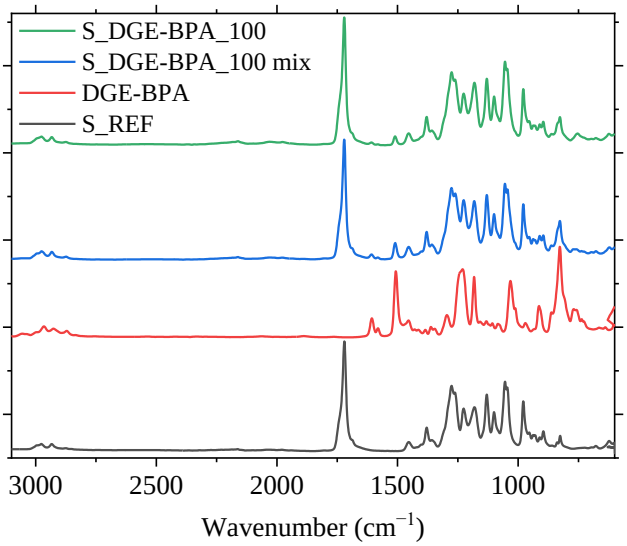

Figure 62 FTIR spectra of the reference, pure diglycidylether bisphenol A, the sample S_DGE-BPA_100 mix (as prepared), and S_DGE-BPA_100 (after the reaction)

TMP-TGE was more effective in increasing the solution viscosity in the lower amount tested – 2-fold molar overdose towards PHB chain ends. The sample with 0.2 wt% addition had 5% higher

viscosity than the reference and 83% higher number average MW. In line with this, also its characteristic temperatures, T_g and T_m, rose. In the case of a 100-fold sample, the viscosity dropped by 4% in comparison with the reference. This is partially the effect of the simple addition of the additive, as it causes a 2% decrease in viscosity (Figure 60). However, the sample has a 118% increase in M_n (the second highest value among the samples prepared in the solution), and its thermal properties were affected as well, with higher T_g and 4 °C lower T_m.

Table 22 The results of GPC and DSC analysis for neat PHB expressed as mean value ± standard deviation from 5 measurement, and for samples prepared by solution method with hydroxy additives expressed as the change of mean values (values differing for more than 2σ are underlined)

	GPC results		**DSC 2nd cycle**			
Sample name and reagent amount	**M_n (kDa)**	**M_w (kDa)**	**T_g (°C)**	**T_m (°C)**	**X_c (%)**	**Tc (°C)**
REF	47 ± 6	268 ± 16	−4.4 ± 0.7	172.2 ± 0.3	60.0 ± 0.6	73.8 ± 1.2
	ΔM_n (kDa)	**ΔM_w (kDa)**	**ΔT_g (°C)**	**ΔT_m (°C)**	**ΔX_c (%)**	**ΔT_c (°C)**
S_DGE-BPA_2 0.4 wt%	+34	+0	+1.6	−0.2	+0.2	−0.5
S_DGE-BPA_ 100 15.7 wt%	+52	+30	−1.2	−6.6	+2.1	−20.0
S_TMP-TGE_2 0.2 wt%	+39	−8	+3.5	+1.1	−2.0	+0.9
S_TMP-TGE_100 9.9 wt%	+56	+20	+4.4	−3.8	+0.8	−4.8
M_PGMA_2 0.3 wt%	−4	−9	−4.0	−0.1	−4.6	+1.3
M_PGMA_100 13.5 wt%	+48	−16	+1.6	+1.8	−3.1	−15.6

In Figure 63, there are FTIR spectra of the reference, the reagent and both samples with a 100-fold overdose of TMP-TGE for comparison.

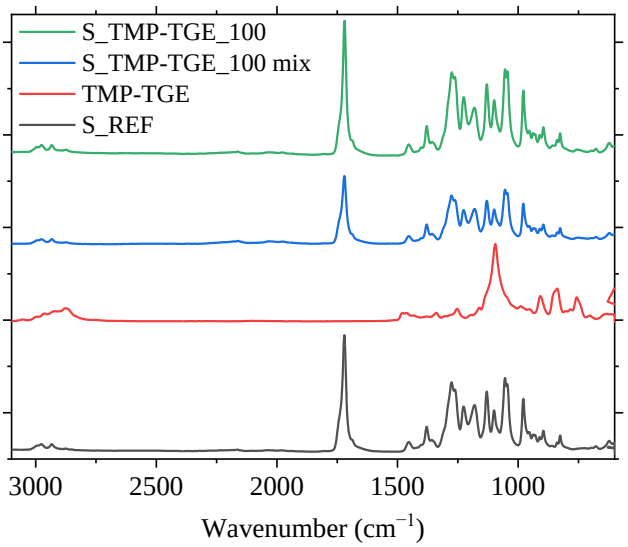

Figure 63 FTIR spectra of the reference, pure trimethylolpropane triglycidyl ether, the sample S_TMP-TGE_100 mix (as prepared), and S_TMP-TGE_100 (after the reaction)

The spectrum of TMP-TGE contains aliphatic -CH- peaks and, similarly to DGE-BPA, peaks corresponding to ether and oxirane, such as a strong characteristic peak of C–O–C stretching at 1095 cm^{-1}. For us, the typical peak of oxirane at 827 cm^{-1} is of main importance.[103,108] This peak is slightly visible in both spectra of S_TMP-TGE_100 samples (reactive and unreactive). However, the peak is very weak in both cases.

As far as PGMA is concerned, its effect on the solution viscosity is minor, with only a 1% increase for the sample with 100-fold overdose, as can be seen in Figure 60. The sample S_PGMA_2 showed no significant change in the molecular weight and had the lowest PHB glass transition temperature among all prepared samples in the melt and in the solution, −8.5 °C. S_PGMA_100 had a 101% increase in the number average MW. The crystallization of PHB with the addition of 13.5% PGMA was hindered, with a 16 °C drop of T_c (12.5 °C decrease for melt-prepared sample) and 3% of the crystallinity.

Infrared spectra of the high-dosage sample were compared with the reference and are depicted in Figure 64. The spectrum of pure PGMA was discussed in chapter 4.1 Synthetized poly(glycidyl methacrylate). However, similarly to both preceding epoxy functional reagents, as the relevant oxirane peak lies in the fingerprint region, and their intensity is very small in the blends, the differences in the spectra are inconclusive.

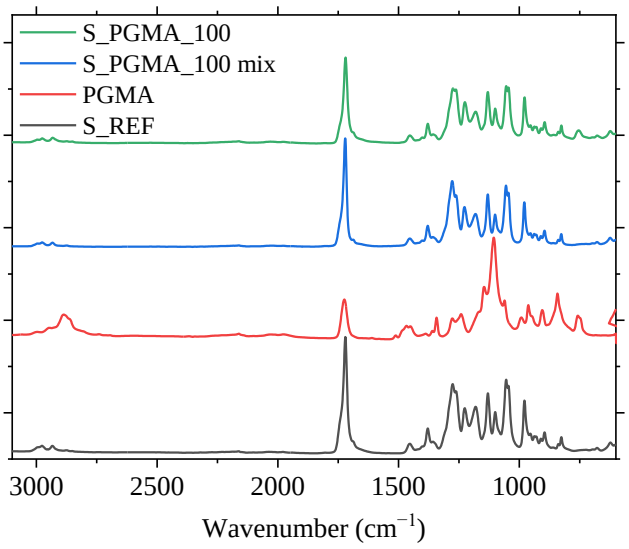

Figure 64 FTIR spectra of the reference, pure poly(glycidyl methacrylate), the sample S_PGMA_100 mix (as prepared), and S_PGMA_100 (after the reaction)

4.4.5. Discussion

Solution reaction offered a convenient way of the preparation of high-dosage samples with a 100-fold molar overdose of the additive over the poly(3-hydroxybutyrate) reactive chain ends. For each additive, also low-dosage (2-fold overdose) samples were prepared in order to cover both extremes. The viscosity of prepared solutions was measured, and dried samples were characterised by means of molecular weight, thermal properties and their absorbance in the infrared spectrum.

For a better understanding of the changes in viscosity, comparative samples where the additives were simply mixed with PHB solution prior to the measurement were prepared for all bifunctional and trifunctional additives. In most cases, the pure addition had zero or slightly negative effect on the solution viscosity, only in the case of glycerol, it caused a 2% increase in viscosity. Therefore, observed increases in viscosity can be attributed to the changes in PHB molecular structure. The greatest change in viscosity was achieved for the samples with Raschig 9000, where the increase is one order higher than for the rest of the samples – 101% higher than for the reference. The sample with a 100-fold amount of glycerol follows with 17% higher viscosity than neat PHB. The only two reagents causing a decrease in the solution viscosity compared to the reference were trifunctional poly(hexamethylene diisocyanate) and trimethylolpropane triglycidyl ether. However, due to the limited informative value of viscosity for non-linear macromolecules, it is necessary to look also at other measured characteristics.

For the majority of samples, the changes were reflected in the number average MW probably due to the high mobility of low molecular weight fraction of the polymer in the solution and, therefore, good accessibility towards chain extension and branching reaction. Moreover, the weight average of the reference PHB prepared by the solution method was higher than kneaded PHB, and its determination is burdened by high measurement error. Therefore, although there are some more promising samples, only in three cases a significant increase was achieved. That was for 100-fold samples with HMDI and Stabaxol and a 2-fold sample with Raschig 9000.

The reference PHB has lower characteristic temperatures than the kneaded sample, which may be caused by different molar mass distribution, with identical M_n and higher M_w (polydispersity index of almost 6). Therefore, a low molecular weight fraction can act as a plasticizer lowering all T_g, T_m and T_c. For the samples with carbodiimides and epoxides, this is in line with the increase in glass transition temperature observed for the samples, which also exhibited the already discussed increase in the number average molecular weight. However, this presumption would have to be verified.

As for the melting point, for 2-fold samples, it either did not change or increased and if so, the crystallinity of the sample dropped at the same time. On the other hand, 100-fold samples often exhibit lower melting point and higher crystallinity compared to the reference. This may be attributed to the plasticizing effect of the additives in such high dosages. The exceptions are Raschig and PGMA, which decreased the crystallinity, and the latter also increased the melting point. For carbodiimide and epoxy additives, the higher dosage samples had a greater effect on the crystallization temperature, shifting it to lower temperatures.

Further insight into what is happening between PHB and the additives was gained from infrared spectra measurement. For that, non-reactive samples with 100-fold dosage were prepared by simple mixing of PHB with the additive and were compared with the samples prepared by the reaction in the solution. For isocyanate reagents, the consumption of the reactive NCO group was confirmed by the disappearance of the characteristic peak at 2250 cm^{-1} in the spectra of the reactive samples. In the case

of HMDI, the formation of an amide group was observed as well. In the case of carbodiimide samples, on the other hand, no reduction of the peak intensity of the reagent's reactive groups due to the solution reaction was observed. For Raschig, the addition of 100-fold molar overdose (11.8 wt%) is counterproductive, as also shown by viscosity and molecular weight results. For example, for the blend of PHB with polylactide, more than 0.5 wt% of Raschig was proven ineffective.[109] Diethylene glycol and glycerol both have a wide peak of hydroxyl functional group between 3500 and 3200 cm^{-1} visible in the spectra of non-reactive samples. The peak disappears for the samples after the reaction time, meaning the reactive groups were consumed. In the case of epoxy additivated samples, the changes were not detected, as the characteristic peak of the oxirane group had too low intensity and no newly formed hydroxyl groups were detected. Generally, we are often unable to track the products of the reaction between PHB and the additives, and furthermore, we have to take into account also the impurities present in PHB, which can react with the reagents as well. Therefore, successful consumption of the reagent functional groups does not necessarily mean the reaction with PHB.

It is necessary to say that from the results of only one of above-mentioned methods, one can neither prove nor disprove the reaction of the selected additive with PHB. It is when they are combined that you can draw some conclusions. Carbodiimide additives showed a superior positive effect on the solution viscosity and molar mass of PHB. Isocyanate and epoxy compounds were more effective with increasing dosage, while hydroxyl compounds reached better performance in the lower dosages tested.

4.5. Rheological studies

Melt reaction in the kneader gave us useful information about the processing changes of poly(3-hydroxybutyrate) upon the addition of selected reagents, which is of high practical importance. Solution reaction enabled us to study the effect of high dosages for those additives, for which it was not possible in the melt. Using rheology, we can study the possible reaction of thermally unstable PHB with selected additives *in situ* and with great precision.

4.5.1. Time sweep test

For the time test, all samples were prepared with a 10-fold molar overdose of the additive towards PHB chain ends, as this dosage was the highest possible and, at the same time, feasible for all additives during the melt tests. However, during this study, it became obvious that the sample homogeneity was an issue due to two key reasons:

1) the low amount of the additive is localized in the small part of the testing specimen, as is demonstrated below in Figure 65 below for HMDI,
2) proper mixing in the rheometer cannot be achieved even with the optimization of the conditioning step or a distinctive increase in the deformation during the test.

Figure 65 The rheology testing specimen (2.5 cm diameter) R_HMDI_10 before (on the left) and after (on the right) the time sweep test

Ten-minute time sweep test at 185 °C with 1 Hz frequency and 1% deformation (in the LVR) was performed. After this time, the viscosity of pure PHB drops from the initial 10,000 Pa·s to 22 % after at minute 10 of the measurement. Overall, the viscosity loss due to the degradation after 10 minutes is so severe that the differences between the samples vanish. Therefore, the following graphs will present the first five minutes of the test, where 47 % of the initial viscosity of the reference is retained. The final values of complex viscosity measured for all samples are given in Table 23. The samples with HMDI and PGMA, in this order, achieved significantly higher values than neat PHB, which was 2264 ± 145 Pa·s. The samples with PVAl and TMP-TGE also seemed promising, but the difference was within the measurement error.

Table 23 The complex viscosity after 10 min time test at 185 °C expressed as mean ± standard deviation from at least 3 measurements (the values significantly different from the reference are underlined)

Complex viscosity after ten minute time test at 185 °C (Pa·s)				
	Isocyanates	**Epoxy**	**Carbodiimides**	**Alcohols**
Bifunctional	R_HMDI_10 2898 ± 145	R_ST-LF_10 2306 ± 215	R_DEG_10 2369 ± 369	R_DGE-BPA_10 2349 ± 250
Trifunctional	R_PHMDI_10 2440 ± 46		R_GLYC_10 2472 ± 170	R_ TMP-TGE_10 2588 ± 326
Polyfunctional		R_R9_10 2463 ± 170	R_PVAl_10 2516 ± 315	R_PGMA_10 2670 ± 187

Hexamethylene isocyanate showed exciting results in both melt and solution tests and as well during the rheology studies. During the time sweep, the initial complex viscosity (further on referred to simply as viscosity) of the sample R_HMDI_10 was approximately half of the value of the reference. This is probably the effect of the simple addition of less viscous liquid into the polymer melt. Therefore, analogously to the kneading experiment, we also observe the relative viscosity normalized to the initial value. Both measured and calculated viscosities during the first five minutes of the test are in Figure 66. Clearly, the slope of the viscosity decrease for the R_HMDI_10 sample is noticeably lower than for the reference at the end of the test, reaching 28% higher complex viscosity.

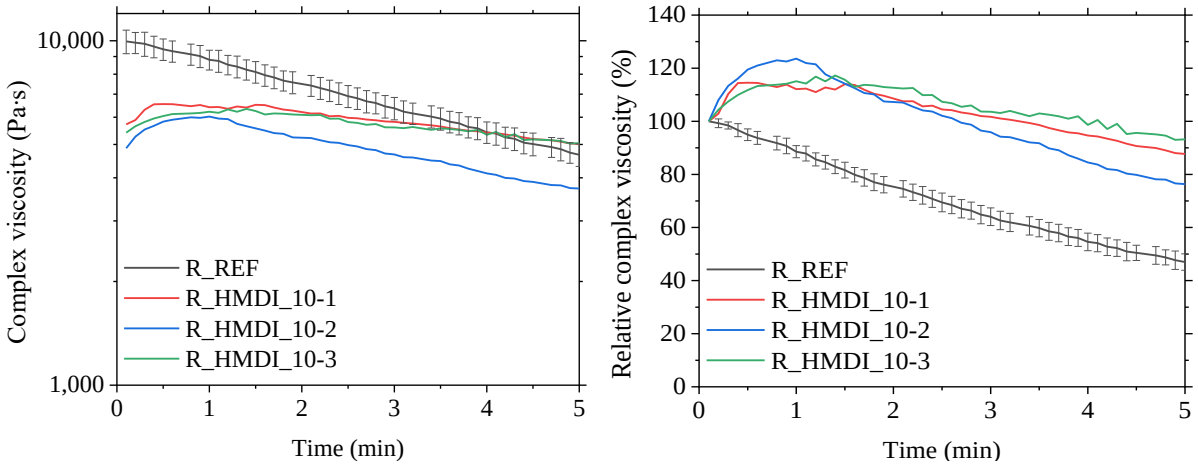

Figure 66 The time evolution of complex viscosity (on the left) and relative viscosity (on the right) for the reference PHB and the sample R_HMDI_10

Its oligomeric form, poly(hexamethylene isocyanate), exhibited similar behaviour. Its initial viscosity was between the values of the reference and R_HMDI_10. Subsequently, the viscosity increased and, after two minutes, began to drop steadily. At the end of the test, the R_PHMDI_10 viscosity was comparable to that of the reference. From the graphs in Figure 67, it is evident that PHMDI can enhance PHB viscosity during the first minutes of the thermal stress, which could be exploited during its processing.

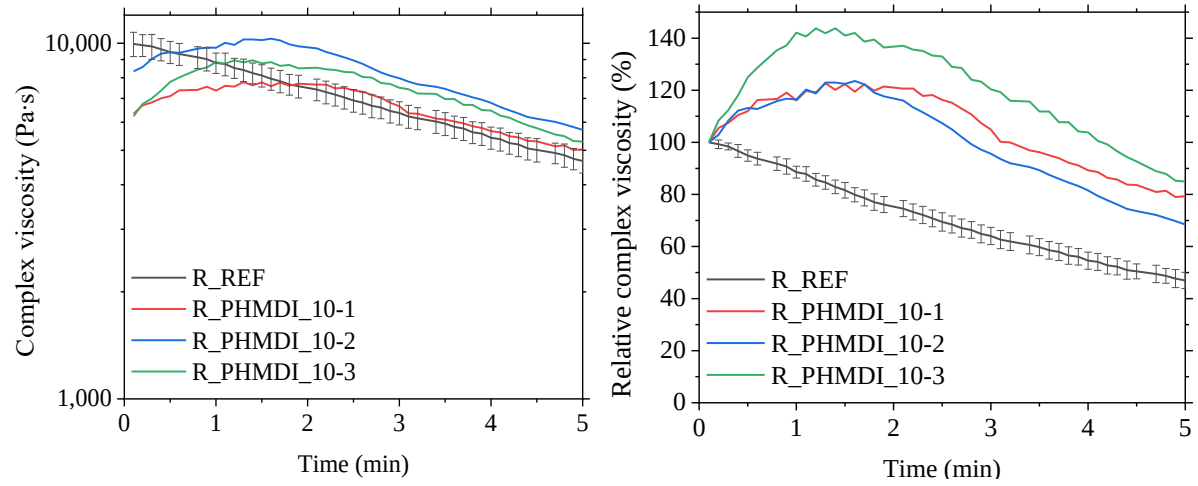

Figure 67 The time evolution of complex viscosity (on the left) and relative viscosity (on the right) for the reference PHB and the sample R_PHMDI_10

Commercial additives with the carbodiimide functional group, although showing remarkable results in the previous test, did not excel in the time sweep test. Contrary to the samples with isocyanate reagents, the initial viscosity and its change in time during 10 min of the measurement closely matched that of the reference for the samples wih Stabaxol and Raschig. The same applies to the relative viscosities shown in Figure 68.

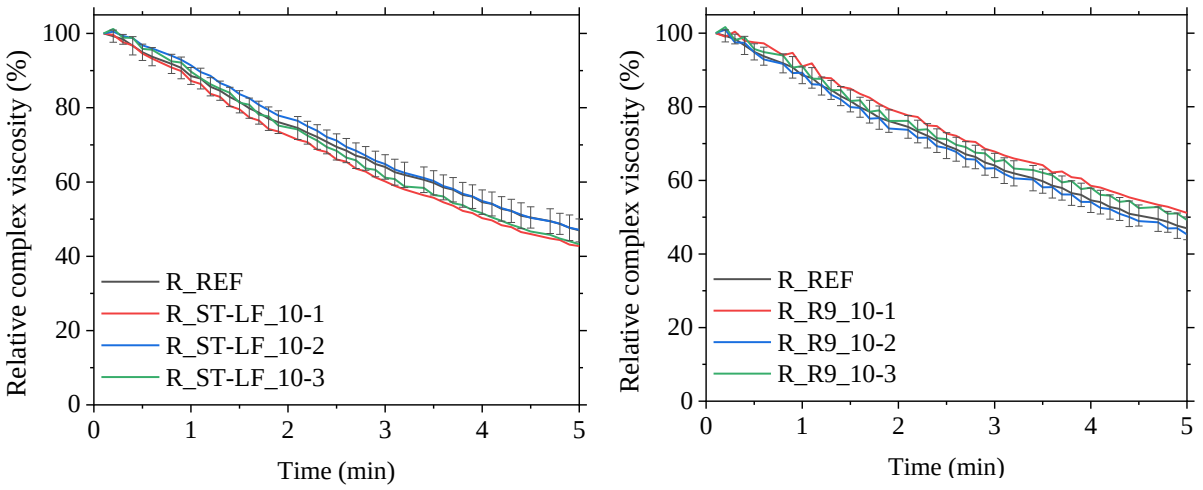

Figure 68 The time evolution of the relative viscosity of R_ST-LF_10 (on the left) and the sample R_R9_10 (on the right) compared with the reference PHB

This behaviour was also observed for low functionality reagents with hydroxyl functional group, diethylene glycol and glycerol, as can be seen in Figure 69. A slight exception is poly(vinyl alcohol), which has a mildly less steep decrease in the relative torque in the first two minutes of the test, as can be observed in Figure 70.

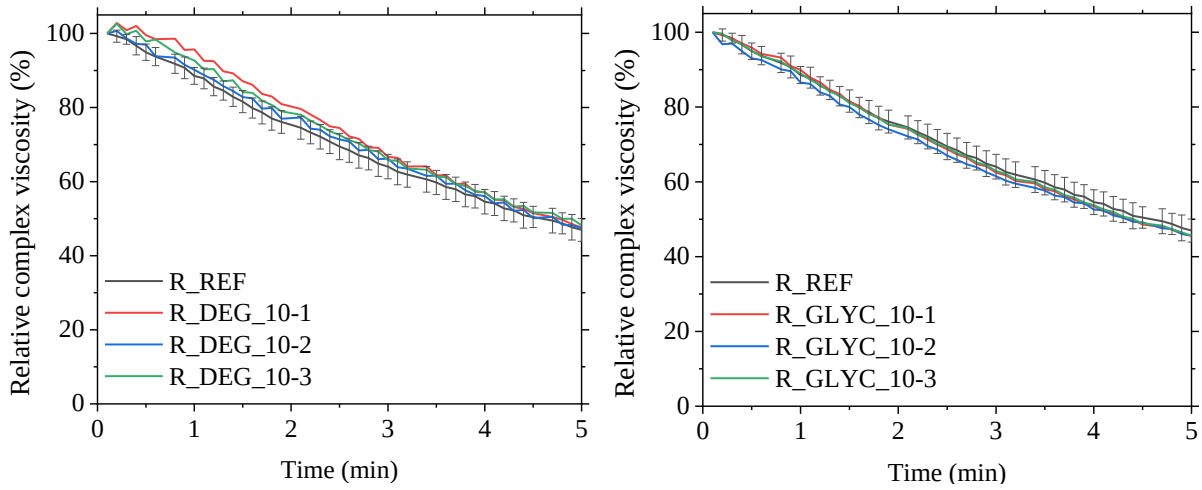

Figure 69 The time evolution of the relative viscosity of R_DEG_10 (on the left) and the sample R_GLYC_10 (on the right) compared with the reference PHB

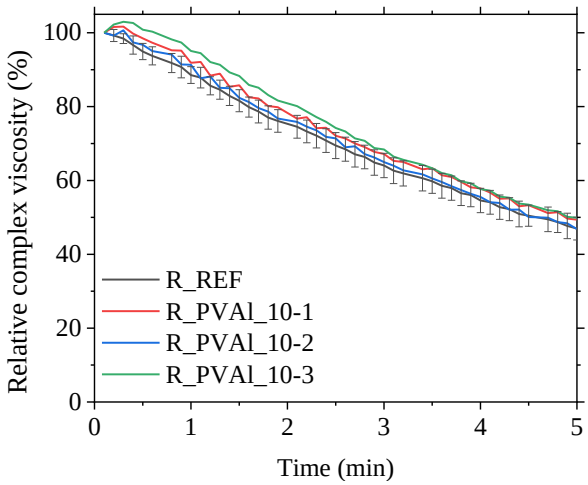

Figure 70 The time evolution of relative viscosity for the reference PHB and the sample R_PVAl_10

Figure 71 shows the time evolution of the relative viscosity during the first five minutes of the measurement of PHB with epoxy reagents diglycidyl ether of bisphenol A and trimethylolpropane triglycidyl ether. DGE-BPA seems to slightly positively impact the viscosity change, while TMP-TGE does not behave any differently than pure PHB.

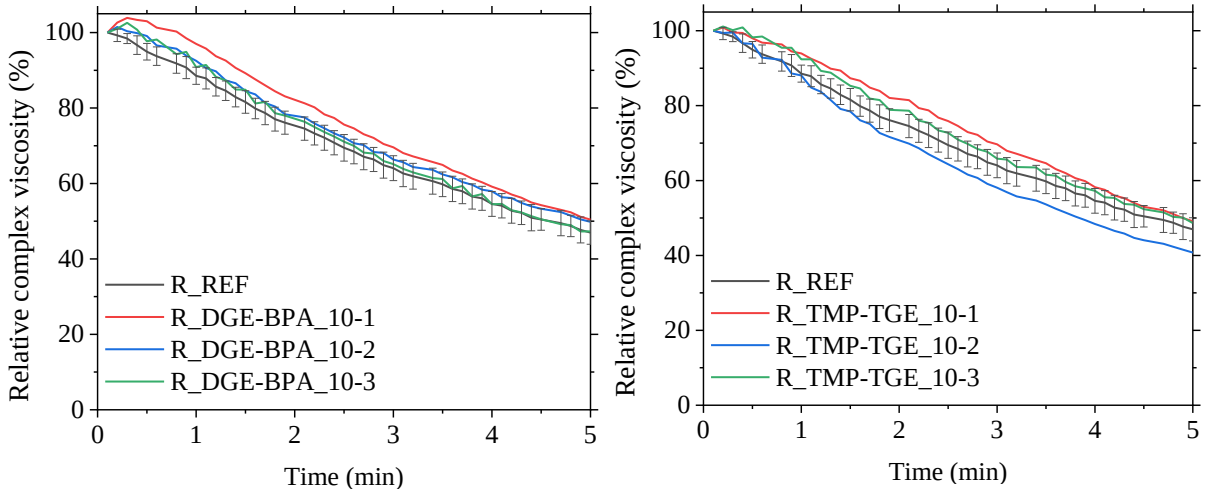

Figure 71 The time evolution of the relative viscosity of R_DGE-BPA_10 (on the left) and the sample R_TMP-TGE_10 (on the right) compared with the reference PHB

Poly(glycidyl methacrylate), as the only one among tested reagents, reached higher absolute viscosities during the time frame of the test. After ten minutes, its complex viscosity was 18% higher than for the neat PHB. The difference between the relative change of viscosity for the reference and R_PGMA_10 is in Figure 72. Similarly to PVAl, PGMA is clearly capable of suppressing the viscosity loss of PHB caused by degradation during the first few minutes of processing.

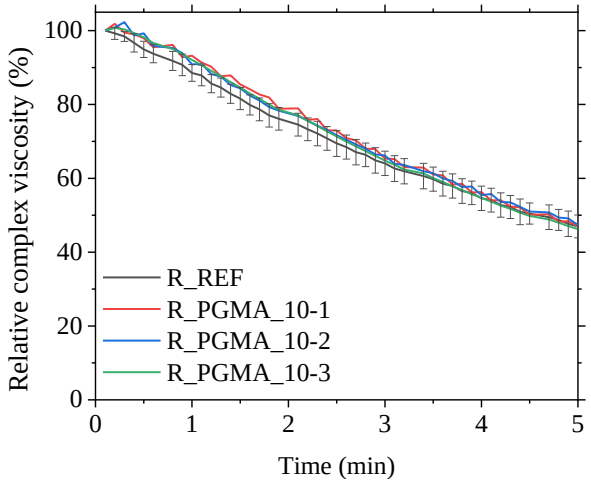

Figure 72 The time evolution of relative viscosity for the reference PHB and the sample R_PGMA_10

4.5.2. Degradation kinetics

It is evident that the previous test did not meet the expectations of characterization of the degradation behaviour of pure polyhydroxybutyrate and its mixture with reagents of different specificity and functionality. Therefore, a measurement containing four subsequent frequency steps (FS) was carried out, as described in the chapter 3.3.3 Multiple frequency sweeps. For this test, a 100-fold overdose

dosage of the reagent was chosen, which should overcome the problem of insufficient homogenization of the lower amount in the rheometer. The representative of the measurement record for the reference is in Figure 73.

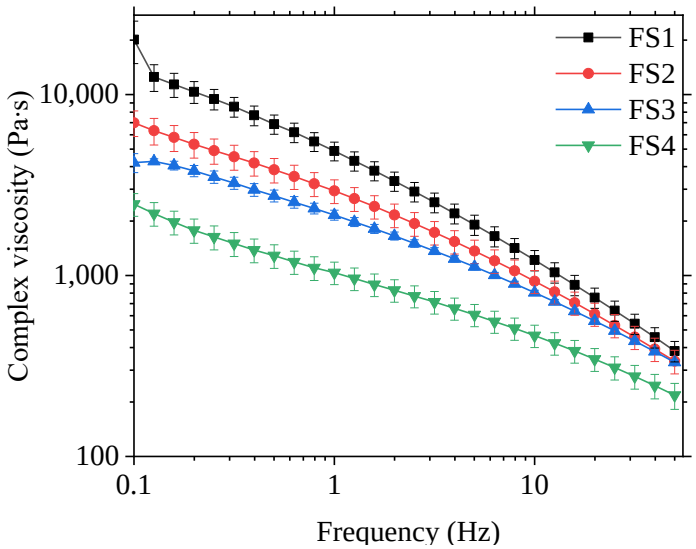

Figure 73 Frequency dependency of complex viscosity for four subsequent runs

As the material acts more solid-like with increasing frequency, the viscosity decreases, which can be observed for all four FS. A gradual shift to lower viscosities due to the thermal degradation, which was observed in all previous experiments, is also clear.

Logarithms of obtained viscosity values were plotted as a function of the measurement time for each frequency separately, obtaining the graph in Figure 74.

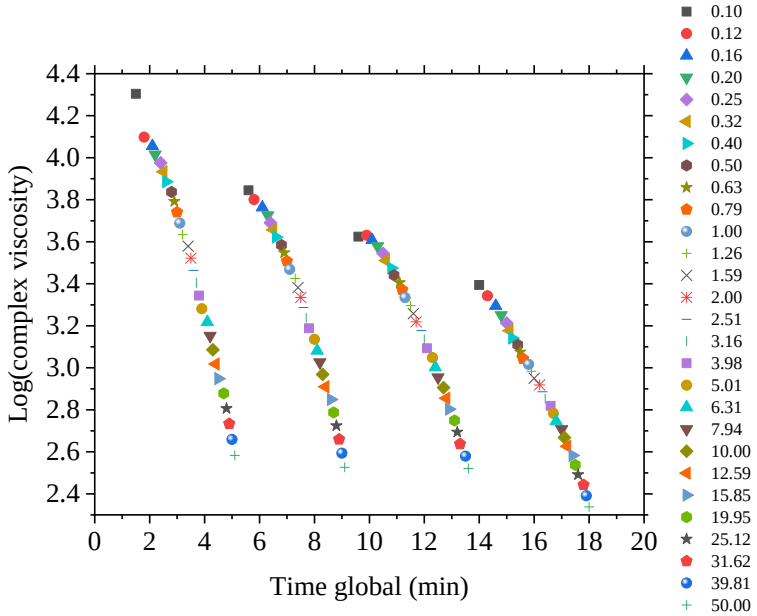

Figure 74 Complex viscosity as a function of the measurement time for all measured frequencies

You can easily notice that the first value for 0.1 Hz is quite remote, which is also apparent in the original FS plot. This is probably a consequence of insufficient melting at the start of the measurement due to the minimal preheating time. Therefore, this frequency was excluded from further calculations. Afterwards, the data for each frequency were fitted with linear regression. For example, for 0.13 Hz:

$$y = 4.18 - 0.059x, R^2 = 0.9901. \quad \text{Eq. 27}$$

Looking at Eq. 14, from the first coefficient of the obtained linear equation, we can calculate the complex viscosity at time zero for this frequency $\eta^*(\omega,t = 0)$, and the second coefficient corresponds to the first-order viscosity loss rate R_{v1} for given frequency as follows:

$$\eta_0^*(0.13\ \text{Hz}, t = 0) = 10^{4.18} = 15262\ \text{Pa} \cdot \text{s}, \quad R_{v1} = 0.059\ \text{min}^{-1}. \quad \text{Eq. 28}$$

This procedure was repeated for each measured frequency, and obtained data are in Figure 75. The time zero viscosity rapidly decreases with frequency, as observed for measured data. The viscosity loss rate starts at 0.06 min^{-1}, and is constant up to 0.5 Hz, slowly decreasing until 1 Hz from when it falls more rapidly. At 50 Hz, it reaches 0.02 min^{-1}. At higher frequencies, the molecular movement is hindered and therefore, the degradation is suppressed. Harrison and Melik described the same shape of frequency dependency for PHB copolymers poly(3-hydroxybutyrate-co-3-hydroxyvalerate), having higher viscosity loss rate, and poly(3-hydroxybutyrate-co-3-hydroxyhexanoate), which achieves slightly lower values of R_{v1} than PHB used in this work.[53]

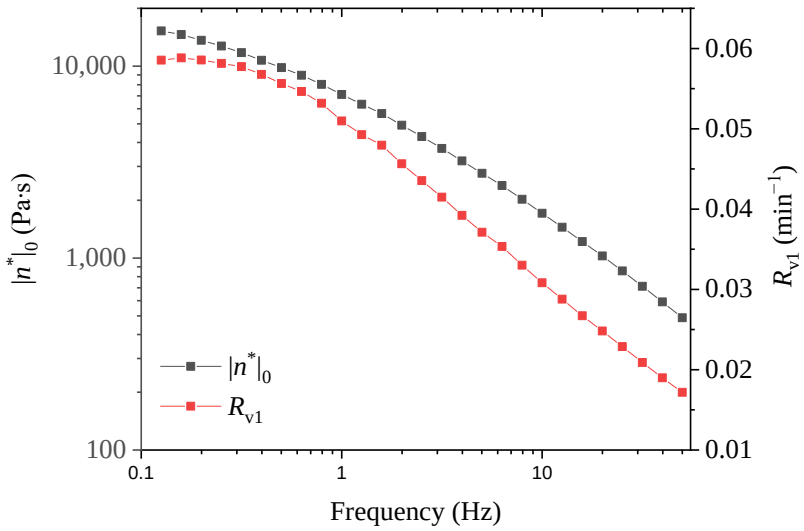

Figure 75 Frequency dependency of complex viscosity at time zero and viscosity loss rate for the reference PHB

This analysis was performed for all samples except for diethylene glycol and glycerol, which showed extreme evaporation in such a high dosage. Measured complex viscosity-frequency curves for PHB with remaining additives are in Figure 76. Looking closely at the viscosity values for all samples, one can see that nitrogenous reagents have overall better performance in the test. Their curves lie very close to the reference despite the high content of the low MW additive. Stabaxol, which has the highest weight fraction in the sample, 16.5%, is the only exception having slightly lower viscosities. Isocyanate additives and Raschig even reached higher complex viscosity than the reference during the fourth FS.

Among the oxygenated reagents, trimethylolpropane triglycidyl ether stands out with substantially lower viscosities than the rest of the samples. However, due to the high dosage, it is too early to draw any conclusion, as its viscosity loss rate may still be lower than for other samples. PGMA and PVAl show values similar to the reference.

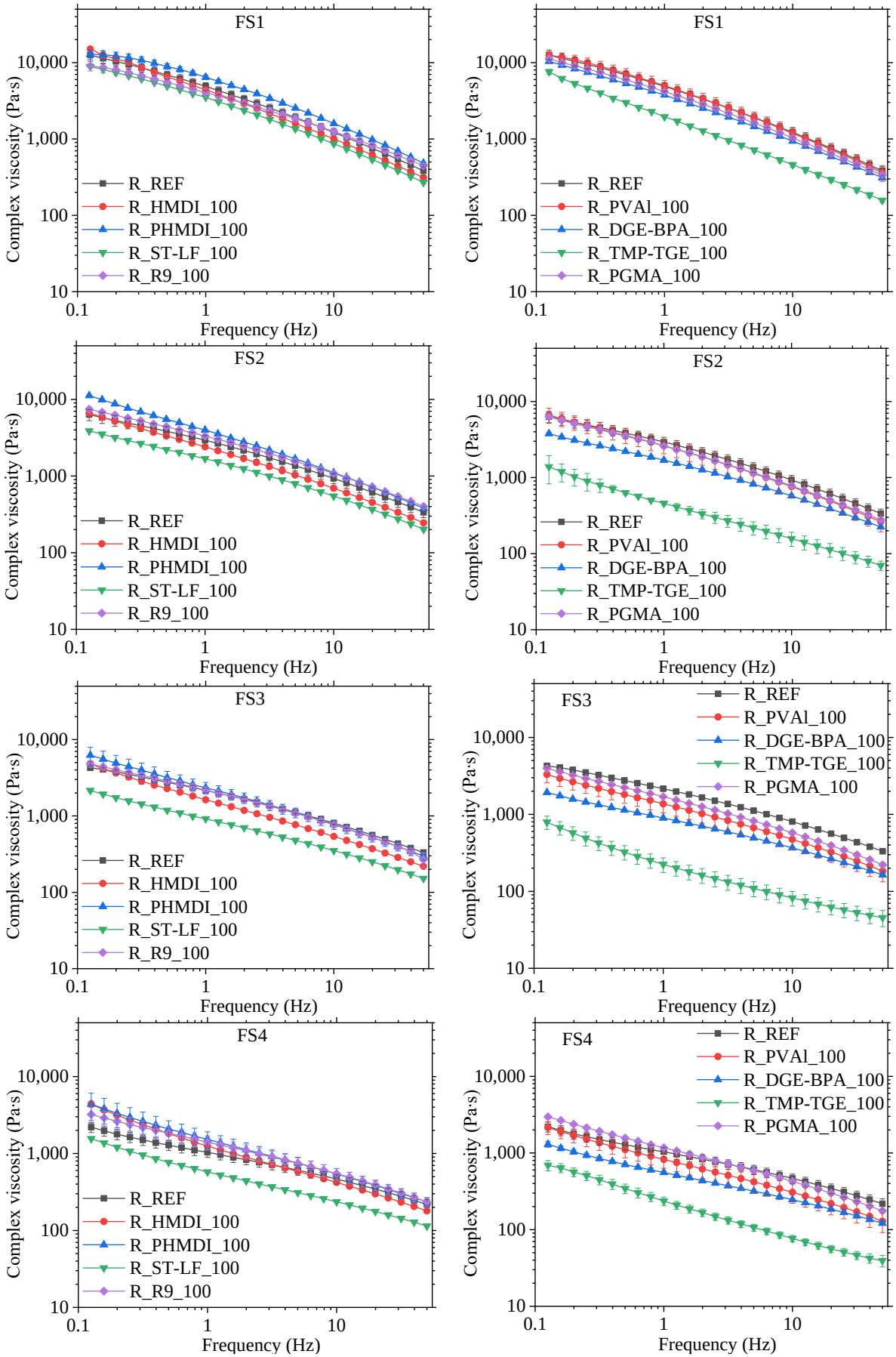

Figure 76 FS for the samples with isocyanates and carbodiimides (left column) and the samples with hydroxy and epoxy additives (right column)

The data measured for each sample were processed in the same ways as those of the reference using first-order fits for the complex viscosity-measurement time data sets. Obtained time zero viscosity-frequency plots compared with the reference are in Figure 77 for isocyanate and carbodiimide additivated samples and in Figure 78 for the samples with hydroxy and epoxy reagents. In the first graph, we can see that R_PHMDI_100 lies above the reference curve for all tested frequencies. PHB mixed HMDI and Stabaxol exhibit lower time zero viscosity than neat PHB. The curve of the R_R9_100 sample lies below the reference up to 10 Hz frequency, from where it slowly rises.

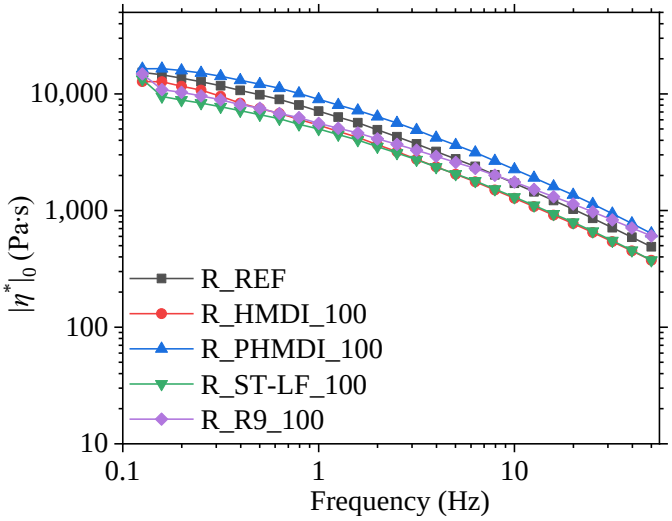

Figure 77 Calculated values of the viscosity at time zero – prior to any degradation for the reference and the samples with HMDI, PHMDI, ST-LF and R9

As for the oxygenated additives, none of the samples reached higher time zero viscosity than the reference. Among them, the PVAl-PHB blend reached the highest values copying the curve of the neat PHB. The epoxy additivated samples R_DGE-BPA_100 and R_PGMA_100 exhibited almost identical values of calculated zero time viscosity a little lower than the reference PHB. The sample with trifunctional TMP-TGE, as expected from the FS curves, had the lowest values among tested mixtures. In fact, its time zero viscosity at a given frequency is less than half of the value of other epoxy reagents.

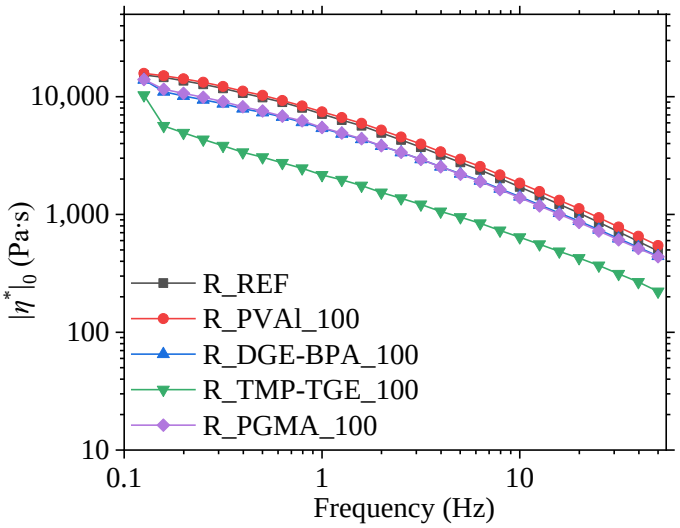

Figure 78 Calculated values of the viscosity at time zero – prior to any degradation for the reference and the samples with PVAl, DGE-BPA, TMP-TGE and PGMA

Also, viscosity loss rates as a function of frequency were calculated for all samples and compared with the values calculated for the reference PHB. The resulting curves for the samples mixed with nitrogenous additives are in Figure 79. In contrast with the zero time viscosity, with viscosity loss factor, we hope to obtain lower values than neat PHB. This was achieved for three samples in the limited frequency region. R_PHMDI_100, although being the only sample which reached higher time zero viscosity, had an R_{v1} factor lower than the reference only for the frequencies under 1.3 Hz. Moreover, R_R9_100 showed the lowest viscosity loss rate than the reference in the frequency region ranging from 0.13 to 16 Hz. Except for the two highest frequencies measured, the sample with HMDI had lower values of the viscosity loss coefficient than the reference in the whole frequency region.

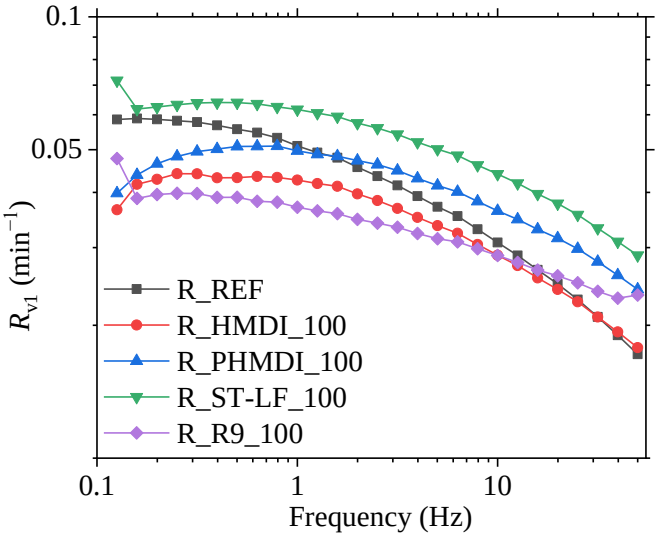

Figure 79 Calculated viscosity loss rate for each frequency for the reference and the samples with HMDI, PHMDI, ST-LF and R9

In Figure 80, we can see the resulting R_{v1} values for PVAl and all epoxy-functional reagents. The highest values of the viscosity loss factor among all tested samples were obtained for the PHB sample additivated with TMP-TGE. The curve corresponding to R_DGE-BPA_100 reaches comparable values of R_{v1} as the R_TMP-TGE_100 for the frequencies up to 1 Hz but afterwards drops. Similarly, PVAl addition did not have any positive effect on the viscosity loss rate despite the promising values of the time zero viscosity. Last but not least, the sample with PGMA showed distinctly lower R_{v1} than neat PHB for the frequencies 0.13–16 Hz, similar behaviour to R_R9_100 with values comparable to those of R_HMDI_100.

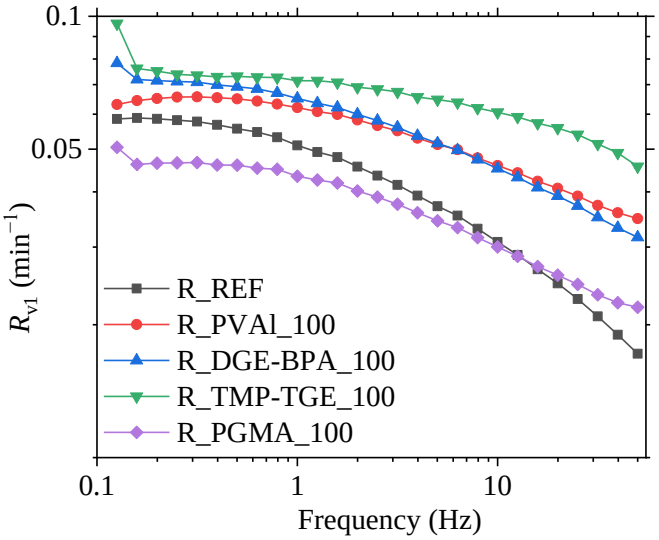

Figure 80 Calculated viscosity loss rate for each frequency for the reference and the samples with PVAl, DGE-BPA, TMP-TGE and PGMA

4.5.3. Discussion

In this chapter, two different rheology tests were exploited in order to characterize the kinetics of poly(3-hydroxybutyrate) degradation during thermal treatment, which is of great importance for its processing.

The first test was simple 10 minutes time sweep at 185 °C with one minute of preheating, which was performed in order to observe the differences in viscosity loss during the measurement among the prepared samples. On the basis of previous tests, significant variations in the effects of individual reagents on PHB were expected. However, this methodology was proven very ineffective, as except for isocyanate samples, there were only minor differences between the samples and also with the reference. The reason lies partly in the low dosage of the reagent, which is, although well homogenized in the dry state, localized in the small part of the testing specimen. The second part of the problem is that the melt is not mixed during the measurement, such as during kneading experiments, for example. Therefore, the additive has only a limited working area, which is predestined by specimen preparation. However, low shear rates during the measurement are inevitable. The parameters of the measurement (frequency and deformation) are chosen so that the test takes place in the linear viscoelastic region to avoid any irrelevant changes in the macromolecular structure (and hence the viscosity) due to shear thinning.

Despite all this, hexamethylene diisocyanate and poly(hexamethylene diisocyanate) addition to PHB caused a profound change in the slope of relative viscosity decrease. Both samples also exceeded the complex viscosity values of the reference during the time frame of the test, HMDI sample reaching 28% higher final viscosity than neat PHB. A positive effect was also observed with poly(glycidyl methacrylate) addition. The sample with 10-fold overdose exhibited higher values of both absolute and relative viscosity than the reference having 18% higher complex viscosity after 10 minutes than PHB.

The second performed test was composed of four identical subsequent frequency sweeps. Seeing the PHB viscosity drops to 22% of the original value in ten minutes at 185 °C, the parameters were set so

that the test is as short as possible and, at the same time, covers a wide range of frequencies. The final frequency range is 0.1–50 Hz, and the length of the test is 18 minutes therefore, the random chain scission kinetics is applicable during the whole test.[50]

The test results were processed using a kinetic model from the literature, and for each measured frequency, two parameters of high practical importance were calculated:

- time zero viscosity, a theoretical value of complex viscosity, which would have been measured if the material did not degrade. It tells us information about the influence of the reagent on the absolute value of viscosity,
- viscosity loss factor, a kinetic parameter characterizing the viscosity decrease in time, regardless of its absolute value.

With these two parameters, we can separate the effect of simple the addition of the reagent into PHB on melt viscosity and the reagent's effect on the degradation rate. In the previous test, we had both of these effects working simultaneously. However, as most of the reagents are low-viscosity liquids, their addition also causes a decrease in the viscosity of PHB, which does not necessarily mean they also act as pro-degradants. Likewise, polymeric additives can in theory increase the melt viscosity without having any stabilizing effect.

This was observed for HMDI samples, which had lower time zero viscosity than neat PHB due to the addition of 8.4 wt% of low-molecular weight fraction. Nevertheless, the viscosity loss factor was lower than for PHB for almost all measured frequencies except the last two. PHMDI additivated sample alone reached higher time zero viscosities than the reference, but its viscosity loss rate was lower only in the low frequency range. The lowest overall viscosity loss factor was obtained for the sample with Raschig addition. On the contrary, its dimer analogue, Stabaxol, did not prove itself an effective stabilizer for PHB. Due to the high evaporation rate of diethylene glycol and glycerol, poly(vinyl alcohol) was the only representative of hydroxyl-functional compounds. Although the sample with PVAl had promising values of viscosity matching those of the reference, it was only due to the simple mixing rule, as its loss viscosity rate is higher than for neat PHB. Moreover, both epoxy reagents with low functionality, diglycidyl ether of bisphenol A and trimethylolpropane triglycidyl ether failed to suppress PHB's natural degradation and decrease its viscosity loss rate. The sample with poly(glycidyl methacrylate), on the other hand, showed comparable zero time viscosity with the reference and, at the same time, lower viscosity loss rate for a high range of frequencies, making it one of the most effective reagents in PHB thermal stabilization.

This chapter showed that with a proper methodology, it is possible to distinguish two influences of the reagents on PHB: the change in viscosity caused by simple addition and the pro-degrading or stabilizing effect. This can put into perspective the results of the previous chapters in which the additivated samples prepared by two different techniques were characterised.

4.6. Biodegradability *in vitro*

In order to investigate if the addition of the reagent and its possible incorporation into PHB structure changes the biodegradability of this polymer, enzymatic biodegradability *in vitro* test with simultaneous measurement in purely abiotic conditions was performed. In Figure 81 and Figure 82, there are measured weight changes for nonenzymatic and enzymatic conditions, respectively. Evidently, the changes in weight change are minimal, given the specimen size, they are usually under half a milligram. Therefore, they come with a great measurement error, which I assume would remain in the same dimension even if the weight change was bigger. Nevertheless, the reference did not exhibit any weight loss in purely abiotic conditions of PBS buffer. Moreover, after 90 days weight gain of 0.3% (corresponds to 0.15 mg) was recorded.

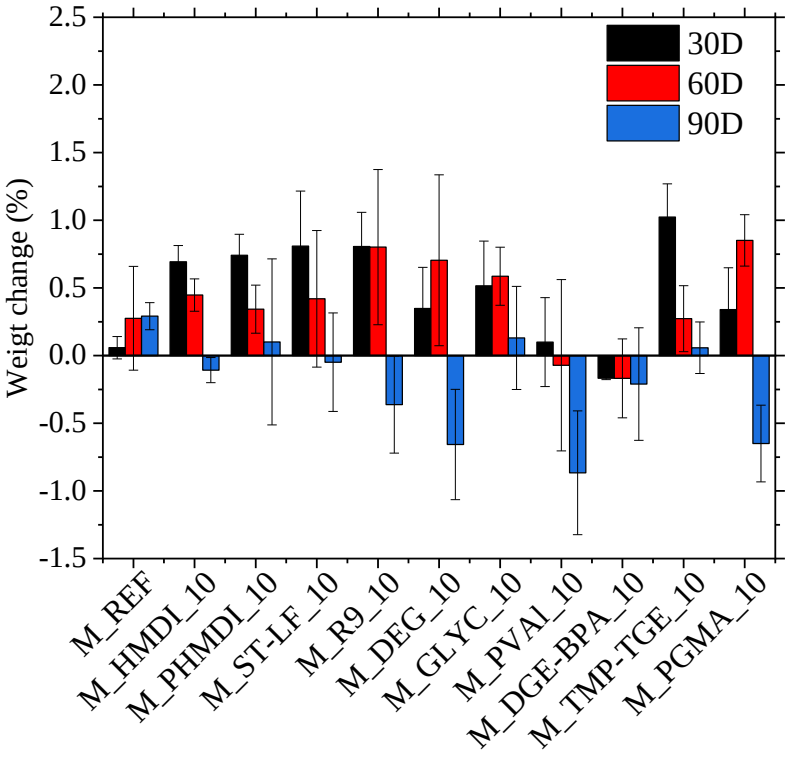

Figure 81 Weight change during the biodegradation test in abiotic conditions

For most of the samples with reagents, especially during the first 60 days of the test, weight gain was observed as well. This can be caused by the absorption of water, which was not removed during drying. Or simple measurement error is possible in such small weights. After 90 days, the sample additivated with DEG, PVAl and PGMA showed weight loss of slightly above 0.5 wt%.

The weight loss in the environment with the enzyme should be a combination of weight loss caused by abiotic contribution and enzyme action. In this case, the measured weight changes are too small to draw any conclusion. It is important to note that changes can be seen for the reference, which has 0.3 wt% weight loss after 90 days. M_PVAl_10 and M_PGMA_10 show similar weight loss after 90 days as in the abiotic conditions.

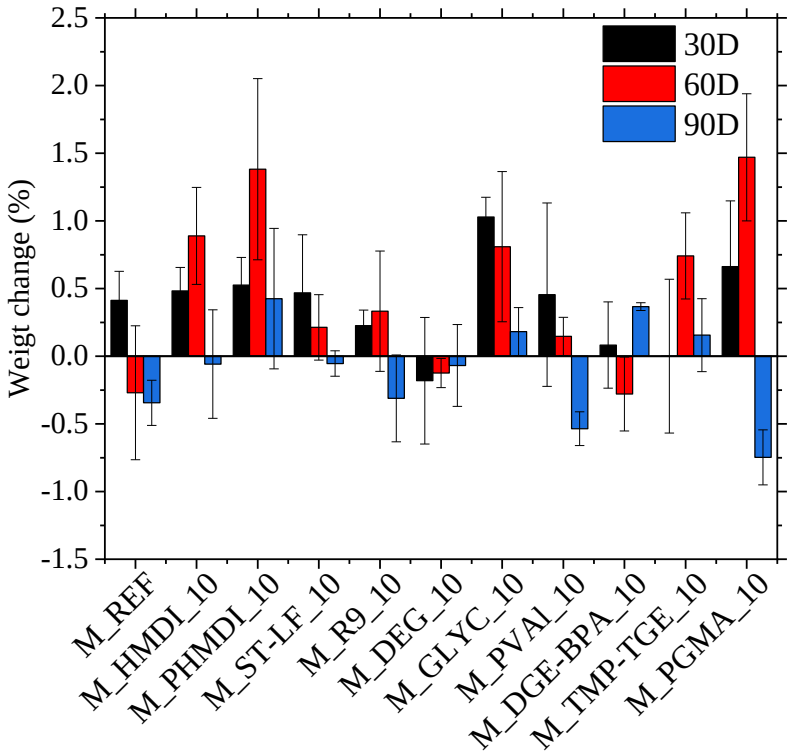

Figure 82 Weight change during the biodegradation test in enzymatic solution

More prominent changes are observed in the results of molar mass measurement. Weight average molecular weight has a smaller experimental error and is of great practical importance and, therefore, its changes are are presented in Figure 83 for the nonenzymatic test and in Figure 84 for samples treated with lipase solution. Obtained data were analysed using one-way ANOVA test in order to find out if there is a statistically significant difference between the individual samples.

After 30 days of non-enzymatic biodegradation, the highest decrease of M_w was observed for the samples containing PHMDI (−21 %) and PGMA (−26 %). Both samples had a statistically higher loss than those with HMDI, ST-LF, R9 and TMP-TGE, which showed only minor changes in molecular weight.

After 60 days, for most of the samples, the extent of MW change increased or remained unchanged in comparison with the results from 30-day measurement. The samples M_PGMA_10 (−19%), M_PVAl_10 (−19%) and M_GLYC_10 (−14%) exhibited the greates change in MW, while the lowest drop was observed for the samples with R9, PHMDI, ST-LF, and TMP-TGE.

The sample M_R9_10 showed the highest final MW loss in abiotic conditions, −31%, which is statistically higher than all the remaining samples except those with PGMA and PVAl. M_PGMA_10 and M_PVAl_10 also showed a profound decrease in M_w at the end of the test, −22% and −19%, respectively. The reference PHB showed 15% molar mass loss after 90 days of this test. The lowest change in M_w after 90 days was observed for the samples M_PHMDI_10 and M_ST-LF_10.

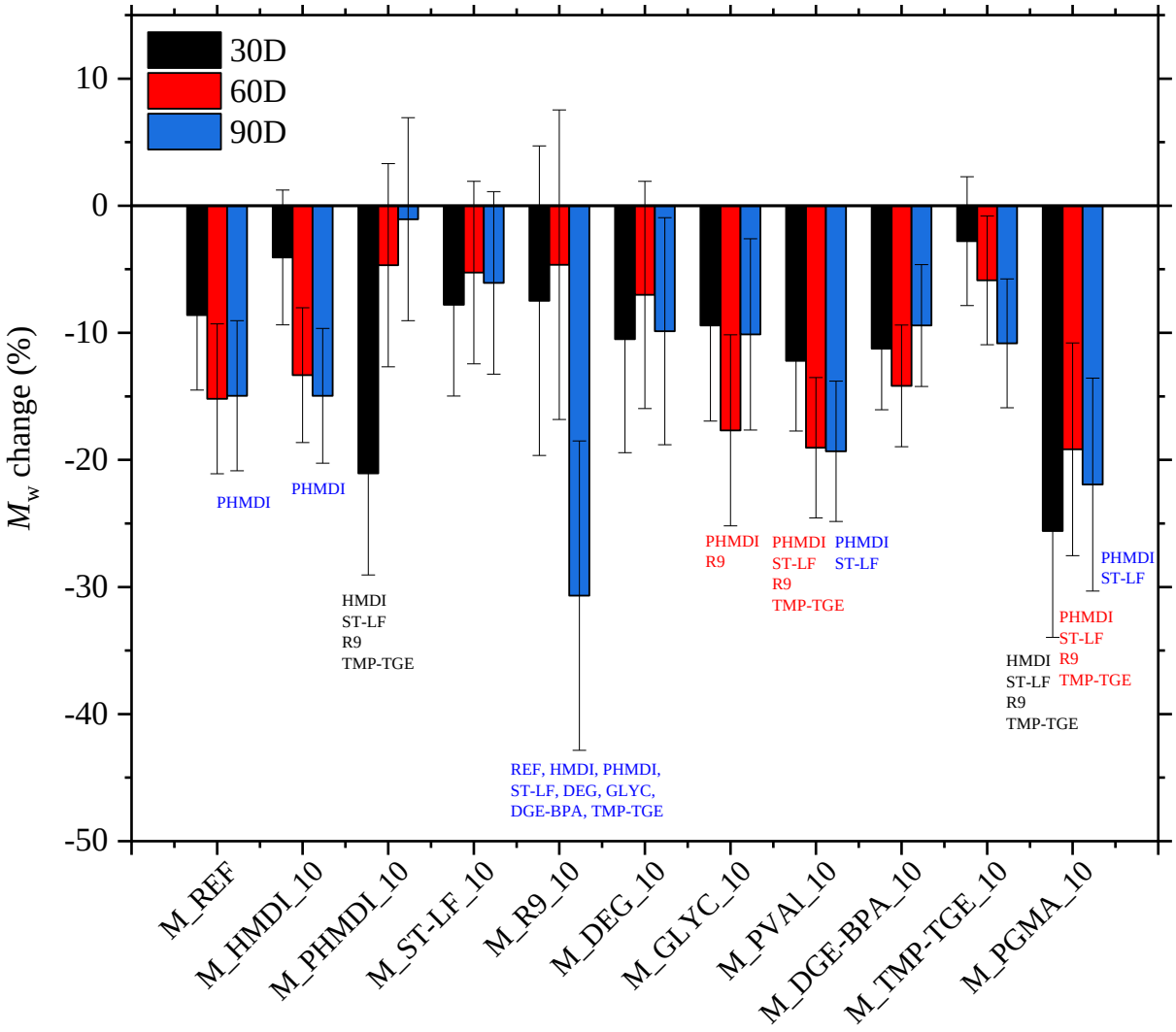

Figure 83 Weight average molecular weight change during the biodegradation test in abiotic conditions, marks above columns indicates the samples with statistically significant differences ($p < 0.05$, Fisher)

The change in molecular weight after 30 days in a solution containing lipase was the most significant for M_PGMA_10, −26 %. Similarly as in abiotic conditions, the lowest drop in M_w was observed for the sample with Raschig, followed by the sample containing PHMDI, which also showed only a slight change of MW in the non-enzymatic test.

After 60 days at 37 °C in enzymatic conditions, the differences among the samples enhanced. The greatest extent of biodegradation was observed for the samples with PGMA (−28%), PVAl (−22%), DEG (−21%) and the reference (−20%). Their M_w loss was significantly higher than for the samples showing the lowest change: M_HMDI_10 (+1%), M_PHMDI_10, M_TMP-TGE_10, M_R9_10, and M_DGE-BPA_10 (−7%).

After 90 days in the medium, most of the samples exhibited the highest decrease in M_w measured in the time frame of the measurement. The reference PHB showed 20% molar mass loss at the end of the test. A significantly higher decrease was measured only for M_R9_10, −35%, such as in the non-enzymatic test. The smallest drop in M_w was observed for M_ST-LF_10 (−6%) and M_HMDI_10 (−9%).

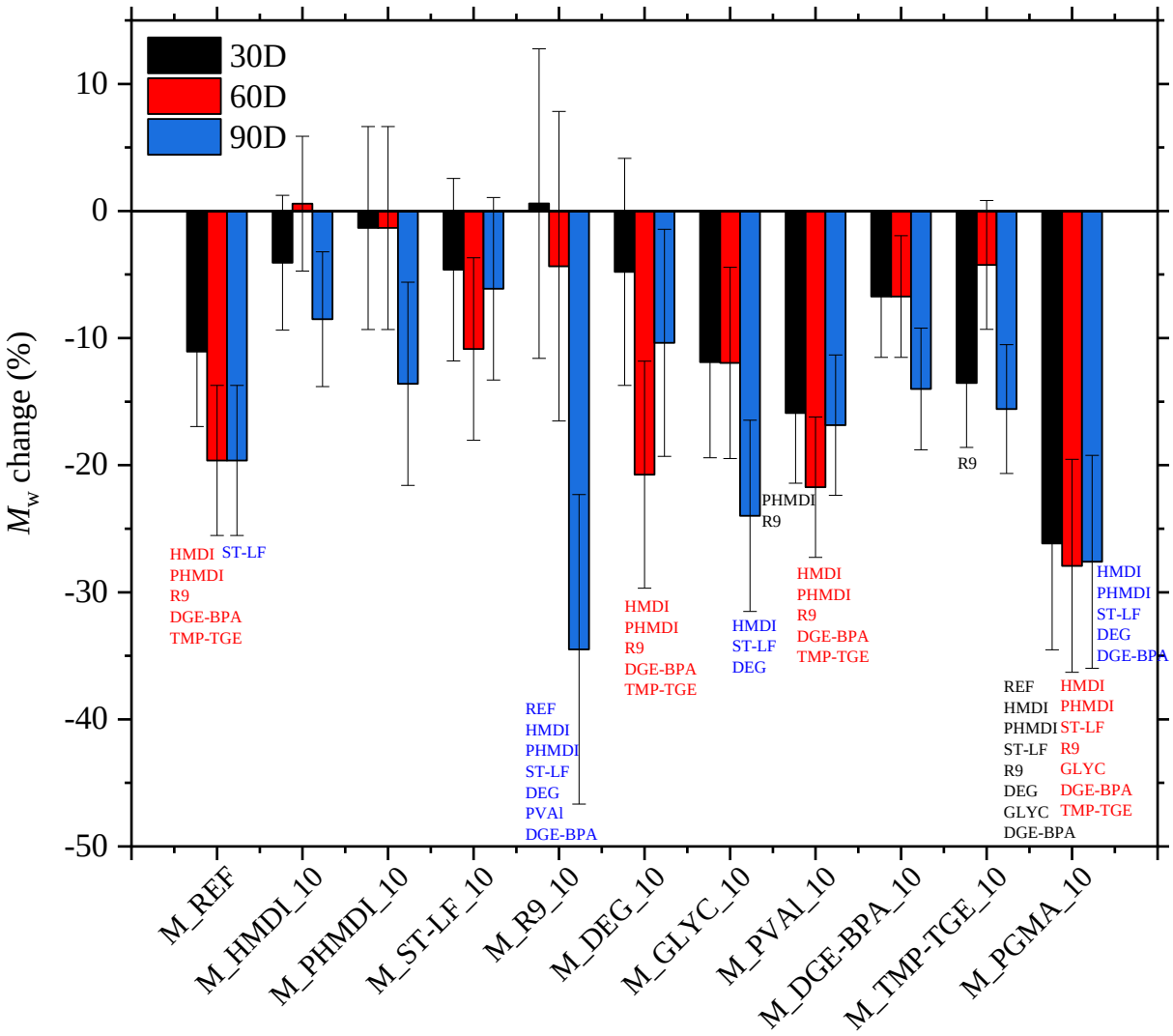

Figure 84 Weight average molecular weight change during the biodegradation test in enzymatic solution, marks above columns indicates the samples with statistically significant differences ($p < 0.05$, Fisher)

The data gathered from the measurement in non-enzymatic conditions were treated with a first-order kinetic model for the change of number average molecular weight in time in the case of random cleavage given in Eq. 1. The expression was expanded to obtain a linear expression:

$$\ln M_n^0 = \ln M_n^t - kt, \qquad \text{Eq. 29}$$

where M_n^0 is the number average molecular weight at time 0, M_n^t is the number average MW at time t, and k is the rate constant. Obtained linear regression for the reference in abiotic conditions is:

$$y = 10.74 - 8.11 \cdot 10^{-3}x, R^2 = 0.5783. \qquad \text{Eq. 30}$$

As you can see from the R^2 value, the data do not fit the model well for the reference sample (R^2 = 0.6). The results for all measured samples are given in Table 24. For the samples with Stabaxol, glycerol, PVAl, TMP-TGE and PGMA, the first-order kinetics work very well (R^2 > 0.8). The values calculated for the remaining samples are not considered reliable. Obtained rate constants range from $-2.5 \cdot 10^{-3}$ in the case of M_TMP-TGE_10 to $-8.24 \cdot 10^{-3}$ days^{-1} for M_PGMA_10.

Table 24 Data obtained by fitting a linear kinetic model for the degradability test in abiotic conditions, rate constant, calculated and measured values of time zero number average molecular weight (the calculated rate constant from the linear fit with $R^2 > 0.8$ are undelined)

Sample name	k (day^{-1})	lnM_{n0}	R_2	Calculated M_{n0} (Da)	Measured M_{n0} (Da)
M_REF	$-8.11 \cdot 10^{-3}$	10.74	0.5783	46246	55147
M_HMDI_10	$-4.77 \cdot 10^{-3}$	11.11	0.4176	67020	70373
M_PHMDI_10	$2.66 \cdot 10^{-4}$	10.96	0.0044	57401	66263
M_ST-LF_10	$-3.78 \cdot 10^{-3}$	11.23	0.9171	75328	75680
M_R9_10	$-8.74 \cdot 10^{-3}$	11.25	0.7219	77023	67610
M_DEG_10	$-2.09 \cdot 10^{-3}$	10.95	0.6618	57171	55930
M_GLYC_10	$-4.93 \cdot 10^{-3}$	11.04	0.8774	62268	65048
M_PVAl_10	$-6.93 \cdot 10^{-3}$	11.09	0.8352	65377	62178
M_DGE-BPA_10	$-4.40 \cdot 10^{-3}$	11.00	0.6846	60063	63310
M_TMP-TGE_10	$-2.49 \cdot 10^{-3}$	11.10	0.9434	66120	66983
M_PGMA_10	$-8.24 \cdot 10^{-3}$	10.82	0.8518	50054	51503

4.6.1. Discussion

In this last part of the work, the samples prepared by kneading poly(3-hydroxybutyrate) with studied additives were subjected to a laboratory enzymatic biodegradation test with lipase with parallel measurement in purely abiotic conditions phosphate buffer saline. It is important to notice that for each sampling time (30, 60 and 90 days), individual sets of the testing specimen were prepared, which may be a source of discrepancies in the results. The samples were characterised by means of weight and molar mass change.

The majority of detected weight changes were within 1%, which means we are on the limits of the scale resolution with weight differences under one microgram. Many samples also exhibited weight gain, which can be explained either by the measurement error or by the reaction of the additives with water. These results are in agreement with the study of Koyama et al., who observed a zero weight change for 50 μm PHB film in 0.01 M potassium phosphate buffer at 37 °C and pH 7.4 for 150 days.[28] However, it is contradictory to the study of Bonartsev et al., which reported 10.5% weight loss for 40 μm PHB films with 150 kDa in 90 days in abiotic conditions.[25]

In addition, the molecular weight of the samples was measured after 30, 60 and 90 days of the test. In nonenzymatic conditions, the reference PHB reached a 15% drop in weight average molecular weight at the end of the test. For thin films, up to a 75% decrease can be expected.[25] In the presence of lipase, the degradation of most of the samples was enhanced. Only with HMDI the biodegradation of PHB was hindered in enzymatic conditions. The reference achieved a 19% loss in weight average MW after 90 days in medium containing lipase.

The changes in the weight average molecular weight were analysed using the ANOVA test. The samples with polyfunctional additives, Raschig 9000, poly(vinyl alcohol) and poly(glycidyl methacrylate), showed the most significant M_w drop in both environments. For the sample with Raschig, the drop was especially profound at the end of the test and was statistically higher than for the reference

PHB, −31% in non-enzymatic and −35% in enzymatic conditions. On the contrary, samples additivated with carbodiimide Stabaxol, hexamethylene diisocyanate, and poly(hexamethylene diisocyanate showed the lowest decrease in weight average MW during both tests. Furthermore, the change in the number average molecular weight was analyzed and fitted to the first-order kinetic model for random cleavage, which should match the conditions of the test. For the samples with Stabaxol, glycerol, PVAl, TMP-TGE and PGMA, reliable values of rate constants for degradation by hydrolysis were obtained. The sample with PGMA has the greatest value, $-8.24 \cdot 10^{-3}$ $days^{-1}$.

It is important to state, at this point, that the presence of studied additives in the polymer matrix and possibly in its chemical structure did not cause complete inhibition of the biodegradation. Only HMDI showed deceleration of MW decrease in the presence of the lipase. Overall, a bulk hydrolysis behaviour was observed, as MW of PHB decreased profoundly while the weight remained unchanged. Weight loss is expected in the more advanced stages of degradation.[23]

5. CONCLUSION

This thesis's two questions of interest were: *(i)* Is it possible to suppress the thermal degradation of poly(3-hydroxybutyrate) during processing? and *(ii)* If so, will this affect its biodegradability?

In order to answer the first question, ten compounds of different functionality (2-, 3- or polyfunctional) and with four different functional groups were studied:

1) Nitrogenous derivates
    a. Isocyanates – bifunctional hexamethylene diisocyanate and trifunctional poly(hexamethylene diisocyanate),
    b. Carbodiimides –bifunctional bis(2,6-diisopropylphenyl)carbodiimide (Stabaxol® 1 LF) and its polymeric form Raschig® 9000
2) Oxygenous derivates
    a. Alcohols – bifunctional diethylene glycol, trifunctional glycerol, and polyfunctional poly(vinyl alcohol)
    b. Epoxides – bifunctional diglycidyl ether of bisphenol A, trifunctional trimethylolpropane triglycidyl ether, and polyfunctional poly(glycidyl methacrylate) synthesised for the purpose of this work by atom transfer radical polymerisation in the emulsion, having the final molecular weight around 20 kDa.

Mentioned additives were mixed with poly(3-hydroxybutyrate) in the melt, which is the target application, and also in the solution. Moreover, the effect of the additive amount expressed as the molar overdose toward the reactive carboxyl chain ends of the polymer was studied. For most of the additives, the amounts corresponding to the 2-fold to 10-fold overdose showed the most promising effect on the molecular weight of melt-prepared samples. For the reaction intensification in the rheometer and for the infrared spectra measurement, 100-fold overdose samples were prepared in the solution and for the rheological test as well.

Poly(3-hydroxybutyrate) is a material nature-designed for residence in mild temperature conditions and during the processing using traditional machines for plastic production, it undergoes cis-elimination and its molecular weight, and overall performance deteriorates. During 5 minutes at 185 °C, its weight average molecular weight drops to 53% in the press and to 30% in the kneader, where the decrease is also accompanied by a decrease of the torque to 20% of initial values. The complex viscosity measured at 1 Hz of frequency and 1 % of the relative deformations decreases to 47% of the initial value after 5 minutes at the selected temperature.

The kinetics of the polymer's degradation was successfully estimated by measuring four subsequent frequency sweeps and fitting the measured data into the model for the first-order reaction of random cleavage of the macromolecules. Two values were calculated: *(i)* time zero viscosity, a theoretical value of complex viscosity in the case of no degradation; and *(ii)* the viscosity loss factor, a kinetic parameter

which characterizes the viscosity decrease in time. Notably, this allowed to distinguish between the change in viscosity caused by a simple addition of the reagents and the supportive/suppressive effect on the degradation. Among the tested additives, polymeric carbodiimide Raschig 9000, hexamethylene diisocyanate, poly(glycidyl methacrylate), and poly(hexamethylene diisocyanate), in this order, had substantially lower viscosity loss factor than pure poly(3-hydroxybutyrate) in the lower frequencies of the tested range. The sample with Raschig had a 20–30% lower value of the viscosity loss factor than the reference in the frequency region 0.1–5 Hz.

All four reagents also showed a positive effect during the kneading and solution test. The positive effect of hexamethylene diisocyanate and poly(glycidyl methacrylate) on molecular weight, processing torque during kneading, and the solution viscosity increases with increasing dosage. Hexamethylene diisocyanate led to a 13% increase in the weight average molecular weight of the polymer in a 10-fold overdose in the kneader and a 19% increase on a 100-fold overdose in the solution. Moreover, its reaction with the polymer was proved by infrared spectroscopy, as the original functional isocyanate groups were consumed, and the peaks of newly formed amide bonds arose. Poly(glycidyl methacrylate) is the most effective in the melt, where its addition in a 100-fold amount led to an 87% increase in the final torque after five minutes of kneading and a 25% higher final weight average molecular weight. On the contrary, in the solution, the effect on molecular weight was observed only for the number average. Raschig's addition above 10-fold overdose (approximately 1.3 wt%) is counterproductive. In the kneader, the sample with a 10-fold dosage showed the greatest effect on the torque change, while in the solution, the 2-fold overdose addition caused a stagerring 101% increase of the solution viscosity and 49% increase in weight average molecular weight of poly(3-hydroxybutyrate). Poly(hexamethylene diisocyanate) influence was more prominent in the kneader than in the solution, where it successfully caused and increased both the final melt torque (by 61%) and the resulting molecular weight (by 19%) in a 2-fold overdose.

Although for diethylene glycol and glycerol, consumption of their functional groups was proven by infrared spectra, due to their volatility in the melt reactions, they were not used in the analysis of the degradation kinetics. However, diethylene glycol addition had a generally negligible effect on poly(3-hydroxybutyrate). As for glycerol, its addition in 2-fold overdose had a profound effect on the kneading torque and the resulting molecular weight of the polymer was the highest out of all melt-prepared samples, 44% higher than the reference polymer. This additive is, therefore, also suitable for further studies.

As for the remaining additives, poly(vinyl alcohol), diglycidyl ether of bisphenol A, and trimethylol-propane triglycidyl ether, they showed positive effect in the melt test and both epoxy reagents also in the solution test. However, these were not supported by the kinetic measurement and therefore, it is assumed that these reagents may protect poly(3-hydroxybutyrate) from the effect of shear stress rather than the effect of the temperature itself.

As for the second question asked in this thesis, the test of the enzymatic biodegradability with lipase was conducted for all melt-prepared samples in a 10-fold dosage. Also, abiotic degradation was monitored parallelly. After three months, the weight of the samples remained unchanged. On the other hand, the effect of molecular weight was significant, which corresponds to the bulk degradation behaviour. For all samples except that with hexamethylene diisocyanate, the extent of the biodegradation was greater with the lipase than in the buffer. For some samples, the first-order kinetics was applied to the measured data of the number average molecular weight, and the degradation rate constant was calculated. The highest rate was obtained for the sample with poly(glycidyl methacrylate), $-8.24 \cdot 10^{-3}$ $days^{-1}$.

To conclude, the goals of the doctoral thesis were successfully achieved. Four reagents capable of suppressing the degradation rate of poly(3-hydroxybutyrate) were identified, and their effect was quantified. In addition, the melt-prepared samples with those additives showed a loss of molecular weight during three months in abiotic conditions and in the presence of lipase as well.

REFERENCES

1. Biopolymers: Polyesters I Biological system and Biotechnological Production. Weinheim: Wiley-VCH, 2002, 460 s. ISBN 35-273-0224-7.
2. LEMOIGNE, Maurice, 1926. Produit de déshydratation et de polymérisation de l'acide *β*-oxybutyrique. *Soc. De Chim. Biol. Bul.* **8**, 770-782.
3. SUDESH, K, H. ABE and Y. DOI, 2000. Synthesis, structure and properties of polyhydroxyalkanoates: biological polyesters. *Prog. Polym. Sci.* **25**(10), 1503-1555. DOI: 10.1016/S0079-6700(00)00035-6.
4. DOUDOROFF, M. and R. Y. STANIER, Role of poly-*β*-hydroxybutyric acid in the assimilation of organic carbon by bacteria. *Nature*. **183**, 1440-1442.
5. OBRUCA, S., P. SEDLACEK, E. SLANINOVA, I. FRITZ, CH. DAFFERT, K. MEIXNER, Z. SEDRLOVA and M. KOLLER, 2020. Novel unexpected functions of PHA granules. *Appl. Microbiol. Biotechnol.* **104**(11), 4795-4810. DOI:10.1007/s00253-020-10568-1
6. KAUR, G., 2015. Strategies for large-scale production of polyhydroxyalkanoates. *Chem. Biochem. l Eng. Q.* **29**(2), 157-172. DOI: 10.15255/CABEQ.2014.2255.
7. Microbial PHA Production from Waste Raw Materials, c2010. *Plastics from bacteria: Natural functions and applications*. New York: Springer, s. 85-119. Microbiology monographs, 14. ISBN 978-3-642-03286-8.
8. KUNASUNDARI, B. and K. SUDESH, 2011. Isolation and recovery of microbial polyhydroxyalkanoates. *Express Polym. Lett.* **5**(7), 620-634. DOI: 10.3144/expresspolymlett.2011.60.
9. FIORESE, M.L., F. FREITAS, J. PAIS, A.M. RAMOS, G.M.F. DE ARAGÃ£O and M.A.M. REIS, 2009. Recovery of polyhydroxybutyrate (PHB) from Cupriavidus necator biomass by solvent extraction with 1,2-propylene carbonate. *Eng. Life Sci.* **9**(6), 454-461. DOI: 10.1002/elsc.200900034.
10. RAMSAY, J. A., E. BERGER, R. VOYER, C. CHAVARIE and B. A. RAMSAY, 1994. Extraction of poly-3-hydroxybutyrate using chlorinated solvents. *Biotechnol. Tech.* **8**(8), 589-594. DOI: 10.1007/BF00152152.
11. RAMSAY, J. A., E. BERGER, B. A. RAMSAY and C. CHAVARIE, 1990. Recovery of poly-3-hydroxyalkanoic acid granules by a surfactant-hypochlorite treatment. *Biotechnol. Tech.* **4**(4), 221-226. DOI: 10.1007/BF00158833.
12. LEE, S.Y., J. CHOI, K. HAN and J. Y. SONG, 1999. Removal of endotoxin during purification of poly(3-hydroxybutyrate) from gram-negative bacteria. *Appl. Environ. Microbiol.*, **65**, 2762-2764.
13. CHEN, Y., H. YANG, Q. ZHOU, J. CHEN and G. GU, 2001. Cleaner recovery of poly(3-hydroxybutyric acid) synthesized in Alcaligenes eutrophus. *Process Biochem.* **36**(6), 501-506. DOI: 10.1016/S0032-9592(00)00225-9.
14. KAPRITCHKOFF, F.M., A.P. VIOTTI, R. C.P. ALLI, M. ZUCCOLO, J.G.C. PRADELLA, A.E. MAIORANO, E.A. MIRANDA and A. BONOMI, 2006. Enzymatic recovery and purification of polyhydroxybutyrate produced by Ralstonia eutropha. *J. Biotechnol.* **122**(4), 453-462. DOI: 10.1016/j.jbiotec.2005.09.009.
15. YOKOUCHI, M., Y. CHATANI, H. TADOKORO, K. TERANISHI and H. TANI, 1973. Structural studies of polyesters: 5. Molecular and crystal structures of optically active and racemic poly(*β*-hydroxybutyrate). *Polymer*.**14**(6), 267-272. DOI:10.1016/0032-3861(73)90087-6.

16. BARHAM, P. J., A. KELLER, E. L. OTUN and P. A. HOLMES, 1984. Crystallization and morphology of a bacterial thermoplastic: poly-3-hydroxybutyrate. *J. Mater. Sci*. **19**(9), 2781-2794. DOI: 10.1007/BF01026954.

17. Degradation of Natural and Artificial Poly[(R)-3-hydroxyalkanoate]s: From Biodegradation to Hydrolysis, 2010. *Plastics from bacteria: Natural functions and applications*. New York: Springer, s. 288-321. Microbiology monographs, 14. ISBN 978-3-642-03286-8.

18. LUCAS, N., Ch. BIENAIME, Ch. BELLOY, M. QUENEUDEC, F. SILVESTRE and J-E. NAVA-SAUCEDO, 2008. Polymer biodegradation: Mechanisms and estimation techniques – A review. *Chemosphere*. **73**(4), 429-442. DOI: 10.1016/j.chemosphere.2008.06.064.

19. SADI, R. K., G. J.M. FECHINE and N. R. DEMARQUETTE, 2010. Photodegradation of poly(3-hydroxybutyrate). *Polym. Degrad. Stabil*. 95(12), 2318-2327. DOI: 10.1016/j.polymdegradstab.2010.09.003.

20. Fundamentals on Biodegradability, 2016. *Introduction to bioplastics engineering*. Boston, MA: Elsevier, s. 61-80. ISBN 978-0-323-39396-6.

21. Biodegradability Testing of Compostable Polymer Materials, 2013. *Handbook of biopolymers and biodegradable plastics: properties, processing and applications*. Waltham, MA: Elsevier/William Andrew, s. 213-263. ISBN 978-1-4557-2834-3.

22. GU, Ji-G. and Ji-D. GU, 2005. Methods currently used in testing microbiological degradation and deterioration of a wide range of polymeric materials with various degree of degradability: A Review. *J. Polym. Environ*. **13**(1), 65-74. DOI: 10.1007/s10924-004-1230-7.

23. ARTSIS, M. I., A. P. BONARTSEV, A. L. IORDANSKII, G. A. BONARTSEVA and G. E. ZAIKOV, 2012. Biodegradation and medical application of microbial poly(3-hydroxybutyrate). *Mol. Cryst. Liq. Cryst*. **555**(1), 232-262. DOI: 10.1080/15421406.2012.635549.

24. CHA, Y. a C.G. PITT, 1990. The biodegradability of polyester blends. *Biomaterials*. **1**(2), 108-112. ISSN 01429612. DOI:10.1016/0142-9612(90)90124-9

25. BONARTSEV, A. P., A. P. BOSKHOMODGIEV, A. L. IORDANSKII, et al. 2012. Hydrolytic degradation of poly(3-hydroxybutyrate), polylactide and their derivatives: kinetics, crystallinity, and surface morphology. *Mol. Cryst. Liquid. Cryst*. **556**(1), 288-300. DOI: 10.1080/15421406.2012.635982.

26. FINDRIK BALOGOVÁ, Alena, Marianna TREBUŇOVÁ, Gabriela IŽARÍKOVÁ, et al., 2021. In Vitro Degradation of Specimens Produced from PLA/PHB by Additive Manufacturing in Simulated Conditions. *Polymers*. **13**(10). ISSN 2073-4360. DOI: 10.3390/polym13101542

27. SHISHATSKAYA, E. I., T. G. VOLOVA, S. A. GORDEEV a A. P. PUZYR, 2012. Degradation of P(3HB) and P(3HB-co-3HV) in biological media. *J. Biomat. Sci*., Polymer Edition. **16**(5), 643-657. ISSN 0920-5063. DOI: 10.1163/1568562053783678

28. KOYAMA, Naoyuki, Yoshiharu DOI, S. A. GORDEEV a A. P. PUZYR, 1995. Morphology and biodegradability of a binary blend of poly((R)-3-hydroxybutyric acid) and poly((R,S)-lactic acid). *Can. J. Microbiol*. **41**(13), 316-322. ISSN 0008-4166. DOI: 10.1139/m95-203

29. ROOHI, M. R. ZAHEER and M. KUDDUS, 2018. PHB (poly-β-hydroxybutyrate) and its enzymatic degradation. *Polym. Adv. Technol*. **29**(1), 30-40. DOI: 10.1002/pat.4126.

30. KUMAGAI, Y., Y. KANESAWA and Y. DOI, Enzymatic degradation of microbial poly(3-hydroxybutyrate) films. *Macromol. Chem*. **193**(1), 53-57. DOI: 10.1002/macp.1992.021930105.

31. FREIER, T., C. KUNZE, C. NISCHAN, S. KRAMER, K. STERNBERG, M. SAß, U. T. HOPT and K-P. SCHMITZ, 2002. In vitro and in vivo degradation studies for development of a biodegradable patch based on poly(3-hydroxybutyrate). *Biomaterials.* **23**(13), 2649-2657. DOI: 10.1016/S0142-9612(01)00405-7.

32. KANMANI, P., K. KUMARESAN, J. ARAVIND, S. KARTHIKEYAN a R. BALAN, 2016. Enzymatic degradation of polyhydroxyalkanoate using lipase from Bacillus subtilis. *Int. J. Environ. Sci. Technol*. 13(6), 1541-1552. ISSN 1735-1472. DOI: 10.1007/s13762-016-0992-5

33. ABOU-ZEID, D-M., R-J. MÜLLER and W-D. DECKWER, 2001. Degradation of natural and synthetic polyesters under anaerobic conditions. *J. Biotech*. **86**(2), 113-126. DOI: 10.1016/S0168-1656(00)00406-5.

34. KASUYA, K., K. TAKAGI, S. ISHIWATARI, Y. YOSHIDA and Y. DOI, 1998. Biodegradabilities of various aliphatic polyesters in natural waters. *Polym. Degrad. Stabil*. **59**(1-3), 327-332. DOI: 10.1016/S0141-3910(97)00155-9.

35. MERGAERT, J, A WEBB, C ANDERSON, A WOUTERS and J SWINGS, 1993. Microbial degradation of poly(3-hydroxybutyrate) and poly(3-hydroxybutyrate-co-3-hydroxyvalerate) in soils. *Appl Environ Microbiol*. **59**(10), 3233–3238. ISSN 0099-2240.

36. YUE, C.L., R.A. GROSS a S.P. MCCARTHY, 1996. Composting studies of poly (β-hydroxybutyrate-co-/gb-hydroxyvalerate). *Polym. Degrad. Stabil.* **51**(2), 205-210. DOI: 10.1016/0141-3910(95)00201-4.

37. SCANDOLA, M., G. CECCORULLI and M. PIZZOLI, The physical aging of bacterial poly(D-*β*-hydroxybutyrate). *Makromol. Chem., Rapid Commun*. **10**(2), 47-50. DOI: 10.1002/marc.1989.030100201.

38. DE KONING, G.J.M, P.J LEMSTRA, D.J.T HILL, T.G CARSWELL and J.H O'DONNELL, 1992. Ageing phenomena in bacterial poly[(*R*)-3-hydroxybutyrate]. *Polymer*. **33**(15), 3295-3297. DOI: 10.1016/0032-3861(92)90250-Z.

39. DE KONING, G.J.M. and P.J. LEMSTRA, 1993. Crystallization phenomena in bacterial poly[(*R*)-3-hydroxybutyrate]: 2. Embrittlement and rejuvenation. *Polymer*. **34**(19), 4089-4094. DOI: 10.1016/0032-3861(93)90671-V.

40. DE KONING, G.J.M., A.H.C. SCHEEREN, P.J. LEMSTRA, M. PEETERS and H. REYNAERS, 1994. Crystallization phenomena in bacterial poly[(*R*)-3-hydroxybutyrate]: 3. Toughening via texture changes. *Polymer*. **35**(21), 4598-4605. DOI: 10.1016/0032-3861(94)90809-5.

41. CRÉTOIS, R., J-M. CHENAL, N. SHEIBAT-OTHMAN, A. MONNIER, C. MARTIN, O. ASTRUZ, R. KURUSU and N. R. DEMARQUETTE, 2016. Physical explanations about the improvement of polyhydroxybutyrate ductility: Hidden effect of plasticizer on physical ageing. *Polymer*. **102**, 176-182. DOI: 10.1016/j.polymer.2016.09.017.

42. STRUIK, L. C. E., 1978. *Physical aging in amorphous polymers and other materials*. New York: distributors for the U.S. and Canada, Elsevier North-Holland. ISBN 978-0444416551.

43. WUNDERLICH, Bernhard, c2005. *Thermal analysis of polymeric materials*. Berlin: Springer. ISBN 35-402-3629-5.

44. DI LORENZO, M. L., M. GAZZANO and M. C. RIGHETTI, 2012. The role of the rigid amorphous fraction on cold crystallization of poly(3-hydroxybutyrate). *Macromolecules*. **45**(14), 5684-5691. DOI: 10.1021/ma3010907.

45. DI LORENZO, M. L. and M. C. RIGHETTI, 2013. Effect of thermal history on the evolution of crystal and amorphous fractions of poly[(*R*)-3-hydroxybutyrate] upon storage at ambient temperature. *Europ. Polym. J.* **49**(2), 510-517. DOI: 10.1016/j.eurpolymj.2012.11.004.

46. GRASSIE, N., E.J. MURRAY and P.A. HOLMES, 1984. The thermal degradation of poly(-(D)-*β*-hydroxybutyric acid): Part 1 — Identification and quantitative analysis of products. *Polym. Degrad. Stabil.* **6**(1), 47-61. DOI: 10.1016/0141-3910(84)90016-8.

47. GRASSIE, N., E.J. MURRAY and P.A. HOLMES, 1984. The thermal degradation of poly(-(D)-*β*-hydroxybutyric acid): Part 2 — Changes in molecular weight. *Polym. Degrad. Stabil.* **6**(2), 95-103. DOI: 10.1016/0141-3910(84)90075-2.

48. GRASSIE, N., E.J. MURRAY and P.A. HOLMES, 1984. The thermal degradation of poly(-(D)-*β*-hydroxybutyric acid): Part 3 —The reaction mechanism. Polym. Degrad. Stabil. 6(3), 127-134. DOI: 10.1016/0141-3910(84)90032-6.

49. TOCHÁČEK, J., R. PŘIKRYL, P. MENČÍK, V. MELČOVÁ and S. FIGALLA, 2021. The chances of thermooxidation stabilization of poly(3-hydroxybutyrate) during processing – A critical evaluation. J. Appl. Polym. Sci. 138(27). ISSN 0021-8995. DOI: 10.1002/app.50647

50. KUNIOKA, M., and Y. DOI, 1990. Thermal degradation of microbial copolyesters: poly(3-hydroxybutyrate-co-3-hydroxyvalerate) and poly(3-hydroxybutyrate-co-4-hydroxybutyrate). Macromolecules 23 (7): 1933-1936. DOI: 10.1021/ma00209a009.

51. NGUYEN, S., G.-E. YU, and R. H. MARCHESSAULT, 2002. Thermal degradation of poly(3-hydroxyalkanoates): preparation of well-defined oligomers. *Biomacromolecules* **3** (1): 219-224. DOI: 10.1021/bm0156274.

52. KOPINKE, F.-D., M. REMMLER, and K. MACKENZIE, 1996. Thermal decomposition of biodegradable polyesters—i: poly(*β*-hydroxybutyric acid). *Polym. Degrad. Stabil.* **52** (1): 25-38. DOI: 10.1016/0141-3910(95)00221-9.

53. HARRISON, Graham M. a David H. MELIK. 2006. Application of degradation kinetics to the rheology of poly(hydroxyalkanoates). *J. Appl. Polym. Sc.* 102(2), 1794-1802. ISSN 0021-8995. DOI: 10.1002/app.24473

54. HABLOT, E., P. BORDES, E. POLLET and L. AVÉROUS, 2008. Thermal and thermo-mechanical degradation of poly(3-hydroxybutyrate)-based multiphase systems. *Polym. Degrad. Stabil.* **93**(2), 413-421. DOI: 10.1016/j.polymdegradstab.2007.11.018.

55. CSOMOROVÁ, K., J. RYCHLÝ, D. BAKOŠ and I. JANIGOVÁ, 1994. The effect of inorganic additives on the decomposition of poly(*β*-hydroxybutyrate) into volatile products. *Polym. Degrad. Stabil.* **43**(3): 441-446. DOI: 10.1016/0141-3910(94)90017-5.

56. KIM, K. J., Y. DOI, H. ABE and L. AVÉROUS, 2008. Effect of metal compounds on thermal degradation behavior of aliphatic poly(hydroxyalkanoic acid)s. *Polym. Degrad. Stabil.* **93**(4): 776-785. DOI: 10.1016/j.polymdegradstab.2008.01.026.

57. LARSSON, M., O. MARKBO and P. JANNASCH, 2016. Melt processability and thermomechanical properties of blends based on polyhydroxyalkanoates and poly(butylene adipate-co-terephthalate). *RSC Adv.* **6**(50), 44354-44363. DOI: 10.1039/C6RA06282B.

58. KAWALEC, M., M. SOBOTA, M. SCANDOLA, M. KOWALCZUK and P. KURCOK, 2010. A convenient route to PHB macromonomers via anionically controlled moderate-temperature degradation of PHB. *J. Polym. Sci. A.* **48** (23): 5490-5497 DOI: 10.1002/pola.24357.

59. BORDES, P., E. HABLOT, E. POLLET and L. AVÉROUS, 2009. Effect of clay organomodifiers on degradation of polyhydroxyalkanoates. *Polym. Degrad. Stabil.* **94**(5), 789-796. DOI: 10.1016/j.polymdegradstab.2009.01.027.

60. WANG, L., W. ZHU, X. WANG, X. CHEN, G.-Q. CHEN and K. XU, 2008. Processability modifications of poly(3-hydroxybutyrate) by plasticizing, blending, and stabilizing. *J. Appl. Polym. Sci*. **107**(1), 166-173. DOI: 10.1002/app.27004.

61. AURIEMMA, M., A. PISCITELLI, R. PASQUINO, P. CERRUTI, M. MALINCONICO and Nino GRIZZUTI, 2015. Blending poly(3-hydroxybutyrate) with tannic acid: Influence of a polyphenolic natural additive on the rheological and thermal behavior. *Eur. Polym. J.* **63**, 123-131. DOI: 10.1016/j.eurpolymj.2014.12.021.

62. PERSICO, P., V. AMBROGI, A. BARONI, G. SANTAGATA, C. CARFAGNA, M. MALINCONICO and P. CERRUTI, 2012. Enhancement of poly(3-hydroxybutyrate) thermal and processing stability using a bio-waste derived additive. *Int. J. Biol. Macromol*. **51**(5), 1151-1158. DOI: 10.1016/j.ijbiomac.2012.08.036.

63. HONG, S.-G., T.-K. GAU and S.-C. HUANG, 2011. Enhancement of the crystallization and thermal stability of polyhydroxybutyrate by polymeric additives. *J. Therm. Anal. Calorim*. **103**(3), 967-975. DOI: 10.1007/s10973-010-1180-3.

64. ERCEG, M., T. KOVAČIĆ and I. KLARIĆ, 2005. Thermal degradation of poly(3-hydroxybutyrate) plasticized with acetyl tributyl citrate. *Polym. Degrad. Stabil*. **90**(2), 313-318. DOI: 10.1016/j.polymdegradstab.2005.04.048.

65. EL-HADI, A., R. SCHNABEL, E. STRAUBE, G. MÜLLER and S. HENNING, 2002. Correlation between degree of crystallinity, morphology, glass temperature, mechanical properties and biodegradation of poly (3-hydroxyalkanoate) PHAs and their blends. *Polym. Test.* **21**(6), 665-674. DOI: 10.1016/S0142-9418(01)00142-8.

66. CHOI, J.S. and W.H. PARK, 2004. Effect of biodegradable plasticizers on thermal and mechanical properties of poly(3-hydroxybutyrate). *Polym. Test*, **23**(4), 455-460. DOI: 10.1016/j.polymertesting.2003.09.005.

67. HA, C-S and W-J CHO, Miscibility, properties, and biodegradability of microbial polyester containing blends. *Prog. Polym. Sci.*. **27**(4), 759-809. DOI: 10.1016/S0079-6700(01)00050-8.

68. MOUSAVIOUN, P., W.O.S. DOHERTY and G. GEORGE, 2010. Thermal stability and miscibility of poly(hydroxybutyrate) and soda lignin blends. *Ind. Crop. Prod*. **32**(3), 656-661. DOI: 10.1016/j.indcrop.2010.08.001.

69. ABOU-AIAD, T.H., M.Z. EL-SABEE, K.N. ABD-EL-NOUR, G.R. SAAD, E-S.A. EL-SAYED and E.A. GAAFAR, 2002. Miscibility and the specific interaction of polyhydroxybutyrate blended with polyvinylacetate and poly(vinyl acetate-co-vinyl alcohol) with some biological applications. *J. Appl. Polym. Sci.* **86**(9), 2363-2374. DOI: 10.1002/app.11137.

70. LI, J., T. FUKUOKA, Y. HE, H. UYAMA, S. KOBAYASHI and Y. INOUE, 2005. Thermal and crystallization behavior of hydrogen-bonded miscible blend of poly(3-hydroxybutyrate) and enzymatically polymerized polyphenol. *J. Appl. Polym. Sci*. **97**(6), 2439-2449. DOI: 10.1002/app.22004.

71. XU, S., R. LUO, L. WU, K. XU and G-Q. CHEN, 2006. Blending and characterizations of microbial poly(3-hydroxybutyrate) with dendrimers. *J. Appl. Polym. Sci*. **102**(4), 3782-3790. DOI: 10.1002/app.24742.

72. CHEN, Ch., L. DONG and P.H.F. YU, 2006. Characterization and properties of biodegradable poly(hydroxyalkanoates) and 4,4-dihydroxydiphenylpropane blends: Intermolecular hydrogen bonds, miscibility and crystallization. *Eur. Polym. J.* **42**(10), 2838-2848. DOI: 10.1016/j.eurpolymj.2006.07.005.

73. ROA, J. P. B., P. S. de O. PATRÍCIO, R. L. ORÉFICE and R. M. LAGO, 2013. Improvement of the thermal properties of poly(3-hydroxybutyrate) (PHB) by low molecular weight polypropylene glycol (LMWPPG) addition. *J. Appl. Polym. Sci.* **128**(5), 3019-3025. DOI: 10.1002/app.38484.

74. ARKIN, A. H. and B. HAZER, 2002. Chemical Modification of Chlorinated Microbial Polyesters. *Biomacromolecules*. **3**(6), 1327-1335. DOI: 10.1021/bm020079v.

75. CHEN, Ch., B. FEI, S. PENG, Y. ZHUANG, L. DONG and Z. FENG, 2002. The kinetics of the thermal decomposition of poly(3-hydroxybutyrate) and maleated poly(3-hydroxybutyrate). *J. Appl. Polym. Sci*. **84**(9), 1789-1796. DOI: 10.1002/app.10463.

76. CHEN, Ch., S. PENG, B. FEI, Y. ZHUANG, L. DONG, Z. FENG, S. CHEN and H. XIA, 2003. Synthesis and characterization of maleated poly(3-hydroxybutyrate). *J. Appl. Polym. Sci.* **88**(3), 659-668. DOI: 10.1002/app.11771.

77. YE, H., D. YANG, P. HU, F.B. ZHANG and Q. QI, 2005. Radiation-induced graft polymerization of maleic anhydride onto poly-*β*-hydroxybutyrate. *Key Eng. Mat.* **288-289**, 477-480. DOI: 10.4028/www.scientific.net/KEM.288-289.477.

78. HSIEH, W-Ch., Y. WADA, T. MITOBE, H. MITOMO, N. SEKO and M. TAMADA, 2009. Effect of hydrophilic and hydrophobic monomers grafting on microbial poly(3-hydroxybutyrate). *J. Taiwan Inst. Chem. E.* **40**(4), 413-417. DOI: 10.1016/j.jtice.2008.10.005.

79. WADA, Y., H. MITOMO, K-I. KASUYA, N. NAGASAWA, N. SEKO, A. KATAKAI and M. TAMADA, 2006. Control of biodegradability of poly(3-hydroxybutyric acid) film with grafting acrylic acid and thermal remolding. *J. Appl. Polym. Sci*. **101**(6), 3856-3861. DOI: 10.1002/app.24189. ISSN 0021-8995.

80. MITOMO, H., T. ENJÔJI, Y. WATANABE, F. YOSHII, K. MAKUUCHI and T. SAITO, 2006. Radiation-induced graft polymerization of poly(3-hydroxybutyrate) and its copolymer. *J. Macromol. Sci. A.* **32**(3), 429-442. DOI: 10.1080/10601329508013674.

81. ZHIJIANG, C., H. CHENGWEI and Y. GUANG, 2011. Crystallization behavior, thermal property and biodegradation of poly(3-hydroxybutyrate)/poly(ethylene glycol) grafting copolymer. *Polym. Degrad. Stabil.* **96**(9), 1602-1609. DOI: 10.1016/j.polymdegradstab.2011.06.001.

82. JIANG, T. and P. HU, 2001. Radiation-induced graft polymerization of isoprene onto polyhydroxybutyrate. *Polym. J*. **33**(9). DOI: 10.1295/polymj.33.647.

83. WADA, Y., M. TAMADA, N. SEKO and H. MITOMO, 2008. Emulsion grafting of vinyl acetate onto preirradiated poly(3-hydroxybutyrate) film. *J. Appl. Polym. Sci*. **107**(4), 2289-2294. DOI: 10.1002/app.27219.

84. CASARANO, R., D. F. S. PETRI, M. JAFFE and L. H. CATALANI, 2010. Block copolymers containing (*R*)-3-hydroxybutyrate and isosorbide succinate or (*S*)-lactic acid mers. *J. Polym. Environ*. **18**(1), 33-44. DOI: 10.1007/s10924-009-0157-4.

85. IMPALLOMENI, G., M. GIUFFRIDA, T. BARBUZZI, G. MUSUMARRA and A. BALLISTRERI, 2002. Acid catalyzed transesterification as a route to poly(3-hydroxybutyrate-co-*ε*-caprolactone) copolymers from their homopolymers. *Biomacromolecules*. **3**(4), 835-840. DOI: 10.1021/bm025525t.

86. IMPALLOMENI, G., G. M. CARNEMOLLA, G. PUZZO, A. BALLISTRERI, L. MARTINO and M. SCANDOLA, 2013. Characterization of biodegradable poly(3-hydroxybutyrate-co-butyleneadipate) copolymers obtained from their homopolymers by microwave-assisted transesterification. *Polymer*. **54**(1), 65-74. DOI: 10.1016/j.polymer.2012.11.030.

87. YUAN, Y. and E. RUCKENSTEIN, 1998. Miscibility and transesterification of phenoxy with biodegradable poly(3-hydroxybutyrate). *Polymer*. **39**(10), 1893-1897. DOI: 10.1016/S0032-3861(97)00468-0.

88. SAAD, G. R. and H. SELIGER, 2004. Biodegradable copolymers based on bacterial Poly((*R*)-3-hydroxybutyrate): thermal and mechanical properties and biodegradation behaviour. *Polym. Degrad. Stabil.* **83**(1), 101-110. DOI: 10.1016/S0141-3910(03)00230-1.

89. ZHAO, Q., G. CHENG, H. LI, X. MA and L. ZHANG, 2005. Synthesis and characterization of biodegradable poly(3-hydroxybutyrate) and poly(ethylene glycol) multiblock copolymers. *Polymer*. **46**(23), 10561-10567. DOI: 10.1016/j.polymer.2005.08.014.

90. VOGEL, R., B. TÄNDLER, D. VOIGT, D. JEHNICHEN, L. HÄUßLER and L. PEITZSCH, 2007. Melt spinning of bacterial aliphatic polyester using reactive extrusion for improvement of crystallization. *Macromol. Biosci.* **7**(6), 820-828. DOI: 10.1002/mabi.200700041.

91. WEI, L. and A. G. McDONALD, 2015. Peroxide induced cross-linking by reactive melt processing of two biopolyesters: poly(3-hydroxybutyrate) and poly(L-lactic acid) to improve their melting processability. *J.Appl. Polym.Sci*. **132**(13), DOI: 10.1002/app.41724.

92. KOLAHCHI, A. R., M. KONTOPOULOU, H. W. KAMMER, M. A. BAKAR, L. HÄUßLER and L. PEITZSCH, 2015. Chain extended poly(3-hydroxybutyrate) with improved rheological properties and thermal stability, through reactive modification in the melt state. *Polym. Degrad. Stabil*. **121**(1), 222-229. DOI: 10.1016/j.polymdegradstab.2015.09.008.

93. CHOI, J. Y., J. K. LEE, Y. YOU and W. H. PARK, 2003. Epoxidized polybutadiene as a thermal stabilizer for poly(3-hydroxybutyrate). II. Thermal stabilization of poly(3-hydroxybutyrate) by epoxidized polybutadiene. *Fiber. Polym*. **4**(4), 195-198. DOI: 10.1007/BF02908278.

94. LEE, H. K., J. ISMAIL, H. W. KAMMER and M. A. BAKAR, 2005. Melt reaction in blends of poly(3-hydroxybutyrate) (PHB) and epoxidized natural rubber (ENR-50). *J. Appl. Polym. Sci*. **95**(1), 113-129. DOI: 10.1002/app.20808.

95. LEE, S. N., M. Y. LEE and W.H. PARK, 2002. Thermal stabilization of poly(3-hydroxybutyrate) by poly(glycidyl methacrylate). *J. Appl. Polym. Sci*. **83**(13), 2945-2952. DOI: 10.1002/app.10318.

96. MARTELLI, S. M., M. PIETRINI, E. G. FERNANDES and E. CHIELLINI, 2013. Poly[(*R*)-3-hydroxy butyrate] Melt processing: strategy for prevention of degradation reactions. *J. Polym. Environ*. **21**(1), 39-45. DOI: 10.1007/s10924-012-0550-2.

97. ARZA, C. R., P. JANNASCH, P. JOHANSSON, P. MAGNUSSON, A. WERKER and F. H. J. MAURER, 2015. Effect of additives on the melt rheology and thermal degradation of poly[(*R*)-3-hydroxybutyric acid]. *J. Appl. Polym. Sci*. **132**(15). DOI: 10.1002/app.41836.

98. WADA, Y., H. MITOMO, K. KASUYA, N. NAGASAWA, N. SEKO, A. KATAKAI and M. TAMADA, 2006. Control of biodegradability of poly(3-hydroxybutyric acid) film with grafting acrylic acid and thermal remolding. *J. Appl. Polym. Sci.* **101**(6), 3856-3861. DOI: 10.1002/app.24189.

99. HONGWEI, Y., J. ZHANPENG and S. SHAOQI, 2004. Anaerobic biodegradability of aliphatic compounds and their quantitative structure biodegradability relationship. *Sci. Total Environ.* **322**(1-3), 209-219. DOI: 10.1016/j.scitotenv.2003.09.009.

100. COMMEREUC, S., H. ASKANIAN, V. VERNEY, A. CELLI and P. MARCHESE, 2010. About durability of biodegradable polymers: structure/degradability relationships. *Macromol. Symp*. **296**(1), 378-387. DOI: 10.1002/masy.201051052.

101. KURUSU, R. S., N. R. DEMARQUETTE, C. GAUTHIER and J-M. CHENAL, 2014. Effect of ageing and annealing on the mechanical behaviour and biodegradability of a poly(3-hydroxybutyrate) and poly(ethylene-co-methyl-acrylate-co-glycidyl-methacrylate) blend. *Polym. Int*. **63**(6), 1085-1093. DOI: 10.1002/pi.4616.

102. HALOI, D. J.; MANDAL, P.; SINGHA, N. K. Atom Transfer Radical Polymerization Of Glycidyl Methacrylate (GMA) In Emulsion. *J. Macromol. Sci. A.* 2013, **50**(1), 121-127. DOI: 10.1080/10601325.2013.736270.

103. THEOPHANIDES, Theophile, ed., 2012. Applications of FTIR on Epoxy Resins – Identification, Monitoring the Curing Process, Phase Separation and Water Uptake. In: *Infrared Spectroscopy - Materials Science, Engineering and Technology*. London: IntechOpen, s. 261-284. ISBN 978-953-51-0537-4.

104. POSPISILOVA, A., V. MELCOVA, S. FIGALLA, P. MENCIK and R. PRIKRYL, 2021. Techniques for increasing the thermal stability of poly[(*R*)-3-hydroxybutyrate] recovered by digestion methods. *Polym. Degrad. Stabil.* 2021, **193**. DOI: 10.1016/j.polymdegradstab.2021.109727

105. HIRSCHMANN, R. P., R. N. KNISELEY and V. A. FASSEL, 1965. The infrared spectra of alkyl isocyanates. *Spectrochim. Acta*. **21**(12), 2125-2133. DOI: 10.1016/0371-1951(65)80228-4

106. FETTERS, L. J., A. D. KISS, D. S. PEARSON, G.r F. QUACK and F. J. VITUS, 1993. *Macromolecules*. Rheological behavior of star-shaped polymers. 26(4), 647-654. ISSN 0024-9297. DOI:10.1021/ma00056a015

107. CHEN, A-L., K-L. WEI, R-J. JENG, J-J. LIN and S. A. DAI, 2011. Well-Defined Polyamide Synthesis from Diisocyanates and Diacids Involving Hindered Carbodiimide Intermediates. *Macromol.* **44**(1), 46-59. DOI: 10.1021/ma1022378

108. LASCANO, D., L. QUILES-CARRILLO, R. BALART, T. BORONAT and N. MONTANES, 2019. Kinetic Analysis of the Curing of a Partially Biobased Epoxy Resin Using Dynamic Differential Scanning Calorimetry. *Polymers*. **11**(3). DOI: 10.3390/polym11030391

109. MELCOVA, V., R. PRIKRYL, P. MENCIK and J. TOCHACEK, 2019. Processing Stabilization of Poly(3-Hydroxybutyrate)/Poly(Lactic Acid) Blends with Oligomeric Carbodiimide. *Materials Science Forum* 955, 7-12. DOI:10.4028/www.scientific.net/MSF.955.7

LIST OF ABBREVIATIONS

AA	acrylic acid
AdA	adipic acid
ATBC	acetyl tributyl citrate
ATRP	atomic transfer radical polymerization
BD	1,4−butanediol
BECMA	bis(3,4-epoxycyclohexylmethyl) adipate
BOX	2,2'-bis(2-oxazoline)
bpy	bipyridine
CL	ε-caprolactone
COD	chemical oxygen demand
CTBN	carboxyl terminated butadiene acrylonitrile rubber
DCP	dicumyl peroxide
DEG	diethylene glycol
DGE-BPA	diglycidyl ether bisphenol A
DSC	differential scanning calorimetry
DTA	differential thermal analysis
EPB	epoxidized polybutadiene
FS	frequency sweep
FTIR	Fourier transform infrared spectroscopy
GLYC	glycerol
GMA	glycidyl methacrylate
GMA.MMA	poly(methyl metharylate-co-glycidyl methacrylate)
GPC	gel permeation chromatography
HMDI	1,6−hexamethylene diisocyanate
HEMA	2−hydroxyethyl methacrylate
ICP-OES	inductively coupled plasma atomic emission spectroscopy
IS	isosorbide succinate
LA	lactic acid
LCB	long chain branched
LVR	linear viscoelastic region
MA	maleic acid/maleic anhydride
MAA	methyl acrylate
MBrP	methyl 2-bromopropionate
MDI	methylene diphenyl diisocyanate
MMA	methyl methacrylate
MW	molecular weight
PBA	poly(1,4-butyleneadipate)
PBA−diol	poly(butylene glycol adipate)-diol
PBS	poly(butylene succinate)
PBT	poly(butylene terephtalate)
PCDI	poly(carbodiimide)
PCL	poly(ε-caprolactone)
PDEGA−diol	poly(diethylene glycol adipate) diol
PEG	poly(ethylene glycol)
PEMAGMA	poly(ethylene-co-methyl acrylate-co-glycidyl methacrylate)

PET	poly(ethylene terephtalate)
PETA	pentaerithritol triacrylate
PETAP	trimethylolpropane tris(2-methyl-1-aziridinepropionate)
PGMA	poly(glycidyl methacrylate)
PHA	poly(3-hydroxy alkanoate)
PHB	poly(3-hydroxy butyrate)
PHMDI	poly(hexamethylene diisocyanate)
PIS	poly(isosorbide succinate)
PLA	poly((L)-lactide)
PU	polyurethane
PVAl	poly(vinyl alcohol)
R9	Raschig 9000
RPM	rotations per minute
SEC	size exclusion chromatography
SSS	sodium *p*-styrene sulfonate
St	styrene
ST-LF	stabaxol® 1 LF
TAM	triallyl trimesate
TGA	thermogravimetric analysis
TMP-TGE	trimethylolpropane triglycidyl ether
TNPP	tris(nonyl phenyl) phosphite
TPP	tris(phenyl phosphite)
TPU	termoplastic polyurethane
TS	time sweep